UNIVERSIDAD DE SALAMANCA

TESIS DOCTORAL

Multi-agent architecture for local electricity trading in power distribution systems

---

Departamento de Informática y Automática

Facultad de Ciencias

Autor:

Amin Shokri Gazafroudi

Director:

Dr. Juan Manuel Corchado Rodríguez

Codirectora:

Dra. Zita Maria Almeida do Vale

Salamanca, 2019

Universidad de Salamanca

Tesis Doctoral

Arquitectura multi-agente para el comercio local de electricidad en sistemas de distribución

Departamento de Informática y Automática

Facultad de Ciencias

Autor:

Amin Shokri Gazafroudi

Director:

Dr. Juan Manuel Corchado Rodríguez

Codirectora:

Dra. Zita Maria Almeida do Vale

Salamanca, 2019

Declaración de autoría

D. Amin Shokri Gazafroudi, presenta el proyecto de tesis titulado "Multi-agent architecture for local electricity trading in power distribution systems" para optar al Grado de Doctor en Ingeniería Informática por la Universidad de Salamanca, y declara que ha sido realizado bajo la dirección del Dr. Juan Manuel Corchado Rodríguez González, profesor contratad doctor del Departamento de Informática y Automática de la Universidad de Salamanca, y la Dra. Zita Maria Almeida do Vale, profesora titular en el Grupo de Investigação em Engenharia e Computação Inteligente para a Inovação e o Desenvolvimento (GECAD) de la Instituto Superior de Engenharia do Porto (ISEP).

En Salamanca, a 5 de julio de 2019

El doctorando:

Amin Shokri Gazafroudi

Los directores:

Dr. Juan Manuel Corchado Rodríguez   Dra. Zita Maria Almeida do Vale

Resumen

En la última década, los mercados eléctricos han desarrollado entornos competitivos para sistemas eléctricos complejos. El rápido crecimiento de los recursos energéticos distribuidos ha dificultado mantener la credibilidad y estabilidad del sistema. Sin embargo, debido a la volatilidad de los recursos energéticos distribuidos las estrategias convencionales de gestión de la energía son incapaces de resolver estos problemas de forma centralizada. Además, los mercados centralizados de electricidad no son capaces de adaptarse al comportamiento flexible de los consumidores que ocurre en los programas de respuesta de demanda. Por lo tanto, se requieren nuevas estructuras de comercio de electricidad que proporcionen energía a las redes de distribución de forma descentralizada y distribuida.

Este trabajo presenta un enfoque ascendente de gestión energética basado en una arquitectura multiagente para el comercio local de la electricidad. La estructura propuesta consiste en una clase de organización basada en sistemas multiagente, en la cual cada agente cumple diferentes tareas. Estos agentes están formados por recursos energéticos distribuidos, consumidores eléctricos, prosumidores, vehículos eléctricos (Electricit Vehicles (EV)), agregadores, un operador del sistema de distribución, coordinadores locales y los coordinadores de los EV del sistema. Además, proponemos un enfoque ascendente para el comercio de energía desde los usuarios finales, como agentes prosumidores capaces de proporcionar transacciones energéticas bidireccionales a los agregadores y al gestor de la red de distribución (Distibution System Operator (DSO)).

En este contexto, se presenta una arquitectura basada en sistemas multiagente, para el sistema eléctrico de las casas inteligentes (como ejemplo de usuario final). A continuación, se define el sistema de gestión de la energía en el hogar (HEMS por sus siglas en inglés) para modelar el comportamiento flexible de los usuarios finales residenciales y su incertidumbre basándose en diferentes métodos de optimización (por ejemplo, intervalo, estocástico e intervalo-estocástico). Además, presentamos un método basado en escenarios probabilísticos para la gestión de la energía residencial y el comercio de energía con el mercado local de electricidad basado en una estrategia de licitación óptima. De acuerdo con nuestro modelo de oferta óptimo, el HEMS es capaz de realizar transacciones de energía con otros actores en su vecindario como un agente de fijación de

precios basado en los enfoques de intercambio de energía entre pares o enfoques basados en la comunidad.

Conforme al enfoque ascendente propuesto en nuestro trabajo de doctorado, las decisiones de los agentes en la capa inferior tienen prioridad en comparación con las decisiones de los agentes en las capas superiores. De esta manera, la estrategia propuesta gestiona la energía localmente para lograr una optimización social global. Además, en la red de distribución se pueden comercializar localmente diferentes tipos de productos básicos de electricidad, como la energía y la flexibilidad.

A continuación, hemos propuesto varios enfoques (por ejemplo, descentralizado, monopolístico y basado en juegos) para la gestión de la flexibilidad energética entre los agentes de la red de distribución de energía, teniendo en cuenta el comportamiento flexible de los usuarios finales y los agregadores. Por último, se ha estudiado el impacto de los futuros sistemas de transporte en las redes inteligentes. Así, la gestión de la flexibilidad energética de los usuarios finales y las operaciones de recarga de los vehículos eléctricos se modelan en la red de distribución. Se han presentado tres estrategias de gestión de la energía para abordar la flexibilidad energética y el funcionamiento de los vehículos eléctricos entre los actores de la capa inferior del sistema eléctrico. Además, la incertidumbre causada por la movilidad de los vehículos eléctricos se ha modelado mediante una programación estocástica. Aquí, el reto es modelar un problema multinivel basado en la función objetiva de los agentes considerando la incertidumbre de los parámetros estocásticos del sistema. De esta forma, cada agente puede participar en diferentes tipos de transacciones eléctricas según sus funciones objetivas correspondientes.

Se evalúa el rendimiento del sistema propuesto de gestión de la energía en el hogar (HEMS) comparándolo con los métodos de optimización de intervalos estocásticos propuestos y de bandas estocásticas predichas modificadas. Evaluamos el impacto del modelo de flexibilidad energética y su exactitud de predicción. Ademas, evaluamos el programa de respuesta de demanda en términos de las ganancias esperadas, de la energía eléctrica tramitada y de la credibilidad de los resultados. Para ello, proponemos un modelo de oferta óptima para el sistema de gestión de la energía en el hogar. Así, el sistema puede participar en el comercio local de electricidad. El rendimiento del modelo de oferta óptima propuesto se evalúa en dos casos diferentes. El Caso 1 evalúa el impacto de los coeficientes de optimismo y flexibilidad en el HEMS, considerando la estrategia de licitación óptima. En el caso 2, sin embargo, el rendimiento de los dos métodos de optimización diferentes -llamados InterStoch e Hybrid- en el HEMS se evalúa sin considerar la estrategia de licitación óptima.

Posteriormente, se evalúa el funcionamiento de nuestros enfoques descentralizados, monopolísticos y basados en juegos en términos de su impacto en la incertidumbre de la línea de distribución y el comportamiento flexible de los usuarios finales. Por último, modelamos la gestión de la flexibilidad energética de los usuarios finales y la operación de carga de los EV en la red de distribución. Se presentan tres estrategias de gestión de la energía para abordar la flexibilidad energética y el funcionamiento de los EV entre los actores de la capa inferior del sistema eléctrico.

Abstract

Over the last decade, electricity markets have created competitive environments for complex power systems. The fast growth of distributed energy resources has made it challenging to maintain the reliability and stability of the system. However, conventional energy management strategies are not capable of resolving these concerns centrally due to the volatility of distributed energy resources. Moreover, centralized electricity markets are not complete enough to follow the flexible behavior of consumers due to demand response programs. Therefore, new electricity trading structures are required to provide energy to distribution networks in a decentralized and distributed manner.

This work presents a bottom-up energy management approach based on a multi-agent architecture for local electricity trading. Our proposed structure is defined as a class of organization-based multi-agent systems, where each agent has different tasks. These agents consist of distributed energy resources, electrical consumers, prosumers, electric vehicles, aggregators, a distribution system operator and local coordinators of the system.

According to the proposed bottom-up approach in our Ph.D. work, decisions of agents in the bottom layer have priority in comparison to agents' decisions in the upper layers. In this way, our proposed strategy manages energy locally to pursue global-social optimization. Also, different types of electricity commodities- e.g. energy and flexibility- can be traded locally in the distribution network.

In this Ph.D. work, we define different strategies such as decentralized, partially-decentralized and centralized (community-based) for local electricity trading. Here, the challenge is to model a multi-level problem based on the objective function of agents considering uncertainty of the system's stochastic parameters. In this way, each agent can participate in different types of the electricity transactions on the basis of their corresponding objective functions.

Acknowledgement

I would like to take this opportunity to express my sincere gratitude to all those that have supported me over the course of my PhD. First of all, I would like to thank my supervisor, Prof. Juan Manuel Corchado Rodríguez for his patience, motivation and immense knowledge. His continuous support in my PhD study and related research have been crucial, I could not have achieved any of this without his guidance and help. Besides my supervisor, I would also like to express my gratefulness to my co-supervisor Prof. Zita Maria Almeida do Vale, for her support in my research activities and her help in the writing of this PhD. thesis.

My sincere thanks also goes to Prof. Juan Miguel Morales González and Discovergy GmbH who have given me the opportunity to join their team and company as an intern, and who have provided me with access to the laboratory and research facilities. Without their valuable support it would not have been possible to conduct this research. A special thanks to Prof. João P. S. Catalão, Dr. Javier Prieto Tejedor, Dr. Francisco Prieto Castrillo and Dr. Tiago Pinto, for their collaboration and advice over the last three years. Moreover, I would also like to express my deep gratitude to Maria de Mello for her time and help in editing all my academic and technical documents.

The BISITE Research Group of the University of Salamanca has been an extraordinary host. This Ph.D. work would not have been possible without the technical and financial support of BISITE. I also thank all my lab mates at both BISITE and GECAD, namely, Fernando, Sara, Elena, Alfonso, Pablo, Yeray, Diego, Daniel, Enrique, Javier, Roberto, Alberto, Omid, Ali, Aria, Mahsa, João, Luis, Pedro and Filipe.

Finally, and most importantly, I would like to thank my lovely and dear wife, Elham Fakhr, for her motivation, hope, patience and love. I thank my beloved parents, Teymour Shokri Gazafroudi and Shahrbanoo Pourebrahimi Gazafroudi, who taught me how to fight, live and love with loyalty.

Contents

Declaración de autoría **iii**

Resumen **v**

Abstract **ix**

Acknowledgement **xi**

Contents **xii**

List of Figures **xix**

List of Tables **xxiii**

List of Acronyms **xxv**

1 Introduction
(*introducción*) **1**
1.1 Description the problem 3
1.2 Literature review 5
1.3 Methodology 7
1.4 Structure of the thesis 8

2 Multi-agent architecture for local electricity trading
(*arquitectura multi-agente para el comercio local de electricidad*) **11**
2.1 Introduction 13
2.2 Virtual organization of agents in the power distribution grid 14
2.2.1 End-Users (EU) 14
2.2.2 Aggregators (AGG) 15
2.2.3 Distribution System Operator (DSO) 16
2.3 Agents Organization for the Smart Home 16
Electrical Loads (ELs) 17
Distributed Energy Resources (DERs) 17
Energy Storage Systems (ESSs) 17
Information Provider (IP) 17

Local Electricity Market (LEM) 17
Energy Scheduler (ES) 17
Prediction Engine (PE) 18
Energy Management System (EMS) 18
2.4 Conclusion 20

3 Home energy management system (*sistema de gestión de energía en la hogar*) 21
3.1 Introduction 23
3.2 Home energy management problem using a novel interval optimization method 24
3.2.1 Proposed interval optimization method 25
3.2.1.1 Stochastic Predicted Bands (SPB) Method 25
Step 1 25
Step 2 26
Step 3 26
Step 4 26
3.2.1.2 Modified Stochastic Predicted Bands (MSPB) Method . . 27
3.2.2 Home energy management problem 28
3.2.2.1 Objective function 28
3.2.2.2 First Stage 28
3.2.2.3 Second Stage 29
PV-battery system 29
Electric Vehicle (EV) 30
Wind system 31
Space heater 31
Storage water heater 32
Pool pump 32
Must-run services 32
Spillage limits 33
Load shedding limits 33
3.2.2.4 Integration with the Modified Stochastic Predicted Bands (MSPB) Method 33
3.2.3 Case study 34
3.2.3.1 Energy service system in a smart home 34
3.2.3.2 Impact of uncertainty 34
3.2.3.3 Impact of optimistic coefficient 36
3.2.3.4 Impact of prediction accuracy 36
3.3 Energy flexibility management based on a predictive dispatch model of the HEMS 37
3.3.1 Interval-stochastic optimization method 38
3.3.1.1 Data 38
3.3.2 Interval Model 39
3.3.3 Stochastic Model 40
3.3.4 Home Energy Management Problem 41
3.3.4.1 Day-Ahead Stage 41
3.3.4.2 Real-Time Stage 43

3.3.5 Simulation Results . . . 47
3.3.5.1 Case Study . . . 47
3.3.5.2 Impact of Energy Flexibility . . . 48
3.3.5.3 Impact of Prediction Accuracy . . . 49
3.3.5.4 Impact of Demand Response . . . 49
3.3.5.5 Impact of Uncertainty Modeling . . . 50
3.4 Conclusions . . . 52

4 Optimal offering model for the home energy management system (*modelo óptimo de oferta de sistema de gestión de energía en la hogar*) 53
4.1 Introduction . . . 55
4.2 Uncertainty representation . . . 56
4.3 Problem Formulation . . . 59
4.3.1 Two-stage Interval-Stochastic model . . . 59
4.3.1.1 Objective function . . . 59
4.3.1.2 Day-ahead stage . . . 61
4.3.1.3 Real-time stage . . . 64
4.3.2 Optimal bidding strategy . . . 69
4.3.3 Two-stage Stochastic model . . . 69
4.4 Case studies . . . 73
4.4.1 Cases . . . 73
4.4.2 Results . . . 79
4.4.2.1 Case 1: with optimal offering model . . . 79
a. Impact of α_{pv}, α_{price}, and γ . . . 79
b. Optimal offering and bidding curves . . . 79
4.4.2.2 Case 2: without optimal offering model . . . 84
a. Results of the InterStoch method . . . 84
b. Results of the Hybrid method . . . 85
4.5 Conclusions . . . 88

5 Local electricity trading structure (*estructura local del comercio de electricidad*) 89
5.1 Introduction . . . 91
5.2 Decentralized energy flexibility management . . . 91
5.2.1 Energy flexibility management problem . . . 92
5.2.2 Simulation results . . . 95
5.2.2.1 Case study . . . 95
5.2.2.2 Impact of lines uncertainty . . . 96
5.2.2.3 The impact of flexible behavior . . . 98
5.3 Monopolistic approach to manage energy flexibility . . . 99
5.3.1 Problem formulation . . . 100
5.3.2 The MILP model . . . 102
5.3.2.1 Aggregators-based energy trading problem . . . 104
5.3.2.2 Consumers-based energy trading problem . . . 104
5.3.3 Evaluation of the Monopolistic Approach . . . 105
5.4 Iterative algorithm for trading electricity between aggregators and the DSO 109
5.4.1 The proposed iterative algorithm . . . 109

5.4.2 Assessment of the performance of the iterative algorithm 110
5.5 Iterative algorithm for trading electricity between end-users and the DSO 113
5.5.1 The proposed iterative algorithm 113
5.5.2 Evaluation of iterative algorithms 113
5.6 Conclusions 116

6 Local electricity trading for EVs (*comercio local de electricidad para EVs*) 117
6.1 Introduction 119
6.2 Problem formulation 120
6.3 Strategies to manage energy flexibility 124
6.3.1 Strategy-I 124
6.3.2 Strategy-II 125
6.3.3 Strategy-III 126
6.4 Simulation results 128
6.4.1 Case study 128
6.4.2 Economic evaluation of strategies 131
6.4.3 Energy flexibility evaluation 133
6.4.4 Agent-based Decision-making Evaluation 134
6.5 Conclusions 137

7 Conclusions and future works (*conclusiones y trabajos futuros*) 139
7.1 Introduction 141
7.2 Main contributions 141
7.3 Research findings and conclusions 142
7.3.1 Home energy management system 142
7.3.2 Optimal offering model for the HEMS 143
7.3.3 Local electricity trading structure 144
7.3.4 Local electricity trading for EVs 145
7.4 Recommendations for future works 146
7.5 Introducción 147
7.6 Contribuciones principales 147
7.7 Resultados y conclusiones de la investigación 148
7.7.1 Sistema de gestión de energía en la hogar 148
7.7.2 Modelo óptimo de oferta para el HEMS 149
7.7.3 Estructura local del comercio de electricidad 150
7.7.4 Comercio local de electricidad para EVs 151
7.8 Recomendaciones para trabajos futuros 152

A Publications and related works (*publicaciones y trabajos relacionados*) 153
A.1 Introducción 155
A.1.1 Published papers in international JCR journals 155
A.1.2 Published book chapters 156
A.1.3 Presented international conference papers 156

A.1.4 Participation in projects 157

Bibliography (*bibliografía*) **159**

List of Figures

2.1 Organization of end-user agents [Shokri Gazafroudi et al., 2019]. 14
2.2 Organization of aggregator agents [Shokri Gazafroudi et al., 2019]. 15
2.3 Organization of the DisCo agents [Shokri Gazafroudi et al., 2019]. 16
2.4 The MASHES physical system [Gazafroudi et al., 2017a]. 16
2.5 The MAS architecture for the SHES [Gazafroudi et al., 2017a]. 19

3.1 The simple flowchart of the SPB method [Shokri Gazafroudi et al., 2017]. 27
3.2 An extended sample of a smart home in [Shokri Gazafroudi et al., 2017]. . 35
3.3 Impact of OC on wind energy output and system expected cost [Shokri Gazafroudi et al., 2017]. 37
3.4 Impact of wind power prediction accuracy on wind energy output and system expected cost [Shokri Gazafroudi et al., 2017]. 38
3.5 Impact of energy flexibility on the amounts of total, day-ahead and real-time expected profits [Gazafroudi et al., 2017b]. 48
3.6 Impact of prediction accuracy on the total expected profit of the system [Gazafroudi et al., 2017b]. 49
3.7 Impact of uncertainty modeling on total expected profit of the system [Gazafroudi et al., 2017b]. 51

4.1 Scenario tree representation [Ghazvini et al., 2015] and [Gazafroudi et al., 2019c]. 58
4.2 A generic layout of our residential energy management system [Gazafroudi et al., 2019c]. 60
4.3 Impact of α_{pv} on total, day-ahead and real-time expected profits of the residential energy management problem considering α_{price} and γ equal 1 [Gazafroudi et al., 2019c]. 80
4.4 Impact of α_{price} on total, day-ahead and real-time expected profits of the residential energy management problem considering α_{pv} equals 0 and γ equals 1 [Gazafroudi et al., 2019c]. 80
4.5 Impact of γ on total, day-ahead and real-time expected profits of the residential energy management problem considering α_{pv} equals 0 and α_{price} equals 1 [Gazafroudi et al., 2019c]. 81
4.6 The optimal scheduled transacted energy for the smart home in the day-ahead stage [Gazafroudi et al., 2019c]. 81
4.7 The optimal bidding and offering curves for the smart home in t equals 1, 3, and 6 in the real-time stage [Gazafroudi et al., 2019c]. 82
4.8 Real-time expected electrical consumption of the space heater (a), real-time expected indoor temperature (b) in the optimal offering model of the HEMS [Gazafroudi et al., 2019c]. 82

4.9 Real-time expected electrical consumption of the storage water heater (a), real-time expected electrical consumption of the pool pump (b), real-time operation status of the pool pump (c) in optimal offering model of the HEMS [Gazafroudi et al., 2019c]. 83
4.10 Real-time expected state of charge of the battery in the optimal offering model of the HEMS [Gazafroudi et al., 2019c]. 83
4.11 Real-time state of charge, charged energy, and discharged energy of the battery at t=1 (a), t=3 (b), t=6 (c) [Gazafroudi et al., 2019c]. 84
4.12 Without offering model (InterStoch model): impact of α_{pv} on total, day-ahead and real-time expected profit of the residential energy management problem considering α_{price} and γ equal 1 [Gazafroudi et al., 2019c]. 85
4.13 Without offering model (InterStoch model): impact of α_{price} on total, day-ahead and real-time expected profit of the residential energy management problem considering α_{pv} equals 0 and γ equals 1 [Gazafroudi et al., 2019c]. 85
4.14 Without offering model (InterStoch model): the bidding and offering curves for the smart home in t equals 1, 3, and 6 in the real-time stage [Gazafroudi et al., 2019c]. 86
4.15 Without offering model (Hybrid model): impact of α_{pv} on total, day-ahead and real-time expected profit of the residential energy management problem considering α_{price} and γ equal 1 [Gazafroudi et al., 2019c]. 86
4.16 Without offering model (Hybrid model): impact of α_{price} on total, day-ahead and real-time expected profit of the residential energy management problem considering α_{pv} equals 0 and γ equals 1 [Gazafroudi et al., 2019c]. 87
4.17 Without offering model (Hybrid model): the bidding and offering curves for the smart home in t equals 1, 3, and 6 in the real-time stage [Gazafroudi et al., 2019c]. 87

5.1 Real-time energy transaction framework of the power distribution system [Zhang et al., 2018], [Prieto-Castrillo et al., 2018] and [Gazafroudi et al., 2018]. 92
5.2 The 33-bus test system and aggregators [Zhang et al., 2018], [Prieto-Castrillo et al., 2018], [Mithulananthan et al., 2016] and [Gazafroudi et al., 2018]. 95
5.3 Impact of flexibility behavior on the expected energy traded between the DSO and the RTEM [Gazafroudi et al., 2018]. 99
5.4 Agents and real-time energy transaction framework of the distribution network [Zhang et al., 2018] and [Prieto-Castrillo et al., 2018]. 100
5.5 Real-time energy flexibility transaction flows through end-users, aggregators, the DSO, and the RTEM in the monopolistic approach from perspective of end-users. 107
5.6 Traded energy (a) electricity price (b), and z_{kt} (c) between aggregator 2 and the DSO in $C2$ and $C3$ in monopolistic approach. 107
5.7 Real-time energy flexibility transaction flows through end-users, aggregators, the DSO, and the RTEM in the monopolistic approach from perspective of aggregators. 108

5.8 Game-based interaction to transact energy between aggregators and the DSO. 110
5.9 Impact of flexibility scenarios on real-time energy transaction flows through end-users, aggregators, the DSO, and the RTEM based on the proposed iterative algorithm. 111
5.10 Real-time energy exchanged between the DSO and the RTEM in $A2$ and $A3$. 112
5.11 Energy flexibility (kWh) of end-users $j3$ (in region of aggregator 1), $j15$ (in region of aggregator 2), and $j29$ (in region of aggregator 3) in $A2$ and $A3$. Red and green colours represent negative and positive flexibilities, respectively. 112
5.12 Game-based interaction to transact energy between aggregators and the DSO. 114
5.13 Real-time energy flexibility transaction flows through end-users, aggregators, the DSO, and the RTEM in the game-based interaction between aggregators and aggregators and the DSO. 115
5.14 Real-time energy flexibility transaction flows through end-users, aggregators, the DSO, and the RTEM in the game-based interaction between aggregators and end-users and the DSO. 115
5.15 Real-time energy exchanged between the DSO and the RTEM in $A2$ and $A3$ (a), in $C1$ and $C3$ (b) in game-based iterative algorithms. 116

6.1 Schematic overview of proposed energy flexibility management model [Gazafroudi et al., 2019a]. 121
6.2 General structure for real-time energy transaction considering EVs mobility in the distribution network [Gazafroudi et al., 2019a]. 121
6.3 Decentralized decision-making framework for energy flexibility management problem by end-users in Strategy-I [Gazafroudi et al., 2019a]. 125
6.4 Two-stage sequential decision-making framework to manage energy flexibility and charging state of EVs in Strategy-II [Gazafroudi et al., 2019a]. 126
6.5 Centralized decision-making framework to manage energy flexibility and charging state of EVs in Strategy-III [Gazafroudi et al., 2019a]. 127
6.6 A modified 33-bus test system with corresponding aggregators and PEVs owners [Gazafroudi et al., 2019a]. 128
6.7 24-hour location of PEVs in the 33-bus test system based on their expected mobility patterns after scenario reduction [Gazafroudi et al., 2019a]. 130
6.8 Total Energy traded between real-time electricity market and aggregators with and without flexibility of end-users [Gazafroudi et al., 2019a]. 133
6.9 Real-time energy flexibility provided by end-users in aggregators-based decision-making in Strategy-I considering shiftable load constraint [Gazafroudi et al., 2019a]. 135
6.10 Real-time energy flexibility provided by end-users in aggregators-based decision-making in Strategy-I considering CA-based constraint [Gazafroudi et al., 2019a]. 136

6.11 Real-time energy flexibility provided by end-users in end-users-based decision-making in Strategy-I considering shiftable load constraint [Gazafroudi et al., 2019a]. 136
6.12 Total Energy traded between real-time electricity market and aggregators in aggregators-based decision-making in Strategy-I considering shiftable load and SCA-based constraints [Gazafroudi et al., 2019a]. 137

List of Tables

3.1 Predicted data for uncertain variables [Shokri Gazafroudi et al., 2017]. . . 35
3.2 Price data of the system [Shokri Gazafroudi et al., 2017]. 36
3.3 VOLL and spillage costs [Shokri Gazafroudi et al., 2017]. 36
3.4 Impact of uncertainty on the EC [Shokri Gazafroudi et al., 2017]. 36
3.5 Predicted data of uncertain variables [Gazafroudi et al., 2017b]. 39
3.6 ToU price data of the system [Gazafroudi et al., 2017b]. 47
3.7 The VOLL and spillage costs [Gazafroudi et al., 2017b]. 47
3.8 Impact of demand response program on the amount of expected profit of the system and sold/bought electrical energy to/from the local electricity market [Gazafroudi et al., 2017b]. 50
3.9 Impact of uncertainty modeling on day-ahead, real-time, and total expected profits under optimistic case [Gazafroudi et al., 2017b]. 51
3.10 Impact of uncertainty modeling on day-ahead, real-time, and total expected profits under conservative case [Gazafroudi et al., 2017b]. 51

4.1 Data of the battery [Gazafroudi et al., 2019c]. 74
4.2 Data of the space heater [Gazafroudi et al., 2019c]. 74
4.3 Data of the storage water heater [Gazafroudi et al., 2019c]. 74
4.4 Data of the pool pump [Gazafroudi et al., 2019c]. 74
4.5 Day-ahead predicted energy consumption of the home and predicted load of the must-run services in real-time [Gazafroudi et al., 2019c]. 75
4.6 Central forecasting and interval forecasting error of the market price and the PV energy output in the day-ahead stage [Gazafroudi et al., 2019c]. . 76
4.7 Scenarios of the market price in the real-time stage [Gazafroudi et al., 2019c]. 77
4.8 Scenarios of the PV energy output in the real-time stage [Gazafroudi et al., 2019c]. 77
4.9 Scenario Probabilities in the real-time stage [Gazafroudi et al., 2019c]. . . 78
4.10 Total expected profit of the residential energy management problem considering optimal and non-optimal strategies in the worst scenario (α_{pv} equals 0 and α_{price} equals 1) [Gazafroudi et al., 2019c]. 87

5.1 Price of energy traded between end-users and aggregators [Zhang et al., 2018], [Prieto-Castrillo et al., 2018] and [Gazafroudi et al., 2018]. 96
5.2 The basic $VOLL$ [Gazafroudi et al., 2018]. 97
5.3 The impact of line uncertainty [Gazafroudi et al., 2018]. 98
5.4 Impact of the end-users' flexible behavior [Gazafroudi et al., 2018]. 98
5.5 Prices of energy traded between consumers and aggregators and real-time energy price [Zhang et al., 2018] and [Prieto-Castrillo et al., 2018]. 106

5.6 Flexibility scenarios. 106
5.7 Total expected costs for end-users, aggregators, and the DSO in the monopolistic approach. 107
5.8 Total expected costs for aggregators and the DSO based on the iterative algorithm. 111
5.9 Total expected costs for end-users, aggregators, and the DSO in the game-based approach. 114

6.1 Prices of traded energy between end-users and aggregators [Zhang et al., 2018], [Prieto-Castrillo et al., 2018] and [Gazafroudi et al., 2019a]. 129
6.2 PEVs and their corresponding owners [Gazafroudi et al., 2019a]. 129
6.3 PEVs and their corresponding mobility path scenarios [Gazafroudi et al., 2019a]. 131
6.4 Total expected costs of decision-makers in proposed strategies [Gazafroudi et al., 2019a]. 131
6.5 Total expected costs of aggregators in proposed strategies [Gazafroudi et al., 2019a]. 131
6.6 Expected costs of aggregators and end-users in proposed strategies [Gazafroudi et al., 2019a]. 132
6.7 Impact of energy flexibility on the total expected cost of aggregators [Gazafroudi et al., 2019a]. 133
6.8 Impact of energy flexibility on expected costs of aggregators and end-users in Strategy-I based on aggregators' independent decisions [Gazafroudi et al., 2019a]. 134
6.9 Impact of agent-based decision-making on total expected costs of end-users and aggregators considering shiftable constraint in Strategy-I [Gazafroudi et al., 2019a]. 134

List of Acronyms

AC	**A**lternating **C**urrent
AGG	**AGG**regators
CI	**C**omputational **I**ntelligence
DA	**D**ay-**A**head
DER	**D**istributed **E**nergy **R**esource
DF	**D**emand **F**actor
DMS	**D**ecision **M**aker **S**ystem
DR	**D**emand **R**esponse
DRP	**D**emand **R**esponse **P**rogram
DSO	**D**istribution **S**ystem **O**perator
EC	**E**xpected **C**ost
EL	**E**lectrical **L**oad
EM	**E**lectricity **M**arket
EMS	**E**nergy **M**anagement **S**ystem
EP	**E**xpected **P**rofit
ES	**E**nergy **S**cheduler
ESS	**E**nergy **S**torage **S**ystem
EU	**E**nd-**U**ser
EV	**E**lectric **V**ehicle
EVC	**E**lectric **V**ehicle **C**oordinator
GAMS	**G**eneral **A**lgebraic **M**odeling **S**ystem
HEM	**H**ome **E**nergy **M**anagement
HEMP	**H**ome **E**nergy **M**anagement **P**roblem
HEMS	**H**ome **E**nergy **M**anagement **S**ystem
IP	**I**nformation **P**rovider

LC	**L**ocal **C**oordinator
LEM	**L**ocal **E**lectricity **M**arket
MAEMS	**M**ulti-**A**gent **E**nergy **M**anagement **S**ystem
MAS	**M**ulti-**A**gent **S**ystem
MASCEM	**M**ulti-**A**gent **S**imulator of **C**ompetitive **E**lectricity **M**arkets
MASGriP	**M**ulti-**A**gent **S**mart Home **G**rid **S**imulation **P**latform
MASHES	**M**ulti-**A**gent **S**mart **H**ome **E**nergy **S**ystem
MIB	**M**anagement **I**nformation **B**ase
MILP	**M**ixed **I**nteger **L**inear **P**rogramming
MINLP	**M**ixed **I**nteger **N**on-**L**inear **P**rogramming
MSPB	**M**odified **S**tochastic **P**redicted **B**ands
MRS	**M**ust-**R**un **S**ervices
OC	**O**ptimistic **C**oefficient
OF	**O**bjective **F**unction
PAC	**P**rediction **A**ccuracy **C**oefficient
PDF	**P**robability **D**ensity **F**unction
PE	**P**rediction **E**ngine
PP	**P**ool **P**ump
PSO	**P**article **S**warm **O**ptimization
PV	**P**hoto**V**oltaic
RT	**R**eal-**T**ime
RTEM	**R**eal-**T**ime **E**lectricity **M**arket
RTLEM	**R**eal-**T**ime **L**ocal **E**lectricity **M**arket
SCA	**S**elf-**C**onsumption **A**ggregated
SG	**S**mart **G**rid
SH	**S**pace **H**eater
SHE	**S**mart **H**om**E**
SHES	**S**mart **H**ome **E**nergy **S**ystem
SOC	**S**tate-**O**f-**C**harge
SPB	**S**tochastic **P**redicted **B**ands
SWH	**S**torage **W**ater **H**eater
ToU	**T**ime **O**f **U**se
VOLL	**V**alue **O**f **L**oss **L**oad

Our love story is a mixed-integer problem.
Your non-linearity makes me infinitive from nothing.

Chapter 1

Introduction
(*introducción*)

VNiVERSiDAD
D SALAMANCA
CAMPUS DE EXCELENCIA INTERNACIONAL

Chapter 1

Introduction (*introducción*)

1.1 Description the problem

The power and energy system has been experiencing a complete change in paradigm due to the worldwide increase in the use of renewable energy sources. The distributed and unpredictable nature of these energy sources has posed new challenges to the traditionally centrally operated sector [Lund, 2014]. Moreover, global energy consumption is increasing, especially the consumption of electricity. European reports from 2010 mention an increase in global consumption in EU-27, where the domestic consumers represent about 29.70% of the total electricity usage [Gazafroudi et al., 2017a].

This shift in paradigm requires new perspectives and approaches capable of tackling the new challenges. One of the most consensual solutions is the so-called Smart Grid (SG) [Borlase, 2016], its success, however, depends on active participation from the consumer side. The SGs improve energy efficiency in power and energy systems through intelligent control and automation technologies. Also, the SG is accounted as an appropriate solution to utilize intermittent energy resource. However, these energy resources create challenges due to the uncertainty of its power generations in the system. Moreover, the restructuring in power systems causes to appear new agents in the power system. Different technologies have been used in the SGs to deal with these challenges e.g. Multi-Agent Systems (MASs). The MAS is defined as a set of independent units that can make decisions and interact with each other [Roche et al., 2010].

Multi-Agent Energy Management Systems (MAEMSs) can be classified according to different characteristics, such as goal, scale, strategy and software utilized in the system. Goal of the MAEMSs is one of important characteristics of Energy Management systems (EMSs) which is defined as the main purpose of the system to present an objective function of its corresponding energy management problem. The Goal of the MAEMS indicates its desired strategy. The Scale of the EMS is another characteristic that represents the system's level, it consists of the system-wide, micro-grid, local, and the building. According to the scale of the system, the complexity of the energy management problem can be changed and different tools can be used to solve it. The strategy is another important characteristic of the EMS which is defined as a decision-making path which allows to obtain the optimum amount of the objective function. Centralized, decentralized, and hierarchical are the most common strategies in the EMSs. In MASs, a platform is required to provide interaction and communication between autonomous agents in the systems. There are different software and platforms -e.g. JADE, MATLAB, etc.- that are chosen on the basis of the goal, scale, and strategy of the proposed MAEMS. Hence, MASs are capable of creating an environment for players-e.g. electrical generation, consumers, system operators and aggregators- in which they can act autonomously and communicate with each other [Brazier et al., 2015].

In this environment, the consumer is no longer a static load to be assumed by the system, rather, it is an active player, who can both purchase and sell the generated energy locally [Kok et al., 2009]. Thereby, Home Energy Management (HEM) is becoming crucial, and should include new characteristics and advanced functions, namely, the management of Electric Vehicles (EVs), the interface with external operators. In this sense, management systems are defined as smart home systems. The smart home represents a house with network communication between all devices allowing for the control, monitoring and remote access of the management system [Wi et al., 2013]. Several works view smart home as house management systems designed to effectively manage consumption, storage, distributed generation and participation in Demand Response (DR) programs [Faria and Vale, 2011]. Smart homes will function as prosumers in the SGs. A smart home electricity system includes the electrical loads that consume electricity, Distributed Energy Resources (DERs) that produce electrical energy, and Energy Storage Systems (ESSs) that can store electrical energy. Besides, there is an Energy Scheduler (ES) in the Smart Home Energy System (SHES) that schedules the production/consumption of energy in all of the system's agents. Additionally, the SHES should be able to connect the power grid. Hence, they will be able to sell/buy electrical energy to/from the Local Electricity Market (LEM).

In addition, over the last decade, Electricity Markets (EMs) have created competitive environments for complex power systems. The fast growth of DERs in the bottom-layer of the power systems has made it challenging to maintain the reliability and stability of the system. Unfortunately, conventional energy management strategies capable of solving these concerns centrally due to the generation volatility of DERs. Nonetheless, this need is percieved by the demand-side of the power systems, such as the distribution or retail participants who want to get a real and fair price in the distribution network.

Furthermore, current centralized EMs are not complete enough, and cannot provide dynamic ancillary services that follow flexible consumers behavior due to Demand Response Programs (DRPs). Also, the DERs cannot indicate their potentialities entirely because of the rules of the EMs. As a result, centralized markets are being replaced with decentralized and local electricity markets. In this way, the consumers and the local market interact through price-based signals.

1.2 Literature review

Various researches have presented numerous methods for the energy management of the power system, and following different goals, scales, strategies, and software. For instance in [Bui et al., 2018], the scale is considered to be the power grid, and the goal is to minimize the operating cost. Besides, the hierarchical and decentralized strategy is presented based on MAS, and CPLEX and JADE are used to implement the problem in a real system. Also, multi-micro grid system has been operated cooperatively in [Bui et al., 2018]. In [Vrba et al., 2014], the authors have reviewed the agent-based technologies of large-scale energy systems and the SG projects. A hierarchical central approach of micro-grids has been presented in [Cintuglu et al., 2018]. The primary control is done in level of distributed energy resources, while the secondary control is done in the level of the micro-grid by an automatic generation control to adjust frequency and voltage. Also, the tertiary control is applied to provide the ancillary services for load regulation in the host-grid level. In [Miao and Fan, 2018], a new method has been presented to solve Alternating Current (AC) optimal power flow problem in the multi-agent decision-making framework. In [Degefa et al., 2016], the multi-objective problem has been defined to minimize energy costs and estimate state based on bottom-up approach. In [Loia and Vaccaro, 2014], the economic dispatch problem has been solved by decentralized and self-organizing strategies. The proposed strategy of [Loia and Vaccaro, 2014] was non-hierarchical, and the operation costs have been minimized locally and then applied to the system globally. In [Pereira et al., 2015], an energy management system has been presented based on the integration of smart meters. The hierarchical method for the management of the energy has been proposed in [Pereira et al., 2015]. In [Wang and Paranjape, 2017], a MAS has been demonstrated in the scale of the distribution network, while agents consist of home agents and retailer agents. In [Wang and Paranjape, 2017], the purpose of the authors was to minimize the payment cost of the electricity. In [Venayagamoorthy et al., 2016], an intelligent method has been demonstrated to manage energy dynamically in the micro-grid. The proposed method of [Venayagamoorthy et al., 2016] has been defined to optimal or sub-optimal. Besides, providing the critical loads continuously is the purpose of [Venayagamoorthy et al., 2016]. In the model of [Venayagamoorthy et al., 2016], the intelligent dynamic energy management system is responsible to send dispatchable control signals of energy. Moreover, forward-looking network is responsible to evaluate the dispatched control signals. The main aims of [Venayagamoorthy et al., 2016] are to maximize the reliability, utilization of renewable energies, and consumers' welfare. Moreover, the operating cost has not been considered in the decision-making problem of [Venayagamoorthy et al., 2016]. In [Pereira et al., 2015], an energy management system has been presented based on integration of smart meters. The authors have proposed the hierarchical method to manage the energy in [Pereira et al., 2015]. In [Venayagamoorthy et al., 2016], an intelligent method has been demonstrated to manage energy dynamically in the MG. The proposed method of [Venayagamoorthy et al., 2016] has been defined as either optimal or sub-optimal. Besides, providing the critical loads continuously is the purpose of [Venayagamoorthy et al., 2016]. In [Hurtado et al., 2015], the agent-based approach to optimize the operation costs of SG and HEMS has been presented. Also, the Partical Swarm Optimization (PSO) method has been used to maximize welfare and energy efficiency in the proposed model of [Hurtado et al., 2015]. In [Manic et al., 2016], authors has discussed the necessities of using the Computational Intelligence (CI) in HEMSs. The CI has been applied to three parts of the HEMS in [Manic et al., 2016]. These parts consist of the prediction of building required power, forecasting the purchasing electrical load from the power grid and the controllers. Minimizing the building energy cost is the goal of the controllers. Also, PSO has been utilized for optimization problem of HEMS. In [Li et al., 2015], the HEMS has been defined as an intelligent MAS. In [Zhang et al., 2016], an adaptive and integrated method has been presented for the DRP and the HEMS based on real-life conditions. In [Zhao et al., 2015], a method is proposed to apply the local energy resources optimally through minimizing the loss of energy. In [Ma et al., 2016], the scheduling problem of HEM has been solved considering the DRP. The objective function of [Ma et al., 2016] was the trade-off between the purchasing cost of electricity and dissatisfaction of the consumers. In [Kahrobaee et al., 2013], each smart home has been considered as an autonomous agent that can buy, sell, and store electricity. Furthermore, the uncertainty is modeled through generating the random data and functions in [Kahrobaee et al., 2013]. In [Kahrobaee et al., 2013], the HEM problem in connection with transactive energy nodes has been discussed. Moreover, co-simulation of smart homes and transactive energy market has been studied in [Kahrobaee et al., 2013].

Moreover, there are several studies in the literature to work on energy transaction approach in distribution power grids. Ref. [Pratt et al., 2016] presented the energy transaction nodes that connect buildings and the local electricity market. Authors in [Jokic et al., 2009] proposed a price-based method for energy management. In

[Sajjadi et al., 2016], [Shafie-khah and Catalão, 2015] and [Nunna and Srinivasan, 2017], a multi agent-based transactive energy market is designed to decentralize decisions. Ref. [Warrington et al., 2010] proposed a real-time price-based method in which agents solve their corresponding energy management problems locally and send their optimum decisions to the central price controller. In addition, there are several works in the literature which address the interaction between agents in the distribution network based on the DRP. In [Chai et al., 2014], the DRP has been performed considering several suppliers and consumers. In [Deng et al., 2015], a distributed framework has been presented based on a dual decomposition technique to regulate the demand of end-users. In [Disfani et al., 2015], a distributed model is described to determine optimal power flow in radial networks. Ref. [Bahrami et al., 2018] proposed the centralized energy trading as a bi-level model. In [Bahrami et al., 2018], the DR framework has been presented decentralized. The local electricity market has been defined in Mustafa et al. [2016] that market agents transact electricity to each other independently. In [Park et al., 2016], authors designed a trading mechanism among micro-grids. Ref. [Zhang et al., 2018] proposed a hierarchical framework for energy trading in the distribution networks. In [Prieto-Castrillo et al., 2018], the energy management problem has been addressed among the players in the power distribution system where the authors introduced the Ising-based model of energy flexibility provided by end-users. In [Gazafroudi et al., 2019a] and [Gazafroudi et al., 2018], authors presented a decentralized approach from the perspective of end-users and other relevant decision makers for the management of energy flexibility according to the desired level of reliability in the distribution network.

1.3 Methodology

Systems based on multi-agents for local electricity trading and home energy management systems allow to model different devices in houses and distribution networks through autonomous agents. In this way, the modeling of distributed energy resources that can be connected to the house are also considered. Through multi-agent modeling, it is possible to solve different scenarios taking into account the optimization of the costs related to energy consumption in General Algebraic Modeling System (GAMS) [Soroudi, 2017]. To this end, this MAS includes negotiation methods that allow various devices to reach consensus when it is necessary to reduce the overall energy consumption of a system in order to respond to the changes in energy prices, e.g. times of the day when the tariff is the highest, and to variations in generation due to their variable nature because of climatic conditions. Besides, the task of the energy scheduler, as one of the agents in the system, is to make optimum decisions in the system. An optimum decision depends on the objective(s) of the system. In this case, energy scheduler faces a discrete optimization problem under the uncertainty of the outputs that are provided by the predictor system. This uncertainty causes some problems, such as higher operating costs of the system and computational overload. There are different methods to model the uncertainty in the optimization problems, such as stochastic programming, interval optimization, robust optimization, etc. In this Ph.D. work, stochastic predicted bands, modified stochastic predicted bands, improved stochastic bands, and hybrid stochastic-interval bands methods are defined and used to model the uncertainty in the system.

Moreover, this work is a combination of energy management and transportation problems. Hence, novel intelligent energy management strategies and adequate electricity trading models will be presented in this work to enable demand response (DR) for real-time operation of the smart grid considering EVs in the system. Although the main task of the EV is to meet the transportation needs of users, the EV can be modeled as an energy storage system in the home energy management system. Therefore, modeling the EV can improve the efficiency of energy management for home systems. One of the challenges regarding the modeling of the EV is the uncertainty caused by EV mobility. In other words, the time that the EV leaves and returns to the home are not deterministic, so it is a big problem for the home energy management system to model the uncertainty of the EV. Hence, a complex problem emerges which involves both, energy management and transportation problems.

1.4 Structure of the thesis

The rest of this thesis is organized as follows:

- **Chapter 2.** In this chapter, we propose a virtual organization architecture for agents in the power distribution system to transact energy among agents of the distribution network. Also, an organization-based multi agent architecture for the smart home energy system is proposed in this chapter.
- **Chapter 3.** The home energy management problem is presented in this chapter. We also define two novel optimization methods (an interval method and a hybrid interval-stochastic optimization method) to model uncertainty in the domestic system.
- **Chapter 4.** This chapter presents an optimal offering model to derive optimal offering and bidding curves for the home energy management systems. In this way, each prosumer is able to act as a price-taker agent and send its optimal offering and bidding curves to the local market or participate in peer-to-peer energy transactions with other agents based on the uncertainties of the system.

- **Chapter 5.** We propose different strategies and structures to trade electricity in power distribution systems based on decentralized, monopolistic, and game-based approaches in this chapter. Besides, different types of flexible behavior of end-users and aggregators are modelled and discussed in this chapter.

- **Chapter 6.** This chapter discusses the impact of stochastic EVs mobility on the traded electricity and energy flexibility provided by the end-users in the power distribution grid. Hence, a stochastic energy management problem is defined which models the uncertainty of EV mobility. Furthermore, we propose different strategies for the management of energy flexibility and operation of EVs through end-users and the central coordinator in the distribution network.

- **Chapter 7.** This chapter concludes the thesis by presenting the main contributions and findings of this research work, lessons learned and some suggestions that can improve this line of research in the future.

Chapter 2

Multi-agent architecture for local electricity trading
(*arquitectura multi-agente para el comercio local de electricidad*)

VNiVERSiDAD
D SALAMANCA
CAMPUS DE EXCELENCIA INTERNACIONAL

Chapter 2

Multi-agent architecture for local electricity trading (*arquitectura multi-agente para el comercio local de electricidad*)

2.1 Introduction

According to infrastructure which is provided by smart grids, the DRPs actives players in the power distribution system. Hence, end-users wish to participate as bidirectional energy customers, prosumers, in the distribution network [Gazafroudi et al., 2017a]. Therefore, new market structures are needed to provide energy based on decentralized approaches. Here, there are several studies in the literature to work on energy transaction approach in power distribution grids.

In this chapter, a virtual organization architecture for agents in the power distribution system is proposed to transact energy among agents of the distribution network (end-users, aggregators and the Distribution System Operator (DSO)). Thus, energy is transacted based on a bottom-up hierarchical structure from end-users to aggregators, from aggregator to the DSO, and from the DSO to the wholesale electricity market, respectively. Moreover, Smart Home Energy System (SHES) is defined as a class of organization-based multi-agent system (MASHES) which includes different agents with corresponding tasks in the system.

The rest of this chapter is organized as follows. In Section 2.2, agents and their corresponding virtual organizations are defined. Section 2.3 describes organization of agents for the smart home energy system. Finally, this chapter is concluded in Section 2.4.

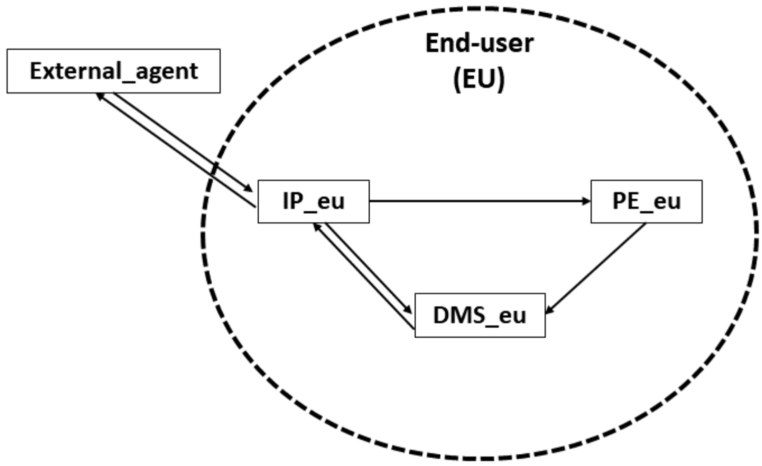

FIG. 2.1: Organization of end-user agents [Shokri Gazafroudi et al., 2019].

2.2 Virtual organization of agents in the power distribution grid

After restructuring in power systems, different players emerged in the system. In this work, the proposed agent architecture in the distribution network is described. Thus, different organizations of agents are defined in the system which consist of end-users, aggregators and the DSO. In the following, each of these agents and their interconnections are described.

2.2.1 End-Users (EU)

End-users are agents in the bottom layer of the power distribution system which act as consumers, producers, or prosumers in the system. In this work, a bottom-up approach is presented to trade energy through end-users, aggregators, the DSO and the wholesale market. Thus, end-users manage their energy production/consumption on the basis of their interactions with the aggregators and the DSO. Also, the end-users have several agents (e.g. Information Provider (IP), Prediction Engine (PE), and Decision Maker System (DMS)) which make up an organization of agents. Each of these agents are described below:

- *Information Provider (IP)* records information of all other agents as well as the environmental conditions. Also, the IP is responsible for sending/receiving information to/from the external agents that correspond to its organization, as shown in Fig. 2.1.

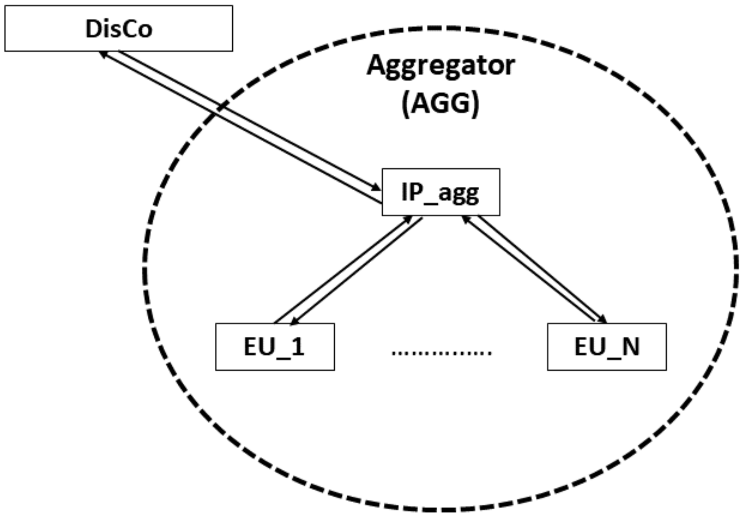

Fig. 2.2: Organization of aggregator agents [Shokri Gazafroudi et al., 2019].

- *Prediction Engine (PE)* forecasts uncertain variables (e.g. the energy generated from distributed energy resources, electrical consumption, electricity price, etc.) of end-users based on information provided by the IP. In this way, the values predicted by the PE are the inputs of the DMS.

- *Decision making system (DMS)* is in charge of making optimum decisions for its corresponding organization (e.g. end-user, aggregator, and the DSO). On the one hand, the inputs of the DMS received from the IP and the PE. On the other hand, the outputs of the DMS are sent to the IP which exchanges them with the external agents from the corresponding organization. Fig. 2.1 shows interactions between agents in the end-user's organization.

2.2.2 Aggregators (AGG)

Aggregators are one type of reseller players in the restructuring power system. In this work, aggregators are defined as agents which are in charge of trading energy with end-users in their corresponding regions. Also, they are able to transact energy with the DSO in this model. In the proposed agent-based architecture, aggregators have several agents such as the IP and the EU for creating agent organizations in each region of the distribution network. Also, according to Fig. 2.2, each aggregator transacts data with the DSO (as an external agent of its organization) through its IP agent.

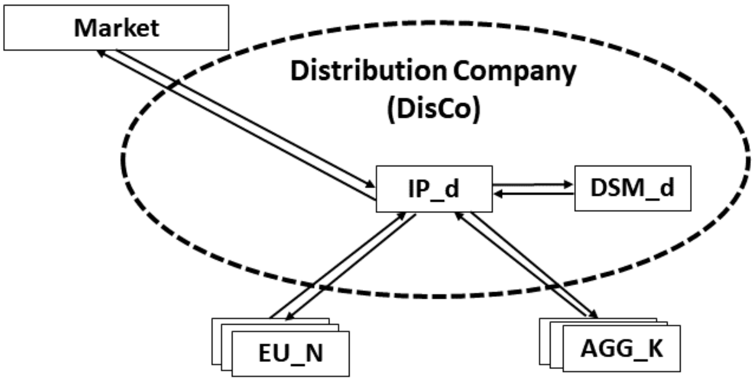

Fig. 2.3: Organization of the DisCo agents [Shokri Gazafroudi et al., 2019].

2.2.3 Distribution System Operator (DSO)

The DSO is the only agent that trades energy with the wholesale market. Moreover, the DSO has the IP and the DMS agents for data exchange with the aggregators and end-users as external agents and makes optimum decisions, respectively, as shown in Fig. 2.3.

2.3 Agents Organization for the Smart Home

The SHES consists of different organization-based agents that each of them has different tasks in the system. In this section, all agents of the SHES will be introduced and their task will be described. Moreover, the physical system of the organization-based MASHES is seen in Fig. 2.4. MASHES includes two layers. First layer is the electricity system which is displayed by black lines. However, second layer is the communication system that is shown by blue lines.

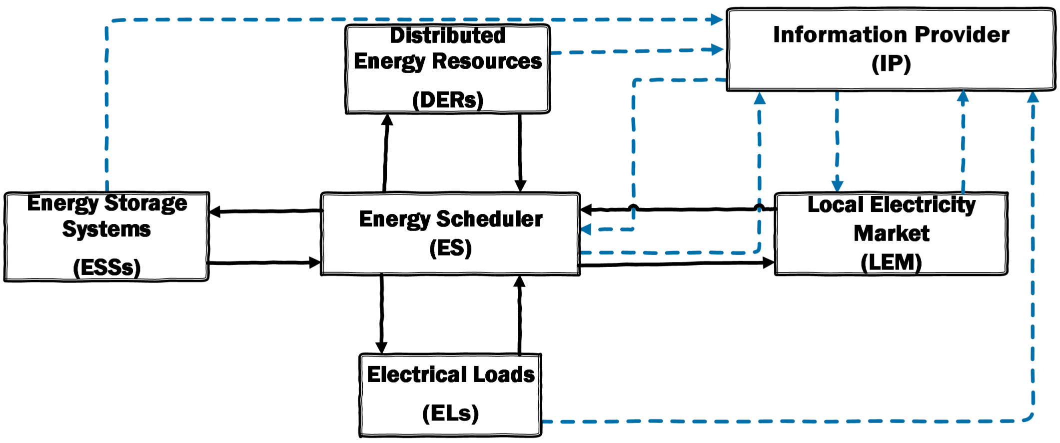

Fig. 2.4: The MASHES physical system [Gazafroudi et al., 2017a].

Electrical Loads (ELs)

The ELs are a group of agents that consume electrical energy in the SHES. Generally, the ELs are classified into different types of loads such as shiftable, controllable, Must-Run Services (MRS), etc. Therefore, the ELs can be considered as an organization basis for different agent types in the MASHES.

Distributed Energy Resources (DERs)

The DERs are a set of agents that are responsible for the generation of electrical energy in a smart home. The DERs are intermittent energy resources, so they inject uncertainty in the system. However, increasing the prediction accuracy of these stochastic variables can decrease the corresponding uncertainty in the system.

Energy Storage Systems (ESSs)

The ESSs are the agents in the MASHES that can store electrical energy such as EVs and batteries. Batteries can help to smooth the electrical demand profile. On the other hand, even though the main purpose of EVs is to provide clean transportation, they can assist the MASHES as the ESSs too.

Information Provider (IP)

The IP is an agent in the SHES that is in charge of providing real-time and historical data information. It senses and records information from all the agents as well as environmental conditions.

Local Electricity Market (LEM)

The LEM is defined as a set of external agents of a building. In this work, external agents consist of a retailer (the energy supplier) and a DR aggregator. Smart homes should be able to connect to the LEM to trade electricity. Hence, electricity price and power are two variables that are exchanged between smart homes and the LEM.

Energy Scheduler (ES)

The ES is a virtual organization of agents who plays as a system operator in the MASHES. The proposed energy scheduling method is based on day-ahead energy management approach. The ES consists of two agents: the Prediction Engine (PE) and the Energy Management System (EMS). The tasks of both are described below:

Prediction Engine (PE)

The PE provides accurate prediction of all stochastic variables of the system (e.g. wind speed, solar radiation, weather temperature, electricity price and electrical unshiftable loads) for EMS. Hence, the outputs of this agent will be the inputs of the EMS. As the DERs utilized in the SHES are non-dispatchable resources, the forecasting of its power output will be very important for the EMS. Hence, accurate forecasting of PE can assist the EMS to make optimum decisions.

Energy Management System (EMS)

The task of the EMS is to make optimum decisions in the MASHES. An optimum decision depends on the objective(s) of the smart home owner. Maximizing the profit of the SHES is the proposed Objective Function (OF) of this chapter. Therefore, after the OF is defined in the system, this agent should make an optimum decision. In this case, EMS faces a discrete optimization problem under uncertainty of the PE's outputs. This uncertainty causes some problems for the EMS, such as increasing the operating costs of the MASHES and computational overload.

The MAS for the SHES allows to model different devices in a house through autonomous agents discussed before. In addition to the representation of the different devices through software agents, the modeling of possible existing generation sources that can be connected to the house are also considered. Through this multi-agent modeling, it is possible to simulate different scenarios taking into account the optimization of the costs related to energy consumption. To this end, this MAS includes negotiation methods that allow various devices to reach consensus when it is necessary to reduce the overall energy consumption of a house in order to respond to the changes in energy prices, e.g. times of the day when the tariff is the highest, and to variations in generation due to their variable nature because of climatic conditions. The architecture of the agent society can be seen in Fig. 2.5. The organization-based MAS is composed by:

- *LEM*: Two external agent sets the retailer-the energy supplier- and the DR aggregator.
- *IP*: In our architecture, the Main Agent is created initially when the simulation is performed. It is responsible for creating the remainder agents. Another agent

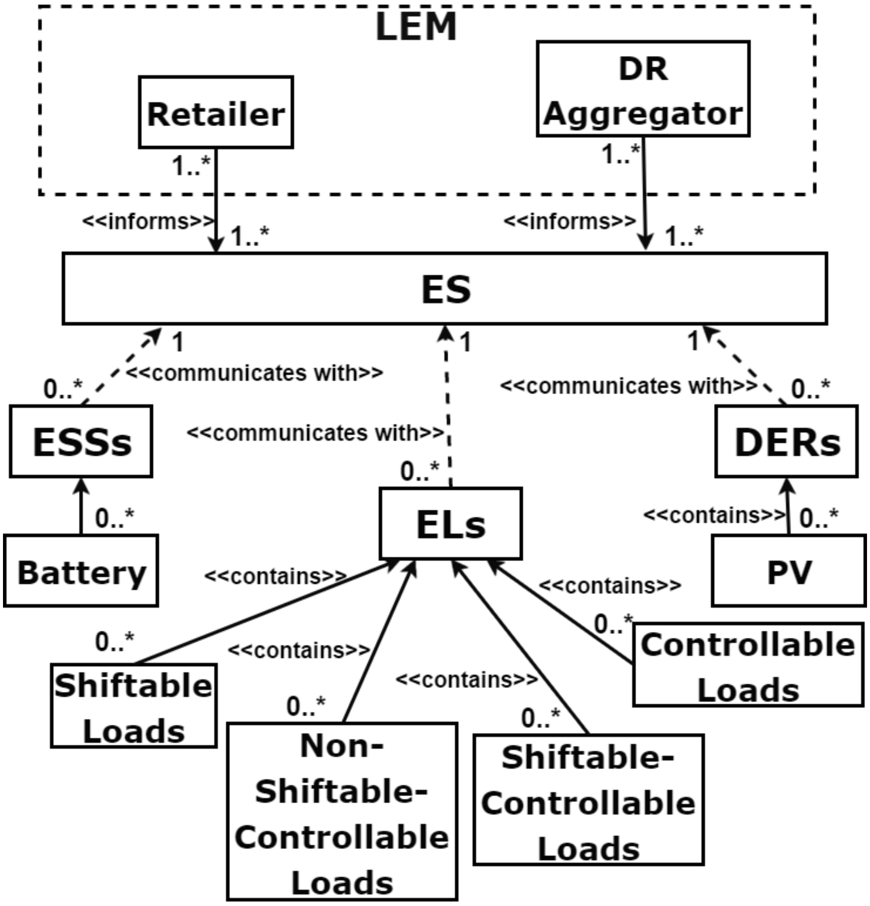

Fig. 2.5: The MAS architecture for the SHES [Gazafroudi et al., 2017a].

in the IP is called Management Information Base (MIB) that is responsible to interconnect agents.

- *ES*: The ES-agent is included in this group of agents because it is responsible for connecting all the agents in a house. In addition, it analyses and predicts data. Also, the energy management is done by the ES.

- *DERs*: This agent is responsible for renewable energy resources, e.g. as wind micro-turbines and PhotoVoltaic (PV) panels.

- *ESSs*: ESSs is a set of agents, that represent the energy storage units, e.g. battery, EVs.

- *ELs*: ELs is an organization of different agents that only consume electrical energy but whose type is different. Shiftable loads are responsible for all units that may have changeable consumption. Shiftable-controllable loads are another type of agents that are responsible for all units which can be controlled and changed in their turn. Controllable loads are the type of agents that are responsible for all units in which only consumption amount can very each time, but not to change their consumption in another time. Non-shiftable-controllable are responsible for all units that have not been included in any of the previously defined agents, i.e. all units that can neither control nor vary their power consumption in time.

In the agents representing the smart home, only the Manager agent is unique for each smart home and is responsible for the energy management of the respective house.

This proposed organization-based MAS architecture is also capable of interacting with the Multi-Agent Smart Grid Simulation Platform (MASGriP) [Oliveira et al., 2012], which is a simulation platform that simulates, manages and controls the most relevant players acting in a smart grid and micro-grid environment. Moreover, the Multi-Agent Simulator of Competitive Electricity Markets (MASCEM) is yet another MAS that enables the simulation of electricity markets [Santos et al., 2016]. Interaction with this system allows for the simulation of the participation of different players, even small players like houses, in distinct types of electricity market negotiations. The interaction between these different MAS is achieved through the use of specifically conceived ontologies, which are used to set a communication language between agents of the different systems, thus allowing them to understand each other and communicate effectively [Santos et al., 2015].

2.4 Conclusion

This chapter has proposed a virtual organization architecture for energy trade between the agents (end-users, aggregators and the DSO) of the distribution network. Also, each of these agents and their interconnections have been described. Then, the organization-based multi-agent system of the smart home electricity system as an example of the end-users has been introduced. In Chapter 3, the home energy management problem is described considering its objective function and the formulation for different agents of the smart home energy system. Moreover, Chapter 5 presents the formulation for end-users, aggregators and the distribution system operator in the power distribution network.

Chapter 3

Home energy management system (*sistema de gestión de energía en la hogar*)

VNiVERSiDAD D SALAMANCA

CAMPUS DE EXCELENCIA INTERNACIONAL

Chapter 3

Home energy management system (*sistema de gestión de energía en la hogar*)

3.1 Introduction

Power systems face new challenges due to the increment in DERs. DERs decrease greenhouse gas emissions and costs related to the electricity production [Abrishambaf et al., 2016b]. However, the integration of these intermittent energy resources leads the energy management problems which are caused by the the scale of the energy system [Vale et al., 2013]. In the last decade, new visions and approaches have been leveraged to deal with reliability and uncertainty due to the increment in DERs. One of the most consensual solutions is the so-called smart grid [Borlase, 2016]. In this scope, buildings can purchase and sell the generated energy locally [Kok et al., 2009]. Thus, residential buildings (as one type of buildings) whose devices are linked to the smart grid via communications channels are called smart homes [Pedrasa et al., 2009]. They are known as *prosumers*– i.e. both consumers and producers– and have an important role in the optimization of electrical energy scheduling [Shokri Gazafroudi et al., 2017]. The HEMS, which incorporates automation technologies, is necessary for economic improvement. In this sense, smart homes can control, monitor and manage the system through network communications [Das et al., 2002], [Wi et al., 2013]. Generally, there are two approaches for energy management of the HEMSs. These approaches consists of centralized and decentralized systems. Based on the approach of the system, different structures of controlling and communicating systems are required [Abrishambaf et al., 2016a]. However, there are challenges in the HEMSs consisting of inaccurate energy generation forecasts and demand patterns, and heavy computational burden [Beaudin et al., 2012] and [Fujimoto et al., 2018].

In addition, customers are going to play a key role in the prospective power systems [Hurtado et al., 2015]. This will be possible because power will no longer be generated at centralized facilities, instead, different technologies will be used to generate energy locally, this is called distributed generation. The infrastructure of the smart grid makes this transition possible [Hurtado et al., 2015]. Thus, in the power distribution systems' demand-side players -e.g. smart homes- will manage their own electrical energy according to the real and fair price [Gazafroudi et al., 2017a]. Besides, current electricity markets are not able to satisfy the customers' strategic behavior based on their autonomous decision-makings [Caramanis et al., 2016]. Hence, decentralized electricity markets are capable of adapting to the flexible behavior of electrical customers. In this way, smart homes are active agents and play a critical role in the bottom layer of the power systems. Hence, smart homes need energy management systems in order to make optimum decisions related to the management of energy inside the home, such as the choice of the best strategies when trading energy with other players (e.g. aggregators, retailers, local market operator, other consumers) in the power distribution network. In this way, power distribution networks are defined as complex ecosystems consisting of machines, networks, procedures, operators, and players which are organized hierarchically in the bottom layer of power systems in order to deliver electric power to end-users [Mithulananthan et al., 2016]. Different studies have considered distinct aspects of the HEMSs, e.g. residential electrical appliances [Gazafroudi et al., 2017a], the main purposes of residential scheduling [Shokri Gazafroudi et al., 2017] and [Gazafroudi et al., 2017b], decision-making under uncertainty [Gazafroudi et al., 2017a], the implementation of the HEMSs [Gazafroudi et al., 2017a], and interaction between the HEMSs and other systems in their neighborhood or up-stream grid [Gazafroudi et al., 2017a].

In this chapter, we model the home energy management problem considering the uncertainty of the system. In Section 3.2, a novel interval optimization method is defined to model uncertainty in the home energy management problem. Section 3.3 proposed a predictive dispatch model to manage energy flexibility by a hybrid interval-stochastic method in the HEMS. Finally, this chapter is concluded in Section 3.4.

3.2 Home energy management problem using a novel interval optimization method

In this chapter, a new interval optimization method is proposed for the management of the uncertainty of stochastic variables in the Home Energy Management Problem (HEMP). This new method is called Stochastic Predicted Bands (SPB) and it considers the uncertainty of decision-making variables without knowledge of the Probability Density Function (PDF). Thus, the uncertainty is modelled by bands which are based on prediction of the stochastic variables. Besides, an auxiliary parameter, which is called *Optimistic Coefficient* (OC), is defined to provide flexibility to the decision-maker to be optimistic or conservative.

3.2.1 Proposed interval optimization method

In this section, we introduce the proposed method for modeling stochastic variables in the decision-making problem. There are similarities between the method proposed in this section and other stochastic optimization methods. However, in this approach, presenting the uncertainty is not done by stating the scenarios. Knowing the PDF of decision-making variables is one of the prerequisites of most stochastic scenario-based methods Soroudi and Amraee [2013]. It is clear that the PDFs of stochastic variables are not always available. Besides, stochastic optimization methods are a large computational burden to the systems. Hence, our proposed method considers the uncertainty of the decision-making variables, taking into account the drawbacks of the stochastic optimization methods.

3.2.1.1 Stochastic Predicted Bands (SPB) Method

In this section, the SPB method is defined to model the uncertainty. It consists of four steps which are described below:

Step 1

This model consists of two stages and it is not a bi-level optimization problem. The first stage is called the shadow stage because it is not actually executed. Also, the uncertainty of variables is not considered in the first stage. The corresponding variables in the first stage are also called shadow variables. The second stage is called the real-time stage where the uncertainty of variables is considered, and the associated variables are called real-time variables. The shadow variables play an important role in converging the real-time variables to their optimum decisions when their uncertainties converge to zero. Hence, the shadow variables should be determined in the first step.

Step 2

In this method, the uncertainty of variables is considered based on their predicted amounts. Hence, short-term forecasting of variables is done in the second step. Besides, σ^{UP} and σ^{DN} are the parameters that are defined to state the amounts of upper and lower variances of the predicted variable in comparison to its actual amount, respectively.

Step 3

In this step, the difference between the shadow amount of variables, E_t^S, and their predicted amount in each time, E_t^P is determined as represented in (3.1). Also, a simple flowchart of the SPB method is illustrated in Fig. 3.1.

$$D_t = E_t^S - E_t^P, t. \tag{3.1}$$

Step 4

According to the state of D_t, the real-time decision-making variables, E_t^{RT}, are limited to the max and min bands. If D_t is positive, it means that the scheduling amount is more than the predicted amount. Hence, the real-time amount should be greater than the predicted amount to converge to the amount of the scheduling variable. If D_t is negative, the predicted amount of the variable is more than the scheduling one. Hence, as the real-time variable likes to converge to the amount of its scheduling variable, the real-time variable will be limited to the predicted amount as its maximum band. Therefore, the minimum limitation of the real-time variable will be based on the upper variance of its prediction because the variable's predicted amount is more than its scheduling amount. Eq. (3.2) is defined to clarify the above explanations:

$$\begin{cases} E_t^P \leq E_t^{RT} \leq E_t^P + \sigma^{UP}, D_t \geq 0. \\ E_t^P - \sigma^{DN} \leq E_t^{RT} \leq E_t^P, D_t < 0. \end{cases} \tag{3.2}$$

For instance, it is assumed that the amount of the shadow variable is determined to be equal to 10 at t=4. Also, the predictor system forecasts that the amount of that stochastic variable equals 11 at t=4, while the upper and lower variances are considered to be 0.5 and 0.3, respectively. Hence, D_t is negative in this case, and the real-time

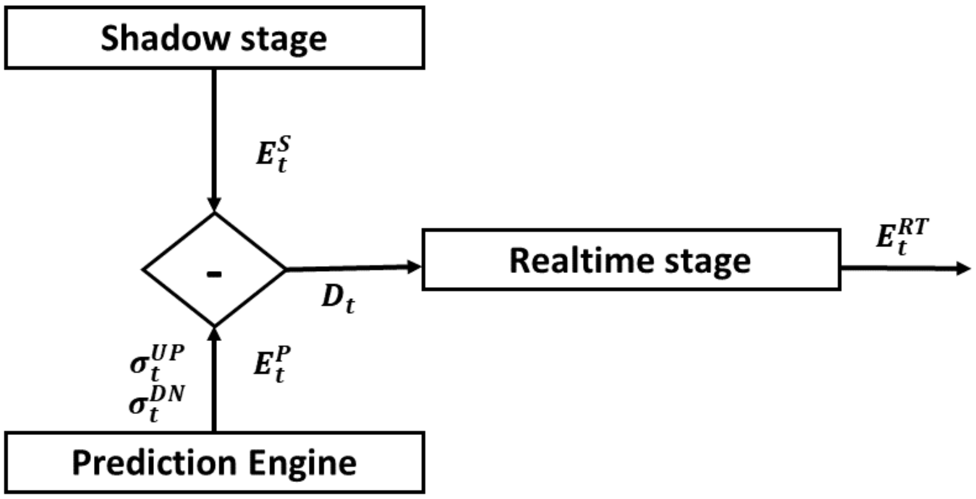

FIG. 3.1: The simple flowchart of the SPB method [Shokri Gazafroudi et al., 2017].

variable should be limited to the bands as follows:

$$D_{t=4} = 10 - 11 = -1.$$
$$11 - 0.3 \leq E_t^{RT} < 11.$$

3.2.1.2 Modified Stochastic Predicted Bands (MSPB) Method

One of the drawbacks of the SPB method is that the uncertainty of the stochastic variables cannot be modeled completely based on the predicted bands. In other words, the variables tend to converge to the maximum and minimum bands based on their amounts in the shadow stage, so the results of the decision-making variables are completely optimistic because they always adapt to the bands to optimize the objective function of the problem. Hence, the stochastic variables stick only to the maximum or minimum bands to optimize the problem.

Here, an auxiliary parameter is defined as a slack parameter that gives the decision-maker the freedom to apply its knowledge regarding the stochastic behavior of the uncertain variable. This parameter is called *optimistic coefficient*, α, and its amount can be between 0 and 1. Consequently, the SPB method considering the *optimistic coefficient* is called Modified Stochastic Predicted Bands (MSPB) optimization method and is represented in (3.3).

$$\begin{cases} E_t^P \alpha + (E_t^P - \sigma_{DN})(1-\alpha) \leq E_t^{RT} \\ \leq (E_t^P + \sigma_{UP})\alpha + E_t^P(1-\alpha), D_t \geq 0. \\ (E_t^P - \sigma_{DN})\alpha + E_t^P(1-\alpha) \leq E_t^{RT} \\ \leq E_t^P \alpha + (E_t^P + \sigma_{UP})(1-\alpha), D_t < 0. \end{cases} \tag{3.3}$$

3.2.2 Home energy management problem

3.2.2.1 Objective function

In this section, a model of power scheduling in a building is presented. The objective is to maximize the revenue of energy services provided in a home energy management system. As seen in (3.4), the objective function includes four parts an d two stage, e.g. shadow and real-time. The first part represents the revenue from selling the electricity to the power grid. The total cost for energy consumption is presented in the second term. The value of energy which is not served is stated in the third term. Finally, the spillage costs of non-dispatchable energies are presented in the last term.

$$\begin{aligned} OF = EC = \sum_{t=1}^{N_t} (&\lambda^{PVB} P_t^{PVB,O,S} + \lambda^W P_t^{W,O,S} \\ &- \lambda^N P_t^{N,S} \\ &+ \lambda^{PVB} P_t^{PVB,O,RT} + \lambda^W P_t^{W,O,RT} + \lambda^{EV} P_t^{EV,O,RT} \\ &- \lambda^N P_t^{N,RT} \\ &- (VOLL^{SH} L_t^{SH,Shed} + VOLL^{SWH} L_t^{SWH,Shed} \\ &+ VOLL^{PP} L_t^{PP,Shed} + VOLL^{MRS} L_t^{MRS,Shed}) \\ &- (V^{W,SP} S_t^W + V^{PVB,SP} S_t^{PVB})) \end{aligned} \tag{3.4}$$

3.2.2.2 First Stage

The uncertainty of decision-making variables is not considered in this stage. Eq. (3.5) establishes the power balance equation of the devices in the smart home. Besides, (3.6) represents the power flow limitation through the distribution line which ended at the building.

$$P_t^{N,S} + P_t^{PVB,I,S} + P_t^{W,I,S} = L_t^{SH,S} + L_t^{SWH,S} + L_t^{PP,S} + L_t^{MRS,S}, \forall t. \tag{3.5}$$

$$-F^{MAX} \leq P_t^{N,S} - (P_t^{PVB,O,S} + P_t^{W,O,S}) \leq F^{max}, \forall t. \tag{3.6}$$

Moreover, there are some limitations corresponding to all appliances. As represented in (3.7)-(3.14), only central prediction of energy produced/consumed by each device is defined in this stage because the uncertainty is not considered in the shadow stage. Also, the components of the HEMS that cause flexibility are not modeled. Hence, the constraints of the energy storage systems and load shedding are not defined in the first stage. This flexibility is needed when the system faces uncertainty, so all the flexible agents are modeled in the second stage.

$$P_t^{PVB,S} = P_t^{PVB,I,S} + P_t^{PVB,O,S}, \forall t. \tag{3.7}$$
$$P_t^{W,S} = P_t^{W,I,S} + P_t^{W,O,S}, \forall t. \tag{3.8}$$
$$P_t^{PVB,S} = P_t^{PVB,P}, \forall t. \tag{3.9}$$
$$P_t^{W,S} = P_t^{W,P}, \forall t. \tag{3.10}$$
$$L_t^{SH,S} = L_t^{SH,P}, \forall t. \tag{3.11}$$
$$L_t^{SWH,S} = L_t^{SWH,P}, \forall t. \tag{3.12}$$
$$L_t^{PP,S} = L_t^{PP,P}, \forall t. \tag{3.13}$$
$$L_t^{MRS,S} = L_t^{MRS,P}, \forall t. \tag{3.14}$$

3.2.2.3 Second Stage

In this stage, the uncertainties of the decision-making variables are considered. In this section, only the uncertainty of the wind and PV power generation is considered, and the uncertainty of the outdoor temperature and the must-run services is ignored for simplicity. Hence, the amounts of these variables are determined on the basis of the outputs of the first stage and the uncertainty in the real-time operation. The power balance equation in the real-time is represented in (3.15). Besides, the power flow limitation through the distribution line in the real-time is described in (3.16).

$$\begin{aligned} &P_t^{N,RT} + P_t^{PVB,I,RT} + P_t^{W,I,RT} + P_t^{EV,I,RT} = L_t^{SH,RT} + L_t^{SWH,RT} + L_t^{PP,RT} \\ &+ L_t^{MRS,RT} - (L_t^{SH,Shed} + L_t^{SWH,Shed} + L_t^{PP,Shed} + L_t^{MRS,Shed}), \forall t. \end{aligned} \tag{3.15}$$
$$- F^{MAX} \leq P_t^{N,RT} - (P_t^{PVB,O,RT} + P_t^{W,O,RT} + P_t^{EV,O,RT}) \leq F^{MAX}, \forall t. \tag{3.16}$$

PV-battery system

The power output of the PV-battery system in the real-time, $P_t^{PVB,RT}$, is obtained based on (3.17). According to (3.17), $P_t^{PV,RT}$ is the power output of the PV panels in the real-time, $P_t^{B,RT}$ is the storage power of the battery in the real-time and S_t^{PVB} is the spillage power of the PV-battery system. Eq. (3.18) indicates that the total power output of the PV-battery system equals its power consumed in the building and the amount of power generation sold to the power grid. Also, minimum and maximum constraints for the power generation of the PV are presented in (3.19).

$$P_t^{PVB,RT} = P_t^{PV,RT} - P_t^{B,RT} - \omega_t - S_t^{PVB}, \forall t. \tag{3.17}$$

$$P_t^{PVB,RT} = P_t^{PVB,I,RT} + P_t^{PVB,O,RT}, \forall t. \tag{3.18}$$

$$P_t^{PV,MIN} \leq P_t^{PV,RT} \leq P_t^{PV,MAX}, \forall t. \tag{3.19}$$

Eq. (3.20) states limitations related to the charge and discharged power of the battery. The state of charge equation is defined on the basis of (3.21). As seen in (3.21), C^i is the initial state of charge of the battery. Also, maximum and minimum limitations of charging/discharging ramp rate of the battery are presented in (3.22).

$$P_t^{B,MIN} - C_{t-1} \leq P_t^{B,RT} \leq P_t^{B,MAX} - C_{t-1}, t \geq 2. \tag{3.20}$$

$$C_t = C_{t-1} + \omega_t, t \geq 2. \tag{3.21}$$

$$C_{t=1} = C^i + \omega_{t=1}, t = 1.$$

$$\omega^{MIN} \leq \omega_t \leq \omega^{MAX}, \forall t. \tag{3.22}$$

Electric Vehicle (EV)

The EV plays as an electrical storage system that can be used economically based on the charging strategies in the HEMS. There are different factors that should be considered when modelling the effect that the use of an EV has on the HEMP. These factors are EV's mobility patterns and battery characteristics. The power generation of the EV is represented in (3.23) and (3.24).

$$P_t^{EV,RT} = -P_t^{EV,B,RT} - \omega_t^C + \omega_t^D, \forall t. \tag{3.23}$$

$$P_t^{EV,RT} = P_t^{EV,I,RT} + P_t^{EV,O,RT}, \forall t. \tag{3.24}$$

Eq. (3.25) represents the state of charge equation in the EV, and $C^{EV,I}$ is the initial state of charge of the EV.

$$C_t^{EV} = C_{t-1}^{EV} + \omega_t^C \eta^{G2V} - \omega_t^D / \eta^{V2G} - \omega_t^M / \eta^{V2T}, t \geq 2. \tag{3.25}$$

$$C_{t=1}^{EV} = C^{EV,I} + \omega_{t=1}^C \eta^{G2V} - \omega_{t=1}^D / \eta^{V2G} - \omega_{t=1}^M / \eta^{V2T}, t = 1.$$

Eqs. (3.26) and (3.28) represent the limitations related to discharging the ramping rate of the EV. However, charging ramping rate's constraints are stated in (3.27) and (3.29).

$$P^{EV,D,MIN}\eta^{V2G}(1-u_t^{EV}) \leq \omega_t^D \leq P^{EV,D,MAX}\eta^{V2G}(1-u_t^{EV}), \forall t. \tag{3.26}$$

$$P^{EV,C,MIN}\eta^{G2V}u_t^{EV} \leq \omega_t^C \leq P^{EV,C,MAX}\eta^{G2V}u_t^{EV}, \forall t. \tag{3.27}$$

$$0 \leq \omega_t^D \leq (C_t^{EV} - P^{EV,D,MIN})\eta^{EV}, \forall t. \tag{3.28}$$

$$0 \leq \omega_t^C \leq (P^{EV,C,MAX} - C_t^{EV})\eta^{EV}, \forall t. \tag{3.29}$$

Eq. (3.30) enforces power limitations of the energy storage system in the EV.

$$P^{EV,D,MAX} - C_{t-1}^{EV} \leq P_t^{EV,B,RT} \leq P^{EV,C,max} - C_{t-1}^{EV}, t \geq 2. \tag{3.30}$$

Wind system

The power output of the wind micro-turbine is calculated according to (3.31). In (3.31), $P_t^{W,RT}$ is the power output of the wind system, $P_t^{W,PT,RT}$ is the potential power output of the wind micro-turbine based on the real-time weather conditions, and S_t^W is the spillage power of the wind system.

$$P_t^{W,RT} = P_t^{W,PT,RT} - S_t^W, \forall t. \tag{3.31}$$

Minimum and maximum limitations of the wind power generation are represented in (3.32). Also, the power output of the wind micro-turbine is split into the power consumed in the home, $P_t^{W,I,RT}$, and the power sold to the power grid, $P_t^{W,O,RT}$, as represented in (3.33).

$$P_t^{W,MIN} \leq P_t^{W,PT,RT} \leq P_t^{W,MAX}, \forall t. \tag{3.32}$$

$$P_t^{W,RT} = P_t^{W,I,RT} + P_t^{W,O,RT}, \forall t. \tag{3.33}$$

Space heater

The space heater is responsible for maintaining the indoor temperature at the desired level. There is a differential equation between the indoor temperature and the power consumed by the space heater device. Eq. (3.34) represents the performance of the space heater based on the relationship between the indoor temperature and the electrical load of the space heater. As seen in (3.34), θ^0 is the initial indoor temperature and it has been proposed that this amount is equal to the desired temperature. Eq. (3.35) represents that the indoor temperature as a controllable variable which is constrained to 1 °C higher or lower than the desired indoor temperature (θ^{DES}). The maximum and minimum limitations for the power consumption of the space heater are presented in (3.36).

$$\theta_{t+1}^{IN} = \theta_t^{IN} e^{-1/RC} + L_t^{SH,RT} R(1 - e^{-1/RC}), \forall t. \tag{3.34}$$

$$+ \theta_t^{OUT,P}(1 - e^{-1/RC}), t \geq 2$$

$$\theta_t^{IN} = \theta^0 = \theta^{DES}, t = 1$$

$$-1 \leq \theta_t^{IN} - \theta^{DES} \leq 1, \forall t. \tag{3.35}$$

$$L_t^{SH,MIN} \leq L_t^{SH,RT} \leq L_t^{SH,MAX}, \forall t. \tag{3.36}$$

Storage water heater

The storage water heater is responsible for storing the heat in the water tank via occupants. The maximum and minimum limitations of the storage water heater's power and consumed energy are expressed in (3.37) and (3.38), respectively.

$$L^{SWH,MIN} \leq L_t^{SWH,RT} \leq L^{SWH,MAX}, \forall t. \tag{3.37}$$

$$U^{SWH,MIN} \leq \sum_{t=1}^{N_t} L_t^{SWH,RT} \leq U^{SWH,max}. \tag{3.38}$$

Pool pump

Running hours of the pool pump should not be more than T^{ON} hours in a day as represented in (3.39). Eq. (3.40) expresses the maximum and minimum constraints of the pool pump power consumed in each hour.

$$\sum_{t=1}^{N_t} z_t \leq T^{ON}. \tag{3.39}$$

$$L^{PP,MIN} z_t \leq L_t^{PP,RT} \leq L^{PP,MAX} z_t, \forall t. \tag{3.40}$$

Must-run services

Must-run services include electrical loads that should be provided quickly, such as lighting, entertainment, etc. According to (3.41), we consider that there is no uncertainty in the prediction of the electrical loads of the must-run services.

$$L_t^{MRS,RT} = L_t^{MRS,P}, \forall t. \tag{3.41}$$

Spillage limits

The spillage amount of the wind and the PV-battery systems are expressed in (3.42) and (3.43), respectively.

$$0 \leq S_t^{W} \leq P_t^{W,PT,rt}, \forall t. \tag{3.42}$$
$$0 \leq S_t^{PVB,RT} \leq P_t^{PVB,RT}, \forall t. \tag{3.43}$$

Load shedding limits

Load shedding is the amount of the electrical load which is not served. Eqs. (3.44)-(3.47) enforce the load shedding constraints of each electrical load.

$$0 \leq L_t^{SH,Shed} \leq L_t^{SH,RT}, \forall t. \tag{3.44}$$
$$0 \leq L_t^{SWH,Shed} \leq L_t^{SWH,RT}, \forall t. \tag{3.45}$$
$$0 \leq L_{pp_t}^{PP,Shed} \leq L_t^{PP,RT}, \forall t. \tag{3.46}$$
$$0 \leq L_t^{MRS,Shed} \leq L_t^{MRS,RT}, \forall t. \tag{3.47}$$

3.2.2.4 Integration with the Modified Stochastic Predicted Bands (MSPB) Method

In our proposed model, the MSPB method is utilized to model the uncertainty of the variables in the HEMP. The uncertainty of wind and PV power generation is considered based on (3.48)-(3.51). Noted that the outdoor temperature is considered as a deterministic variable.

$$D_t^{W} = P_t^{W,S} - P_t^{W,P}, \forall t. \tag{3.48}$$
$$D_t^{PV} = P_t^{PVB,S} - P_t^{PV,P}, \forall t. \tag{3.49}$$

$$\begin{cases} P_t^{W,P}\alpha^w + (P_t^{W,P} - \sigma^{W,UP})(1-\alpha^W) \leq P_t^{W,RT} \\ \leq (P_t^{W,P} + \sigma^{W,DN})\alpha^W + P_t^{W,P}(1-\alpha^W), D_t^W \geq 0 \\ (P_t^{W,P} - \sigma^{W,UP})\alpha^W + P_t^{W,P}(1-\alpha^W) \leq P_t^{W.RT} \\ \leq P_t^{W,P}\alpha^W + (P_t^{W,P} + \sigma^{W,DN})(1-\alpha^W), D_t^W < 0 \end{cases} \tag{3.50}$$

$$\begin{cases} P_t^{PV,P}\alpha^{PV} + (E_t^P - \sigma^{PV,UP})(1-\alpha^{PV}) \leq p_t^{PV,RT} \\ \leq (P_t^{PV,P} + \sigma^{PV,DN})\alpha^{PV} + P_t^{PV,P}(1-\alpha^{PV}), D_t^{PV} \geq 0 \\ (P_t^{PV,P} - \sigma_{PV,UP})\alpha^{PV} + P_t^{PV,P}(1-\alpha^{PV}) \leq P_t^{PV,RT} \\ \leq P_t^{PV,P}\alpha^{pv} + (P_t^{PV,P} + \sigma^{PV,UP})(1-\alpha^{PV}), D_t^{PV} < 0 \end{cases} \tag{3.51}$$

3.2.3 Case study

3.2.3.1 Energy service system in a smart home

To assess the performance of the proposed REM model, the physical system from shokri2017residential is used. The case study is shown in Fig. 3.2. The maximum energy produced by the PV system is 2-kW. The battery can store between 0.48 and 2.4 kWh, and the maximum charging/discharging rates are 400 W. Besides, the charging/discharging efficiencies are 90%. The maximum energy produced by the wind micro-turbine is 6-kW. The EV can store between 1.77 and 5.9 kWh, and the maximum charging/ discharging rates are 3 kW. The charging/discharging efficiencies are 90%. Also, the EV is considered to be out of home between 6 AM and 5 PM. The maximum heating power equals 2 kW to maintain the temperature of the house within ±1 of the desired temperature (23°C). The thermal resistance of the building shell is equal to 18°C/kW, and C equals 0.525 kWh/°C . The energy capacity of the storage water heater is 10.46 kWh (180 L) which has 2 kW heating element. The rated power of the pool pump is 1.1 kW, and it can run for a maximum of 6 hours during the day. The performance of the proposed REM model is assessed in three cases. The implemented program is solved in GAMS 23.7 [Soroudi, 2017]. Table 5.2 presents the predicted data of stochastic variables. Table 3.6 presents the price data of the system. Moreover, the Value of Loss Load (VOLL), and the spillage costs of the wind and the PV-battery power generation are presented in Table 3.7. Note that α^W and α^{PV} to equal 1 in case 1, so the SPB method considers the uncertainty in case 1.

3.2.3.2 Impact of uncertainty

This section presents the impact of uncertainty of wind and PV power output on the EC which is presented in Table 3.8. Table 3.8 states that the uncertainty of the wind and PV power output increases the amount of the EC. According to the SPB method, upper/lower variance of the predicted variables equal zero. Therefore, the decision-making variables can be higher/lower than the predicted amount of these

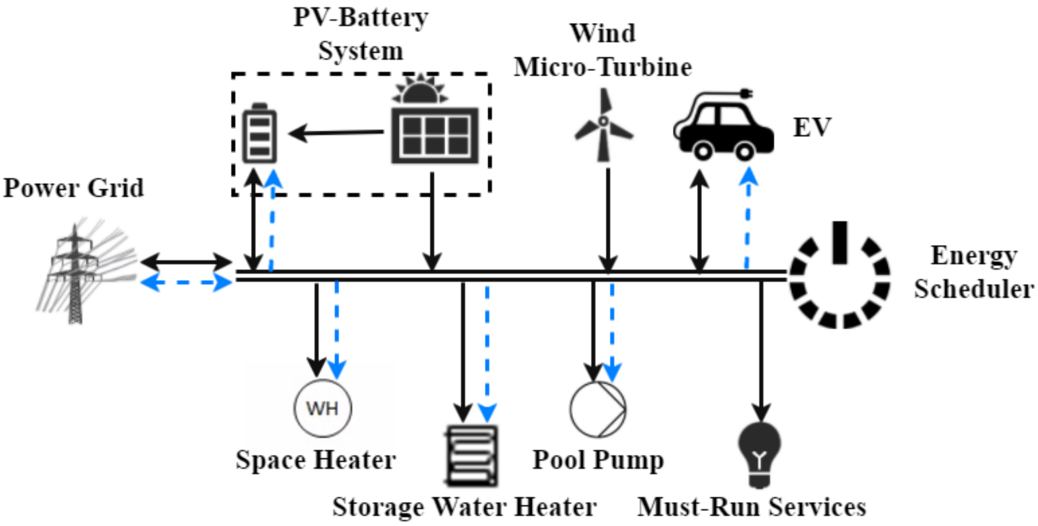

FIG. 3.2: An extended sample of a smart home in [Shokri Gazafroudi et al., 2017].

TAB. 3.1: Predicted data for uncertain variables [Shokri Gazafroudi et al., 2017].

t	$P_t^{PV,P}$	$\sigma^{PV,DN}$	$\sigma^{PV,UP}$	$P_t^{W,P}$	$\sigma^{W,DN}$	$\sigma^{W,UP}$	$\theta_t^{OUT,P}$	$L_t^{MRS,P}$
1	0	0.03	0.01	4	0.28	0.19	5.5	0.3
2	0	0.03	0.01	3.7	0.28	0.19	5.5	0.3
3	0	0.03	0.01	3.6	0.28	0.19	5.2	0.3
4	0	0.03	0.01	3.3	0.28	0.19	5.2	0.3
5	0	0.03	0.01	3.4	0.28	0.19	4.8	0.4
6	0	0.03	0.01	3	0.28	0.19	5.5	0.6
7	0.25	0.03	0.01	2.4	0.28	0.19	6.5	0.8
8	0.75	0.03	0.01	1.8	0.28	0.19	7.5	0.8
9	1.25	0.03	0.01	2	0.28	0.19	9.8	0.7
10	1.75	0.03	0.01	1.5	0.28	0.19	10	0.55
11	1.9	0.03	0.01	1	0.28	0.19	11	0.5
12	1.9	0.03	0.01	0.8	0.28	0.19	12	0.5
13	1.9	0.03	0.01	0.7	0.28	0.19	12	0.5
14	1.75	0.03	0.01	0.6	0.28	0.19	12	0.5
15	1.25	0.03	0.01	1.3	0.28	0.19	11	0.6
16	0.75	0.03	0.01	1.7	0.28	0.19	10	0.8
17	0.25	0.03	0.01	2.1	0.28	0.19	9	1.5
18	0	0.03	0.01	2.9	0.28	0.19	8.5	1.8
19	0	0.03	0.01	3.7	0.28	0.19	8	1.7
20	0	0.03	0.01	3.5	0.28	0.19	7.5	1.1
21	0	0.03	0.01	4	0.28	0.19	7	0.9
22	0	0.03	0.01	5	0.28	0.19	6.5	0.7
23	0	0.03	0.01	5.7	0.28	0.19	6.2	0.6
24	0	0.03	0.01	5.9	0.28	0.19	6	0.4

variables based on the upper/lower variance of the prediction when there is uncertainty in the prediction.

Tab. 3.2: Price data of the system [Shokri Gazafroudi et al., 2017].

	Price (\$/MW)			
Time (h)	λ^{PVB}	λ^{EV}	λ^{w}	λ^{N}
23-7	2.2	1	2.2	0.0814
8-14	2.2	1	2.2	0.1408
15-20	2.2	1	2.2	0.3564
21-22	2.2	1	2.2	0.1408

Tab. 3.3: VOLL and spillage costs [Shokri Gazafroudi et al., 2017].

	VOLL (\$/MW)				Spillage Cost (\$/MW)	
Time (h)	SH	SWH	PP	MRS	PVB	Wind
22-7	1	1	-0.5	2.2	4	6
8-21	1	1	0.25	2.2	4	6

Tab. 3.4: Impact of uncertainty on the EC [Shokri Gazafroudi et al., 2017].

	No uncer. of wind and PV	Uncer. of wind	Uncer. of PV
EC (\$)	652.683	665.087	660.969

3.2.3.3 Impact of optimistic coefficient

In this section, the MSPB method is used to model the uncertainty of wind and PV power generation. Also, only the impact of α^{W} is assessed. It is considered that α^{PV} equals 1. As seen in Fig. 3.3, the increase in the amount of α^{W} increments the EC. However, this increment is not uniform.

3.2.3.4 Impact of prediction accuracy

The impact of wind power prediction accuracy is evaluated in three scenarios based on its *optimistic coefficient*. Fig. 3.4 shows the influence of the Prediction Accuracy Coefficient (PAC) on the EC and wind energy output. In this case, upper prediction accuracy is assumed to equal 15% and the lower prediction accuracy is equal to 10% when the PAC equals 1.

Additionally, upper prediction accuracy equals 10% and lower prediction accuracy is equal to 6.67% when the PAC equals 0.67, and upper prediction accuracy equals 22.5% and down prediction accuracy equals 15% when the PAC equals 1.5. As seen in Fig.

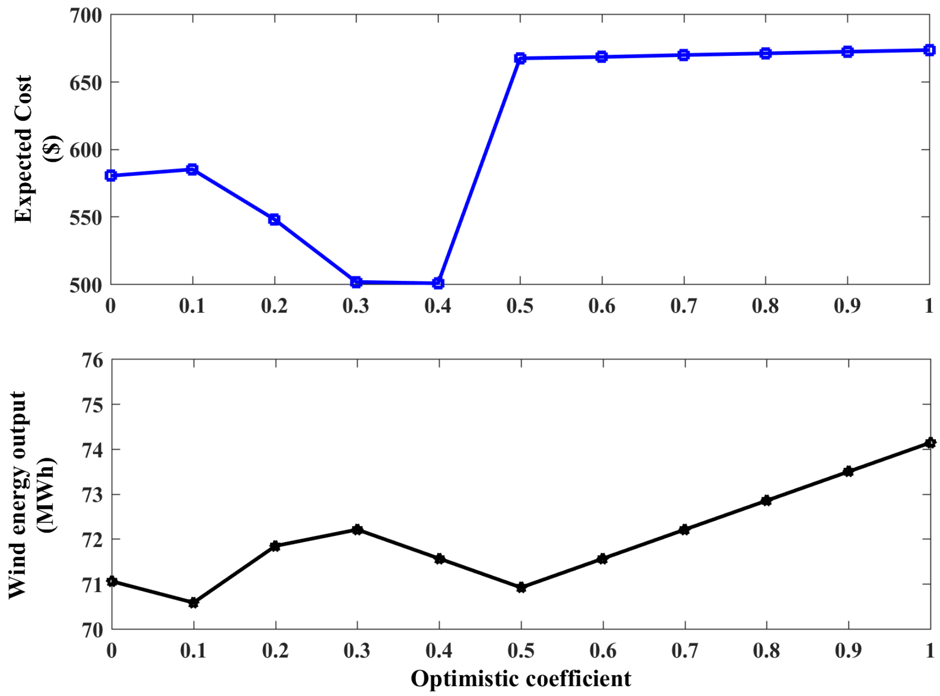

Fig. 3.3: Impact of OC on wind energy output and system expected cost [Shokri Gazafroudi et al., 2017].

3.4, increasing the amount of wind power's PAC has a positive effect on the EC in all scenarios. Note that the simulation results of the system are more realistic when α^W equals zero because increasing prediction error has negative effect on the system's energy output. Hence, this point is seen when α^W equals zero. In this section, the home energy management problem has been modeled to enable the smart home to trade electricity with the power grid. Also, a novel interval optimization method has been introduced to model the uncertainty of wind and PV power generation of the residential scale. In Section 3.3, the impact of energy flexibility on the HEMS by a predictive dispatch model is studied based on findings of [Gazafroudi et al., 2017b].

3.3 Energy flexibility management based on a predictive dispatch model of the HEMS

This section proposes a predictive dispatch model for management of energy flexibility in the HEMS. In this way, EV, battery and shiftable loads are the devices that provide energy flexibility in the proposed residential system. Our energy management problem consists of two stages: day-ahead and real-time. A hybrid method is defined in [Gazafroudi et al., 2017b] to model the uncertainty of the PV power generation based

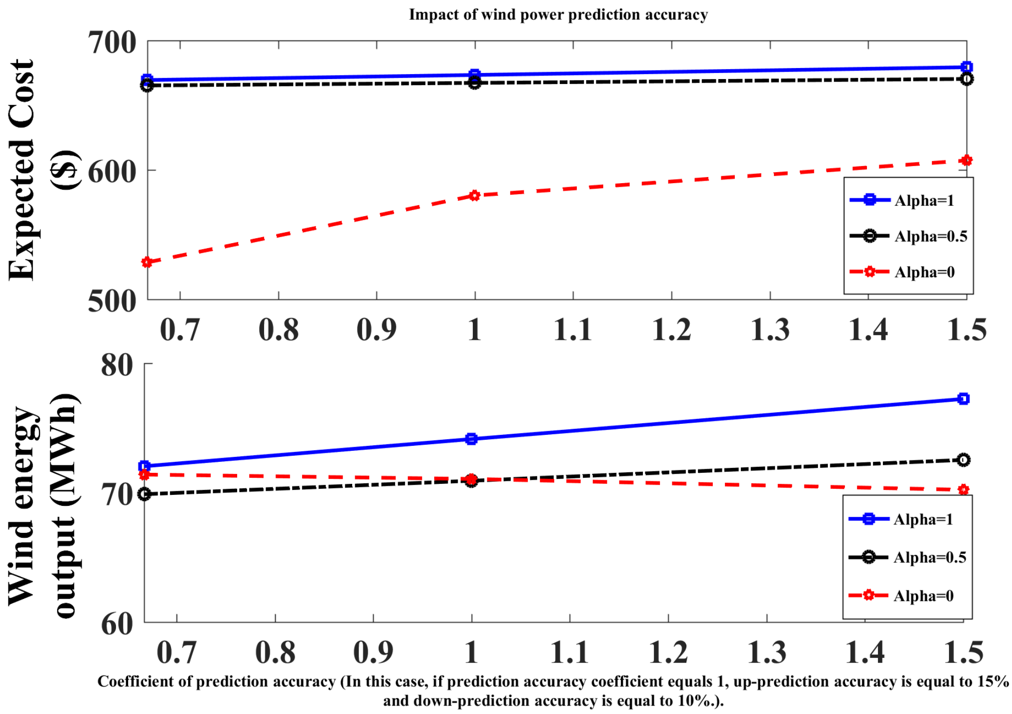

FIG. 3.4: Impact of wind power prediction accuracy on wind energy output and system expected cost [Shokri Gazafroudi et al., 2017].

on its power prediction. In the day-ahead stage, the uncertainty is modeled by interval bands. However, the uncertainty of PV power generation is modeled through a stochastic scenario-based method in the real-time stage. The performance of the proposed hybrid interval-stochastic optimization method is compared with the MSPB method which has been defined in Section 3.2. Moreover, the impacts of energy flexibility and the demand response program on the expected profit and transacted electrical energy of the system are assessed in the case study presented in this section.

The rest of this section is organized as follows. Section 3.3.1 introduces the proposed hybrid interval-stochastic method. Then, the home energy management problem is described in Section 3.3.4. Finally, Section 3.3.5 provides the simulation results.

3.3.1 Interval-stochastic optimization method

3.3.1.1 Data

Here, the data predicted in [Gazafroudi et al., 2017a] and [Gazafroudi et al., 2017b] has been used. As shown in Table 3.5, the predicted data in each time step consists of the central forecasting, and up/down deviation. Hence, the predicted data is limited to upper/lower band based on the central forecasting and up/down deviation. It is noticeable that this section concentrates only on modelling the uncertainty caused by PV power prediction in the system. Hence, the forecasting system is not explained in this section. The data presented in Table 3.5 are inputs of the HEMS. Therefore, the energy management system makes optimum decisions through the interval-stochastic optimization method.

TAB. 3.5: Predicted data of uncertain variables [Gazafroudi et al., 2017b].

t	$P_t^{PV,P}(kW)$	$\sigma^{PV,DN}(kW)$	$\sigma^{PV,UP}(kW)$	$\theta_t^{OUT,P}$(°C)	$L_t^{MRS,P}(kW)$
1	0	0.00	0.00	5.5	0.005
2	0	0.00	0.00	5.5	0.005
3	0	0.00	0.00	5.2	0.005
4	0	0.00	0.00	5.2	0.005
5	0	0.00	0.00	4.8	0.005
6	0	0.00	0.00	5.5	0.005
7	0.10	0.01	0.02	6.5	0.005
8	0.20	0.02	0.04	7.5	0.005
9	0.42	0.03	0.07	9.8	0.005
10	0.76	0.08	0.26	10	0.005
11	1.1	0.12	0.23	11	0.005
12	1.32	0.13	0.26	12	0.005
13	1.91	0.10	0.19	12	0.005
14	0.85	0.02	0.04	12	0.005
15	0.29	0.02	0.04	11	0.005
16	0.31	0.02	0.03	10	0.005
17	0.06	0.01	0.01	9	0.005
18	0	0.00	0.00	8.5	0.005
19	0	0.00	0.00	8	0.005
20	0	0.00	0.00	7.5	1.218
21	0	0.00	0.00	7	0.262
22	0	0.00	0.00	6.5	0.14
23	0	0.00	0.00	6.2	0.127
24	0	0.00	0.00	6	0.005

3.3.2 Interval Model

In the day-ahead stage, PV system power generation is limited to the bands according to the forecasting deviations. The minimum band represents the deviation below the central forecasting, and the maximum band represents the deviation above the central forecasting. $P_{pv_t}^{da}$ intends to converge to the maximum/minimum band in the best/worst case. Therefore, Eq. (3.52) can be divided into Eqs. (3.53) and (3.54) in the best and worst cases, respectively. This way, an auxiliary parameter is added to these equations as a slack parameter for the decision-maker. This parameter is denoted as *Optimistic Coefficient*, α, which has been defined in Section 3.2. Hence, $P_{pv_t}^{da}$ converges to the best/worst case when the decision-maker has the pessimistic/conservative perspective by adding α to (3.53) and (3.54), and sum over them, as seen in (3.55). Then, Eqs. (3.55) and (3.56) are obtained through the simplification of (3.52)-(3.54).

$$P_{pv_t}^{pred} - \sigma_{pv_t}^{down} \leq P_{pv_t}^{da} \leq P_{pv_t}^{pred} + \sigma_{pv_t}^{up}, \forall t. \tag{3.52}$$

$$P_{pv_t}^{pred} \leq P_{pv_t}^{da} \leq P_{pv_t}^{pred} + \sigma_{pv_t}^{up} : OC = 1, \forall t. \tag{3.53}$$

$$P_{pv_t}^{pred} - \sigma_{pv_t}^{down} \leq P_{pv_t}^{da} \leq P_{pv_t}^{pred} : OC = 0, \forall t. \tag{3.54}$$

$$\begin{aligned} & P_{pv_t}^{pred}\alpha_{pv} - (P_{pv_t}^{pred} - \sigma_{pv_t}^{down})(1-\alpha_{pv}) \leq P_{pv_t}^{da} \\ & \leq (P_{pv_t}^{pred} + \sigma_{pv_t}^{up})\alpha_{pv} + P_{pv_t}^{pred}(1-\alpha_{pv}), \forall t. \end{aligned} \tag{3.55}$$

$$P_{pv_t}^{pred} - \sigma_{pv_t}^{down}(1-\alpha_{pv}) \leq P_{pv_t}^{da} \leq P_{pv_t}^{pred} + \sigma_{pv_t}^{up}\alpha_{pv}, \forall t. \tag{3.56}$$

3.3.3 Stochastic Model

In the real-time stage, stochastic programming is used to model the uncertainty of PV power. Therefore, the scenarios and their corresponding probabilities are defined in this section. Thus, the prediction mean and deviation are defined as metric parameters by (3.57) and (3.58), respectively. These are used to generate scenarios of the PV power in the real-time stage. In this step, three scenarios are defined to model the uncertainty of the PV system's power generation. First scenario, up scenario, describes data that has a deviate above the central forecasting. Second scenario, down scenario, represents data that has a deviation below the central forecasting. Then, the third scenario describes the central forecasting data. The amounts of these scenarios are determined through (3.59)-(3.61). Moreover, the corresponding probabilities are obtained according to (3.62)-(3.64).

$$P^{mean}_{pv_t} = P^{pred}_{pv_t} + \frac{\sigma^{up}_{pv_t} - \sigma^{down}_{pv_t}}{2}, \forall t. \tag{3.57}$$

$$\Delta_{pv_t} = \frac{\sigma^{up}_{pv_t} + \sigma^{down}_{pv_t}}{2}, \forall t. \tag{3.58}$$

$$P^{rt}_{pv_t}(\omega = \omega_1) = P^{pred}_{pv_t} + \sigma^{up}_{pv_t}, \forall t. \tag{3.59}$$

$$P^{rt}_{pv_t}(\omega = \omega_2) = P^{pred}_{pv_t} - \sigma^{down}_{pv_t}, \forall t. \tag{3.60}$$

$$P^{rt}_{pv_t}(\omega = \omega_3) = P^{pred}_{pv_t}, \forall t. \tag{3.61}$$

$$\pi(\omega = \omega_1) = Prob(P^{pred}_{pv_t} + \sigma^{up}_{pv_t} > P^{mean}_{pv_t} + \Delta_{pv_t}) \tag{3.62}$$

$$\pi(\omega = \omega_2) = Prob(P^{pred}_{pv_t} - \sigma^{down}_{pv_t} < P^{mean}_{pv_t} - \Delta_{pv_t}) \tag{3.63}$$

$$\pi(\omega = \omega_3) = 1 - \pi(\omega = \omega_1) - \pi(\omega = \omega_2) \tag{3.64}$$

3.3.4 Home Energy Management Problem

We consider that each smart home can participate in two different types of LEM [Gazafroudi et al., 2017a], [Gazafroudi et al., 2017b]. These LEMs are called day-ahead and real-time markets. In practice, the proposed LEMs can be operated by the distribution system operator or the retailers. Hence, the distribution system operator or the retailers are responsible for providing their agents in the region with the local electricity market framework to transact energy with them. Besides, smart homes are considered price-takers in the LEM, and they can buy electricity from the local electricity market on the basis of the Time of Use (ToU) tariff. Also, it is assumed that the sold/bought electricity price to/from the local electricity market are different. The domestic energy management problem is modeled as a two-stage problem. The first stage is called the day-ahead stage, and the second stage is called the real-time stage. Here, the Expected Profit (EP) is defined by an Objective Function (OF) which maximizes the profit of energy services. In 3.65, EP is a summation of the day-ahead EP, EP^{da}, and the real-time EP, EP^{rt}, which are OFs of the day-ahead and real-time stages, respectively.

$$EP = EP^{da} + EP^{rt}. \tag{3.65}$$

3.3.4.1 Day-Ahead Stage

The objective function of the HEMS in the day-ahead local electricity market is defined in the Day-Ahead (DA) stage. The purpose of this function is to make the best decisions in each of the time periods during the day d. However, the DA stage obtains optimum decisions for the system in day $d-1$. Hence, the objective function for the DA stage is represented in (3.66):

$$EP^{da} = \sum_{t=1}^{N_t} (\lambda_t^{'} P_{pv,out_t}^{da} + \sum_{k} \gamma_k \lambda_t^{'} P_{dis,out_t}^{da}(k) - \lambda_t P_{net_t}^{da}) \tag{3.66}$$

EP^{da} consists of three parts. The first and second parts represent the revenue of selling the electrical energy produced by the PV and the Energy Storage Systems (ESSs) to the local market. The third part states the costs of buying the electrical energy from the local market. Noted that participation factor, γ_k, is a binary parameter that is defined for the first time in [Gazafroudi et al., 2017b] in order to consider the participation of the ESSs in the DA stage. If the participation factor is equal to zero, ESSs are used to trade energy only in the real-time LEM. In other words, the HEMS can utilize the full capacity of the ESSs in the day-ahead market if the participation factor equals 1.

As represented in Section 3.3.1, new optimization is used to model the uncertainty in the HEMP. In this way, all the equations stated in Section 3.2 are redefined in this section. Eq. (3.67) establishes the power balance equation due to the power outputs of the PV, P_{pv,in_t}^{da}, and the ESSs, $P_{dis,in_t}^{da}(k)$, injected into the home, the grid power input, $P_{net_t}^{da}$, the electrical loads, L_{jt}^{da}, and the charged power of the ESSs, $P_{ch_t}^{da}(k)$. In this section, power loss is not considered for simplicity. Eq. (3.68) represents the power flow limitation through the distribution line which ends at the building. S_{max} expresses the maximum power capacity of the distribution line that links the smart home with the power distribution network.

$$P_{net_t}^{da} + P_{pv,in_t}^{da} + \sum_{k} \gamma_k P_{dis,in_t}^{da}(k) = \sum_{j=1}^{N_j} L_{jt}^{da} + \gamma_k P_{ch_t}^{da}(k), \forall t. \tag{3.67}$$

$$- S_{max} \leq P_{net_t}^{da} - P_{pv,out_t}^{da} - \sum_{k} \gamma_k P_{dis,out_t}^{da}(k) \leq S_{max}, \forall t. \tag{3.68}$$

Besides, some limitations correspond to all appliances. According to (3.69)-(3.72), only the maximum and minimum limitations of the produced/consumed energy are defined in each device at this stage because the uncertainty is not considered in the DA stage. The total power generation of the PV is stated in (3.69). Eq. (3.70) represents the interval limitations of the PV power generation. Besides, Eqs. (3.71) and (3.72) represents the total electric power consumption.

$$P_{pv_t}^{da} = P_{pv,in_t}^{da} + P_{pv,out_t}^{da}, \forall t. \tag{3.69}$$

$$P_{pv_t}^{pred} - \sigma_{pv_t}^{down}(1-\alpha_{pv}) \leq P_{pv_t}^{da} \leq P_{pv_t}^{pred} + \sigma_{pv_t}^{up}\alpha_{pv}, \forall t. \tag{3.70}$$

$$L_{jt}^{da} = L_{jt}^{pred}, \forall t. \tag{3.71}$$

$$\sum_{j=1}^{N_j} L_{jt}^{da} = L_{sh_t}^{da} + L_{swh_t}^{da} + L_{pp_t}^{da} + L_{mrs_t}^{da}, \forall t. \tag{3.72}$$

ESSs can be utilized economically on the basis of the charging/discharging strategies in the HEMP. The mobility patterns and the storage characteristics of the ESSs are different factors that should be considered in modeling the ESSs. However, the mobility pattern is only related to the EVs.

$$C_t^{da}(k) = C_{t-1}^{da}(k) + P_{ch_t}^{da}(k)\eta_{B2V} - P_{dis_t}^{da}(\omega)/\eta_{V2B}, t \geq 2\forall k. \tag{3.73}$$

$$C_{t=1}^{da}(\omega) = C_i + P_{ch,t=1}^{da}(k)\eta_{B2V} - P_{dis,t=1}^{da}(\omega)/\eta_{V2B}, t = 1, \forall k.$$

$$P_{ev}^{min} \leq C_t^{da}(k) \leq P_{ev}^{max}, \forall t, k. \tag{3.74}$$

$$-w^{min} \leq C_t^{da}(k) - C_{t-1}^{da}(k) \leq w^{max}, t \geq 2, \forall k. \tag{3.75}$$

$$-w^{min} \leq C_t^{da}(k) - C_i(k) \leq w^{max}, t = 1.$$

$$0 \leq P_{dis_t}^{da}(k) \leq w^{max} u_t^{da}, \forall t, k. \tag{3.76}$$

$$0 \leq P_{ch_t}^{da}(k) \leq w^{min}(1-u_t^{da}), \forall t, k. \tag{3.77}$$

$$P_{dis_t}^{da}(k) = P_{dis,in_t}^{da}(k) + P_{dis,out_t}^{da}(k), \forall t, k. \tag{3.78}$$

3.3.4.2 Real-Time Stage

In this stage, the objective function of the HEMP is defined due to participating in the RTLEM. Also, the uncertainty is modeled by a stochastic scenario-based method. Decisions in the real-time stage are made on the basis of the outputs of the first stage and the prediction engine. The energy traded between the home and the real-time market is noticeably different to the energy traded in the day-ahead market because of the PV power generation uncertainty. In other words, the energy traded in the real-time stage can be positive or negative due to the prediction error of PV power generation. The expected profit of the real-time stage, EP^{rt}, is represented as:

$$EP^{rt} = \sum_{t=1}^{N_t}\sum_{\omega=1}^{N_\Omega}\pi(\omega)(\lambda_t(P^{rt}_{pv,out_t}(\omega) - P^{da}_{pv,out_t}) \tag{3.79}$$
$$+ \sum_k(\lambda_t(P^{rt}_{dis,out_t}(k,\omega) - \gamma_k P^{da}_{dis,out_t}(k)) - \lambda_t(P^{rt}_{ch_t}(\omega) - \gamma_k P^{da}_{ch_t}(k))), \forall t.$$
$$- \sum_{j=1}^{N_j} VOLL_j L^{shed}_{jt}(\omega) - V^s_{pv} S_{pv_t}(\omega)).$$

EP^{rt} consists of five parts. The first part represents the revenue for selling energy produced by PV to the real-time local electricity market. The total cost of electrical energy that is bought from the RTLEM is represented in the second part. The third part expresses the profit due to selling the stored electrical energy of ESSs to the local market. The Value of Loss Load (VOLL) cost, $VOLL_j$, is stated in the fourth part. Finally, the spillage cost of the PV system is represented in the last part. As seen in (3.79), it is proposed that if the PV power generation in the real-time stage, $P^{rt}_{pv,out_t}(\omega)$, is more than the PV power generation in the DA stage, the HEMS can only sell its extra power at the net price, λ_t, that is less than the price that is established for the purchase of the power generated by the PV on the day-ahead local market, λ'_t. Hence, the HEMS can increase its expected revenue if it has better day-ahead prediction accuracy of its PV power generation. In the real-time stage, Eq. (3.80) is the power balance equation, and Eq. (3.81) shows the power flow limitations in the distribution line.

$$P^{rt}_{net_t}(\omega) + P^{rt}_{pv,in_t}(\omega) + \sum_k P^{rt}_{dis,in_t}(k,\omega) = \sum_{j=1}^{N_j}(L^{rt}_{jt}(\omega) - L^{shed}_{jt}(\omega)) \tag{3.80}$$
$$+ \sum_k P^{rt}_{ch_t}(k,\omega), \forall t, \omega.$$
$$- S_{max} \leq P^{rt}_{net_t}(\omega) - (P^{rt}_{pv,out_t}(\omega) + \sum_k P^{rt}_{dis,out_t}(k,\omega)) \leq S_{max}, \forall t, \omega. \tag{3.81}$$

The power output of PV in the real-time stage, $P^{rt}_{pv_t}$, is obtained based on (3.82). Here, $P^{rt}_{pv,p_t}(\omega)$ is the potential power generation of the PV in the real-time, and $S_{pv_t}(\omega)$ is the spillage power of the PV system. Eq. (3.83) represents that the total power output of the PV equals its power output consumed in the home, $P^{rt}_{pv,in_t}(\omega)$, and the amount of power generation that is sold to the real-time local market, $P^{rt}_{pv,out_t}(\omega)$. The PV spillage is the amount of power that is spilled in period t. This amount is positive or equal to zero, and is limited to the actual power generation of the PV as represented in (3.84).

$$P^{rt}_{pv_t}(\omega) = P^{rt}_{pv,p_t}(\omega) - S_{pv_t}(\omega), \forall t, \omega. \tag{3.82}$$
$$P^{rt}_{pv_t}(\omega) = P^{rt}_{pv,in_t}(\omega) + P^{rt}_{pv,out_t}(\omega), \forall t, \omega. \tag{3.83}$$
$$0 \leq S_{pv_t}(\omega) \leq P^{rt}_{pv,p_t}(\omega), \forall t, \omega. \tag{3.84}$$

The power generation of the ESSs, $P^{rt}_{dis_t}(\omega)$, is expressed in (3.85). Eq. (3.86) represents the balance equation of the state of charge in an ESS, where C_i is the initial state of charge in the ESS. The maximum and minimum limitations of the ESSs' state of charge and are represented in (3.87). The ramping constraints of the ESSs are represented in (3.88). Moreover, Eqs. (3.89) and (3.90) express constraints of the ESS in the discharge and charge states, respectively.

$$P^{rt}_{dis_t}(k,\omega) = P^{rt}_{dis,in_t}(k,\omega) + P^{rt}_{dis,out_t}(k,\omega), \forall t, k, \omega. \tag{3.85}$$
$$C^{rt}_t(k,\omega) = C^{rt}_{t-1}(k,\omega) + P^{rt}_{ch_t}(k,\omega)\eta_{B2V} - P^{rt}_{dis_t}(k,\omega)/\eta_{V2B}, t \geq 2, \forall k, \omega. \tag{3.86}$$
$$C^{rt}_{t=1}(k,\omega) = C_i + P^{rt}_{ch,t=1}(k,\omega)\eta_{B2V} - P^{rt}_{dis,t=1}(k,\omega)/\eta_{V2B}, t = 1, \forall k, \omega.$$
$$P^{min}_{ev} \leq C^{rt}_t(k,\omega) \leq P^{max}_{ev}, \forall t, k, \omega. \tag{3.87}$$
$$-w^{min} \leq C^{rt}_t(k,\omega) - C^{rt}_{t-1}(k,\omega) \leq w^{max}, t \geq 2, \forall k, \omega. \tag{3.88}$$
$$-w^{min} \leq C^{rt}_t(k,\omega) - C_i \leq w^{max}, t = 1, \forall k, \omega.$$
$$0 \leq P^{rt}_{dis_t}(k,\omega) \leq w^{max}u^{rt}_t, \forall t, k, \omega. \tag{3.89}$$
$$0 \leq P^{rt}_{ch_t}(k,\omega) \leq w^{min}(1-u^{rt}_t), \forall t, k, \omega. \tag{3.90}$$

Electrical loads include controllable and/or shiftable loads. In this section, three types of loads are modelled. The space heater, L_{sh_t}, which is a controllable load, the storage water heater, L_{swh_t}, which is a shiftable load, and must-run services, L_{mrs_t}, which are non-controllable-shiftable loads. Eqs. (3.91) and (3.92) define total electrical load and total load shedding, respectively. These loads are described in the following.

$$\sum_{j=1}^{N_j} L^{rt}_{jt}(\omega) = L^{rt}_{sh_t}(\omega) + L^{rt}_{swh_t}(\omega) + L^{rt}_{pp_t}(\omega) + L^{rt}_{mrs_t}(\omega), \forall t, \omega. \tag{3.91}$$
$$\sum_{j=1}^{N_j} L^{shed}_{jt}(\omega) = L^{shed}_{sh_t}(\omega) + L^{shed}_{swh_t}(\omega) + L^{shed}_{pp_t}(\omega) + L^{shed}_{mrs_t}(\omega), \forall t, \omega. \tag{3.92}$$

The space heater provides the indoor temperature at the desired temperature. Eq. (3.93) represents the relation between the indoor temperature and its power consumption. In

Eq. (3.93), θ_0 is the initial indoor temperature which is assumed to be equal to the desired temperature. Eq. (3.94) limits the variations in the desired indoor temperature to 1°C above or below it. Also, the maximum and minimum bands of the space heater load are represented in (3.95). Also, the load shedding constraint of the space heater is represented in (3.96).

$$\theta_{in_t+1}(\omega) = \theta_{in_t}(\omega)e^{-1/RC} + L^{rt}_{sh_t}(\omega)R(1-e^{-1/RC}) \tag{3.93}$$
$$+\,\theta^{pred}_{out_t}(1-e^{-1/RC}), t \geq 2, \forall\omega.$$
$$\theta^{rt}_{in_t}(\omega) = \theta_0 = \theta_{des}, t = 1, , \forall\omega.$$
$$-1 \leq \theta^{rt}_{in_t}(\omega) - \theta_{des} \leq 1, \forall t, \omega. \tag{3.94}$$
$$L^{min}_{sh} \leq L^{rt}_{sh_t}(\omega) \leq L^{max}_{sh}, \forall t, \omega. \tag{3.95}$$
$$0 \leq L^{shed}_{sh_t}(\omega) \leq L^{rt}_{sh_t}(\omega), \forall t, \omega. \tag{3.96}$$

Storage water heater stores the heat in the water tank. The maximum and minimum limitations of the storage water heater's load and energy consumption are represented in (3.97) and (3.98), respectively. The load shedding constraint of the storage water heater is expressed in (3.99).

$$L^{min}_{swh} \leq L^{rt}_{swh_t}(\omega) \leq L^{max}_{swh}, \forall t, \omega. \tag{3.97}$$
$$\sum_{t=1}^{N_t} L^{rt}_{swh_t}(\omega) = U_{swh}, \forall t, \omega. \tag{3.98}$$
$$0 \leq L^{shed}_{swh_t}(\omega) \leq L^{rt}_{swh_t}(\omega), \forall t, \omega. \tag{3.99}$$

Maximum running hours of the pool pump equals than T_{on} hours per day. Eq. (3.100) represents the limitations of the pool pump power consumption in each hour. Eq. (3.101) represents the maximum-hour constraint that pool pump can be turn on. Moreover, the load shedding constraint related to the pool pump is represented in (3.102).

$$L^{min}_{pp} z_t(\omega) \leq L^{rt}_{pp}(\omega) \leq L^{max}_{pp_t} z_t(\omega), \forall t, \omega. \tag{3.100}$$
$$\sum_{t=1}^{N_t} z_t(\omega) \leq T_{on}, \forall t, \omega. \tag{3.101}$$
$$0 \leq L^{shed}_{pp_t}(\omega) \leq L^{rt}_{pp_t}(\omega), \forall t, \omega. \tag{3.102}$$

Must-run services are defined as loads that should be provided quickly. In this section, it is assumed that there is no uncertainty due to the prediction of must-run services as represented in Eq. (3.103). Also, the load shedding constraint is represented by (3.104).

$$L^{rt}_{mrs_t}(\omega) = L^{pred}_{mrs_t} \tag{3.103}$$

$$0 \leq L^{shed}_{mrs_t}(\omega) \leq L^{rt}_{mrs_t}(\omega) \tag{3.104}$$

3.3.5 Simulation Results

3.3.5.1 Case Study

To evaluate the performance of the proposed HEMS, the home energy system shown in Fig. 3.2 is used. The wind micro-turbine has been omitted from the test system in this section. The maximum power produced by the PV system is 2-kW. The battery can store between 0.48 and 2.4 kWh, and the maximum charging/discharging rates are 400 W. Besides, the charging and discharging efficiencies are 90%. The maximum heating power of the Space Heater (SH) equals 2 kW to maintain the temperature of the house within ±1 of the desired temperature (23°C). The thermal resistance of the building shell equals 18°C/kW, and C equals 0.525 kWh/°C . The energy capacity of the Storage Water Heater (SWH) is 10.46 kWh which has a 2 kW heating element. The rated power of the Pool Pump (PP) is 1.1 kW, and it can run for a maximum of 6 hours during the day. Table 3.6 gives the price data of the system. Moreover, VOLL, and the spillage costs of PV-battery power generation are shown in Table 3.7.

TAB. 3.6: ToU price data of the system [Gazafroudi et al., 2017b].

	Price ($/MW)	
Time (h)	λ'_t	λ_t
23-7	2.2	0.0814
8-14	2.2	0.1408
15-20	2.2	0.3564
21-22	2.2	0.1408

TAB. 3.7: The VOLL and spillage costs [Gazafroudi et al., 2017b].

	VOLL ($/MW)				Spillage Cost ($/MW)
Time (hour)	SH	SWH	PP	MRS	PV
22-7	1	1	-0.5	2.2	4
8-21	1	1	0.25	2.2	4

3.3.5.2 Impact of Energy Flexibility

In this section, the energy flexibility of the proposed HEMS is assessed. Hence, four scenarios are defined to analyze the performance of the system. In Scenario 1, neither the battery nor the EV are defined in the day-ahead stage of the energy management problem ($\gamma_{battery} = \gamma_{EV} = 0$). In Scenario 2, only the battery is considered in the day-ahead stage ($\gamma_{battery} = 1$, $\gamma_{EV} = 0$). However, only the EV is considered in day-ahead stage in Scenario 3 ($\gamma_{battery} = 0$, $\gamma_{EV} = 1$). In Scenario 4, both (the battery and the EV) are modeled in the day-ahead stage ($\gamma_{battery} = \gamma_{EV} = 1$).

The impact of the ESSs on the total, day-ahead and real-time expected profits of the system is shown in Fig. 3.5. Also, the influence of the optimistic coefficient, α, is evaluated in Fig. 3.5. From this figure it is clear that an increment in α increases the total and day-ahead expected profits because α affects the PV system power production directly through the interval bands in the day-ahead stage. Hence, α increases the PV panel power generation in the day-ahead stage and day-ahead expected profit. However, α has a negative impact on the amounts of the real-time expected profit. Moreover, the expected profit of the system is maximum in scenario 4. In other words, increasing the energy flexibility of the system increases the total, day-ahead and real-time expected profits of the system. Hence, the maximum and minimum amounts of the expected profit are obtained in scenarios 4 and 1, respectively. Also, the expected profit in scenario 3 is higher than that in scenario 2 because the ramping rate of EV is higher than that of the battery. Therefore, the EV can provide more energy flexibility than the battery in this proposed system.

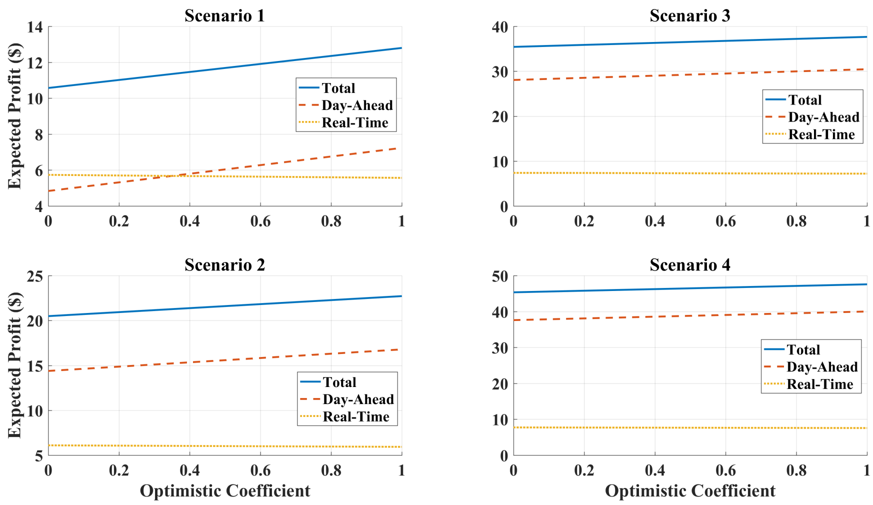

FIG. 3.5: Impact of energy flexibility on the amounts of total, day-ahead and real-time expected profits [Gazafroudi et al., 2017b].

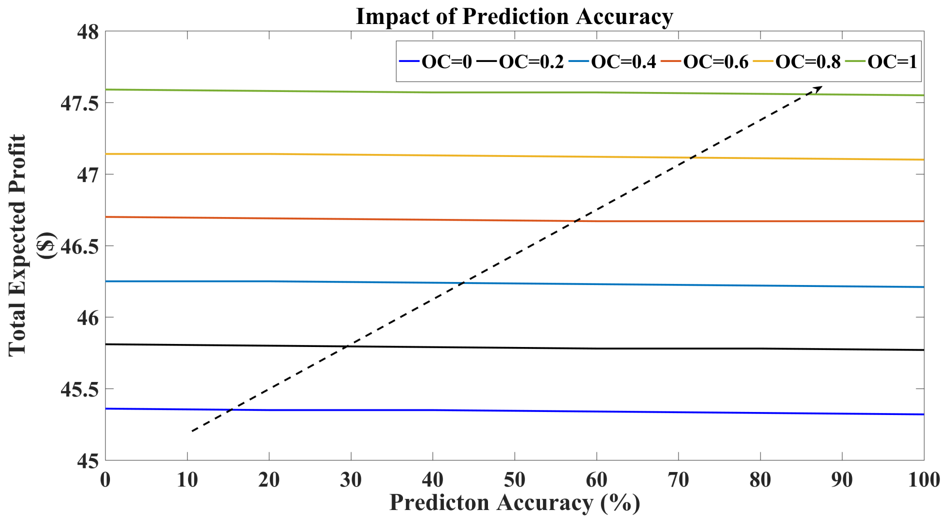

Fig. 3.6: Impact of prediction accuracy on the total expected profit of the system [Gazafroudi et al., 2017b].

3.3.5.3 Impact of Prediction Accuracy

The prediction accuracy of PV power generation and its influence on the total expected profit is analyzed in this section. To simplify the model, in this section, the prediction accuracy of the outdoor temperature of the home and the must-run services is considered to be 100%. Besides, it is considered that the battery and the EV are modeled in the day-ahead stage in this case. As mentioned before, α increases the amount of total expected profit of the system.

Fig. 3.6 evaluates the impact of the prediction accuracy on the total expected profit is evaluated on the basis of the optimistic coefficient. Furthermore, an increase in the prediction accuracy has a smooth negative effect on the expected profit. In other words, in the proposed HEMS, an increment in the prediction accuracy causes to decrease the managed power of the PV. Hence, this decreases the expected profit of the system. According to this assessment, the maximum amount of the total expected profit of the system is where α and prediction accuracy equal 1 and 0, respectively.

3.3.5.4 Impact of Demand Response

In this section, the effect of the DRP on the EPs and the home's electrical energy that is sold/bought to/from the local electricity market is assessed in four scenarios: with the DRP, with flexible VOLL only, with the ToU price only, and without the DRP. Here, the DRP consists of the flexible VOLL and the ToU price.

As seen in Table 3.8, the DRP has a positive effect on the amount of total expected profit of the HEMS. In other words, while EP^{da} increases when the DRP is not considered in the system, EP^{rt} decreases because electrical loads are not flexible when the DRP is not considered in the HEMS. Furthermore, The sold/bought electrical energy of the HEMS considering DRP is more/less than without considering DRP because it makes HEMS able to shift the electrical load in the time horizon of the energy management problem and reduce the loads under some conditions. However, the impacts of the flexible VOLL and the ToU price are not the same. Although both of them increase the sold electrical energy, the total expected profit is higher when only flexible VOLL is considered than when only the ToU price is considered. This is because of the positive effect that the flexible VOLL program has on the real-time stage of the HEMP.

TAB. 3.8: Impact of demand response program on the amount of expected profit of the system and sold/bought electrical energy to/from the local electricity market [Gazafroudi et al., 2017b].

	$\alpha = 1$				
	EP_{total}	EP_{da}	EP_{rt}	E_{sold}	E_{bought}
With the DRP (Flexible VOLL+ToU)	47.571	40.003	7.568	18.605	43.033
With Only Flexible VOLL	47.775	42.409	5.365	14.406	37.995
With Only ToU price	42.071	40.003	2.068	15.236	49.432
Without the DRP	42.275	40.409	-0.135	13.847	47.842

3.3.5.5 Impact of Uncertainty Modeling

In this section, the modeling of uncertainty is evaluated through comparison of the interval-stochastic and the MSPB methods. For simplicity, only the battery has been considered and $\gamma_{battery}$ is equal to 0 in this section. The amounts of total, day-ahead and real-time expected profits are compared in optimistic and conservative cases based on the interval-stochastic and MSPB methods. As seen in Table 3.9, the optimistic case of both methods is where α equals 1. However, the pessimistic case of the interval-stochastic and the MSPB methods is where α equals 0 and 0.4, respectively as seen in Table 3.10. Tables 3.9 and 3.10 show that the difference between the amounts of the expected profits in the optimistic and conservative cases of the interval-stochastic method are less than the profits of the MSPB method. Besides, Fig. 3.7 shows the impact of α on the total expected profit in both methods. Fig. 3.7 also illustrates that the worst case of the HEMS based on the interval-stochastic method is where α equals 0 and there is a linear pattern between increment in the optimistic coefficient and the total expected profit when uncertainty is modeled by the interval-stochastic method. This point makes the system more reliable and easier to analyze, as it is able to further mitigate the uncertainty, dealing with it in such way that its impact on the expected results is highly reduced. Moreover, the amount of the total expected profit in the worst case of the interval-stochastic method is less than its amount in the worst case of the MSPB method. Hence, the interval-stochastic method is more robust than the MSPB method to model the uncertainty in the proposed domestic energy management problem.

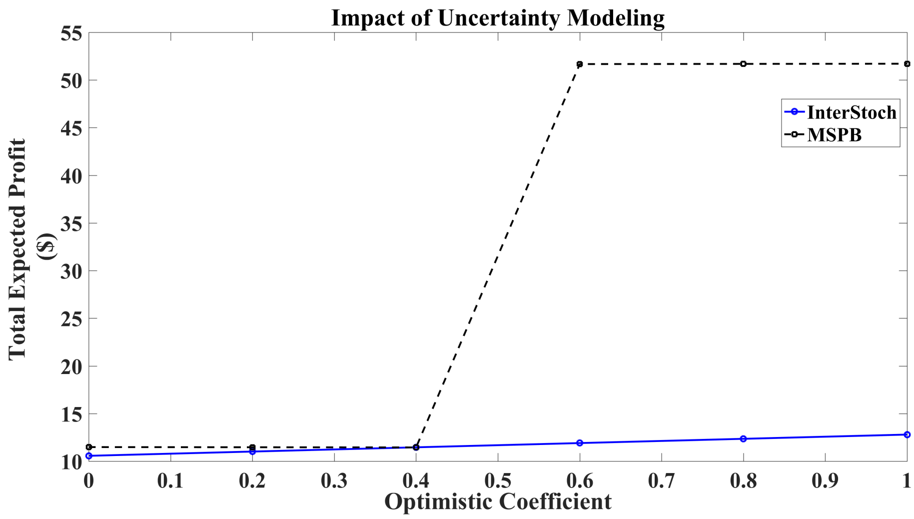

FIG. 3.7: Impact of uncertainty modeling on total expected profit of the system [Gazafroudi et al., 2017b].

TAB. 3.9: Impact of uncertainty modeling on day-ahead, real-time, and total expected profits under optimistic case [Gazafroudi et al., 2017b].

	Interval-stochastic (α=1)		MSPB (α=1)	
	With Uncertainty	Without Uncertainty	With Uncertainty	Without Uncertainty
EP_{total}	12.798	10.549	51.707	51.618
EP_{da}	7.234	4.836	49.232	49.232
EP_{rt}	5.564	5.713	2.475	2.386

TAB. 3.10: Impact of uncertainty modeling on day-ahead, real-time, and total expected profits under conservative case [Gazafroudi et al., 2017b].

	Interval-stochastic (α=0)		MSPB (α=0.4)	
	With Uncertainty	Without Uncertainty	With Uncertainty	Without Uncertainty
EP_{total}	10.569	10.549	11.449	51.618
EP_{da}	4.836	4.836	4.836	49.232
EP_{rt}	5.733	5.713	6.613	2.386

3.4 Conclusions

In this chapter, the HEMS has been defined to model flexible behavior of residential end-users and their uncertainty based on different types of optimization methods (e.g. interval, stochastic, and interval-stochastic). In this way, Stochastic Predicted Bands (SPB) method has been defined as a novel interval method and utilized to model the uncertainty of the decision-making variables in the home energy management problem. The performance of the proposed model has been evaluated based on the influences of the uncertainty of wind and PV power generation. Additionally, the performance of the MSPB has been assessed by analyzing the effects of the optimistic and prediction accuracy coefficients on the system simulation results. According to the simulation results, increasing the amount of the OC can make the optimistic impacts on the system outputs and increase the system EC and the power generation output of the uncertain energy resources.

In addition, the energy flexibility management of the HEMS based on the predictive dispatch model has been introduced. In the first stage, day-ahead domestic energy management problem has been modeled by an interval method to consider the uncertainty due to the prediction error of PV power generation. However, a real-time problem has been represented based on the stochastic method to consider the uncertainty. In this chapter, the HEMS has been modeled as an agent to transact its energy system independently. However, in Chapter 4, we present an optimal offering model for home energy management systems that is going to empower buildings and consumers to participate directly in the local electricity market.

Chapter 4

Optimal offering model for the home energy management system (*modelo óptimo de oferta de sistema de gestión de energía en la hogar*)

VNiVERSiDAD D SALAMANCA
CAMPUS DE EXCELENCIA INTERNACIONAL

Chapter 4

Optimal offering model for the home energy management system (*modelo óptimo de oferta de sistema de gestión de energía en la hogar*)

4.1 Introduction

In chapter 3, the HEMS has been defined to model the flexible behavior of residential end-users and their uncertainty based on different types of optimization methods (e.g. interval, stochastic, and interval-stochastic). However, the HEMS has been modeled as an agent to transact its energy system independently. In this chapter, an optimal offering model is presented for residential energy management systems that would empower buildings and consumers to participate directly as autonomous players in the local electricity market based on the findings of [Gazafroudi et al., 2019c]. This is a significant gap in the literature that should be promptly addressed because local energy markets are quickly becoming a reality, and small consumers and prosumers are not prepared to deal with this paradigm change. This may cause significant problems to the successful implementation and execution of local markets, since the consumer is the central player.

Therefore, this chapter presents a probabilistic scenario-based method for the autonomous management of the production and consumption of residential energy and for deriving optimal offering and bidding curves as a price-taker prosumer in a local electricity market. The proposed residential energy management problem consists of two stages: day-ahead and real-time stages. In the day-ahead stage, uncertainty in the electricity price and PV energy generation is modeled by interval-based scenarios. However, uncertainty in the HEMS is modeled through scenarios in the real-time stage, to determine optimal transactions between the smart home and the local electricity market. In our proposed HEMS, the battery is considered to provide the energy flexibility in the domestic system. According to our proposed model, the HEMS can send its optimal offering and bidding curves to the local market based on the uncertainties of the system a price-taker agent in the local market. On the other hand, our proposed HEMS without optimal bidding strategy is able to participate in peer-to-peer energy transactions with other small consumers, producers, and prosumers in its neighborhood through its optimum decisions in the management of the smart home.

The rest of this chapter is organized as follows. Section 4.2 represents uncertainty modelling. Our two-stage probabilistic scenario-based residential energy management problem is defined in Section 4.3 for which optimal offering and bidding strategies are derived. Finally, Section 4.4 studies the effectiveness of our proposed methodology.

4.2 Uncertainty representation

It is not easy to obtain an accurate market price forecast, due to the main characteristics of market prices. The main features of electricity prices are non-stationary mean and variance, multiple seasonality and the calendar effect. Uncertainty is associated with the predicted values. Although the electricity market prices are highly volatile, the market agents need to obtain an estimation from the price to make optimal decisions in the market [Conejo et al., 2010]. This section discusses the uncertainty modeling for power generation of the PV solar panels and market prices.

The modeling of uncertainty is one of the main concerns of the energy management systems. In [Soroudi and Amraee, 2013], authors studied energy systems from the perspective of decision making under uncertainty. In this way, in [Soroudi and Amraee, 2013], authors classified uncertainty modelling methods into probabilistic, interval, robust, possibilistic, hybrid probabilistic-possibilistic optimization approaches, and information gap decision theory. In [Chen et al., 2016b] and [Chen et al., 2016a], authors presented a combined forecasting technique using time-varying weights to model uncertainty of distributed energy resources in electric power systems. In this way, uncertainties have been modeled by interval bands and stochastic scenarios to be considered in interval linear programming, mixed-integer linear programming, and chance-constrained programming in a general structure. In addition, in [Chen et al., 2016a], bi-level programming has been presented to control air pollution and plan renewable energy resources in an inexact bi-level optimization model. In [Chen et al., 2016a], authors proposed a multi-level algorithm for decision making problems. According to the proposed model of [Chen et al., 2017], authors did not concentrate on interval bands of uncertain parameters as inputs of the system. Hence, solutions of the decision-makers have been represented by interval bands, and authors proposed how optimal solutions could be achieved if the solutions desired by the decision-makers are conflicting.

Among the uncertainties that influence the operation of the residential energy management systems, the solar irradiation and the electricity market prices have the highest impact [Farmani et al., 2018]. Hence, the uncertainties associated with these inputs are considered in the proposed model and the scheduling problem is developed as a stochastic scenario-based optimization model [Soares et al., 2017].

In stochastic models, a set of realizations should be considered, and therefore the foremost problem is to produce a set of scenarios for random variables, which can effectively characterize the probabilistic features of the data [Conejo et al., 2010] and[Ghazvini et al., 2015]. The initial set of scenarios is a large data set generated by the Monte Carlo Simulation (MCS) technique for representing power system uncertainties. The MCS parameters are the probability distribution functions of the forecast errors, which are obtained from the historical data [Ghazvini et al., 2015] and [Wu et al., 2015]. An additional term which can be positive or negative is added to the forecasted profile ($x^{forecasted}(t)$) to include the impact of uncertainty.

$$x^{s}(t) = x^{forecasted}(t) + x^{error,s}(t), \forall t, s. \tag{4.1}$$

According to (4.1), the error term, $x^s(t)$, is a zero-mean noise with standard deviation σ [Ghazvini et al., 2015] and [Bakirtzis et al., 2014]. Scenarios are represented with $x^s(t)$. In this model, the forecast errors are all assumed normally distributed. It is noticeable that electricity prices present very high spikes. However, it depends on the structure of the markets and the behavior of the participants. Some studies, e.g. [Ghalelou et al., 2016], Ref. [Ghalelou et al., 2016] adopts normal distribution to model market price uncertainty. Thus, the scenario tree concept can clearly explain how the discrete outcome for each stochastic input can be combined to construct the larger set of scenarios. A scenario tree consists of nodes that represent the states of the random variable at particular time points, branches to show different realizations of the variable and the root which shows the beginning point where the first stage decisions are made [Ghazvini et al., 2015]. Fig. 4.1 shows the scenario tree model for the proposed scenario-based stochastic programming model [Ghazvini et al., 2015]. $x^s_n(t)$ refers to the n^{th} random

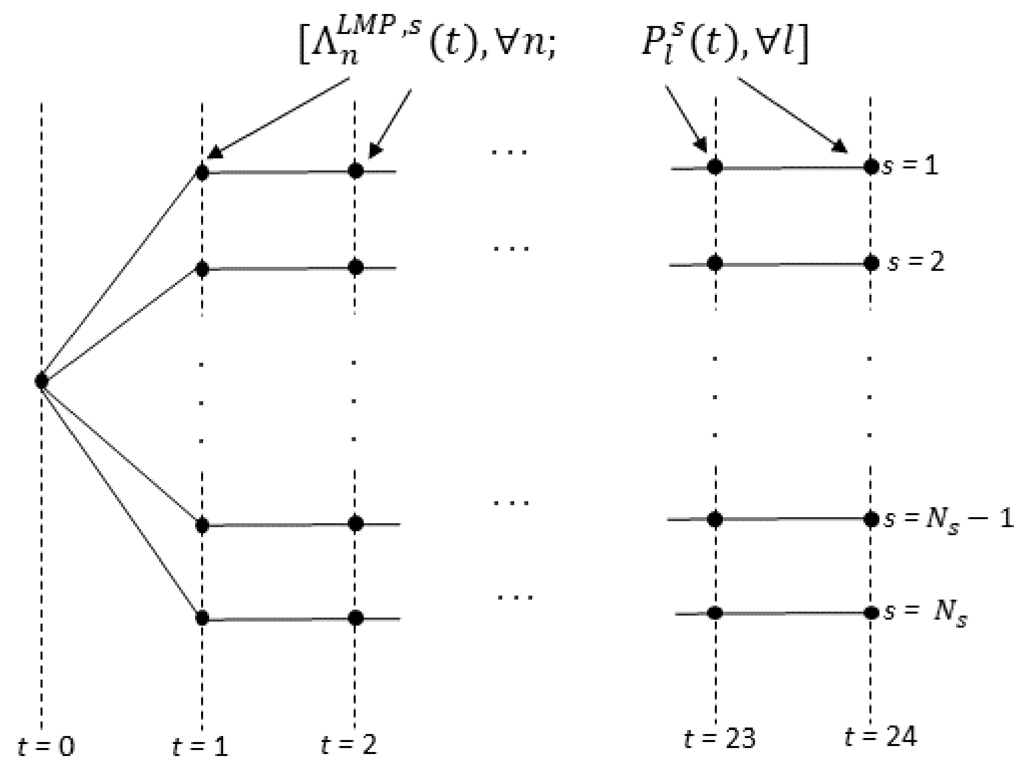

FIG. 4.1: Scenario tree representation [Ghazvini et al., 2015] and [Gazafroudi et al., 2019c].

variable. Variables can be of different nature. In this way, $x_1^s(t)$ may represent PV power generation and $x_2^s(t)$ can denote local market prices. The number of the nodes at the second stage is equal to the total number of scenarios. The occurrence probability of each scenario is equal to the product of the branches' probabilities [Ghazvini et al., 2015] and [Soares et al., 2016].

Using the initial set of generated realizations in the optimization problem will lead to a large-scale optimization model [Ghazvini et al., 2015]. It is essential to obtain a trade-off between model accuracy and the computation speed [Wu et al., 2016] and [Nasri et al., 2016]. In order to handle the computational tractability of the problem, the standard scenario reduction techniques developed in [Growe-Kuska et al., 2003] is implemented. The scenario reduction algorithms exclude the scenarios with low probabilities of occurrence and combines the scenarios that are close to each other in terms of statistic metrics [Growe-Kuska et al., 2003]. They determine a scenario subset of the prescribed cardinality and probability which is closest to the initial distribution in terms of a probability metric [Wu et al., 2015]. The main purpose of scenario reduction is to reduce the dimension of the problem through decreasing the number of variables and equations.

Thus, it would be possible to obtain the solutions more efficiently, without losing the main statistical characteristics of the initial dataset [Momber et al., 2015]. The drawback of applying these approaches is introducing imprecision in the final solution [Nasri et al., 2016]. The reduction algorithms proposed in [Growe-Kuska et al., 2003] incorporate algorithms with different computational performance and accuracy, namely fast backward method, fast backward/forward method and fast backward/backward method. The selection of the algorithms depends on the problem size and the expected solution accuracy [Wu et al., 2015] and [Growe-Kuska et al., 2003]. For instance, the best computational performance with the worst accuracy can be provided by the fast-backward method for large scenario trees. Furthermore, the forward method provides the best accuracy and the highest computational time. Thus, it is usually used where the size of reduced subset is small [Wu et al., 2015].

4.3 Problem Formulation

This section addresses a two-stage probabilistic residential energy problem in which it is necessary to determine optimal offering and bidding curves in the Day-Ahead (DA) and Real-Time (RT) Local Electricity Markets (LEMs). Energy is defined to be the only electrical commodity that is exchanged with the DA and RT local electricity markets. In the DA stage, the uncertainty of the PV energy generation and electricity price is modeled through interval-based scenarios, but the scenarios are used to model the corresponding uncertainty of the PV generation and electrical price in the RT stage. In this way, the two-stage interval-stochastic optimization method to solve the residential energy management problem is described. Then, our proposed problem is modeled by a two-stage stochastic programming. The difference between these two methods is to model the DA stage. While the uncertainties in the DA stage are modeled by interval bands in interval-optimization method, the stochastic interval-based scenarios are used to model the DA stage's uncertainty in the two-stage stochastic programming.

4.3.1 Two-stage Interval-Stochastic model

4.3.1.1 Objective function

In the context of this section, smart home- as a prosumer- is defined as an active player that can trade energy with the LEM in the DA and RT stages. Fig. 4.2 shows a schematic of our proposed residential energy management system. Thus, the objective is to maximize the expected profit of the energy served in the home and the energy transacted with the market. In this section, the PV system is considered as the

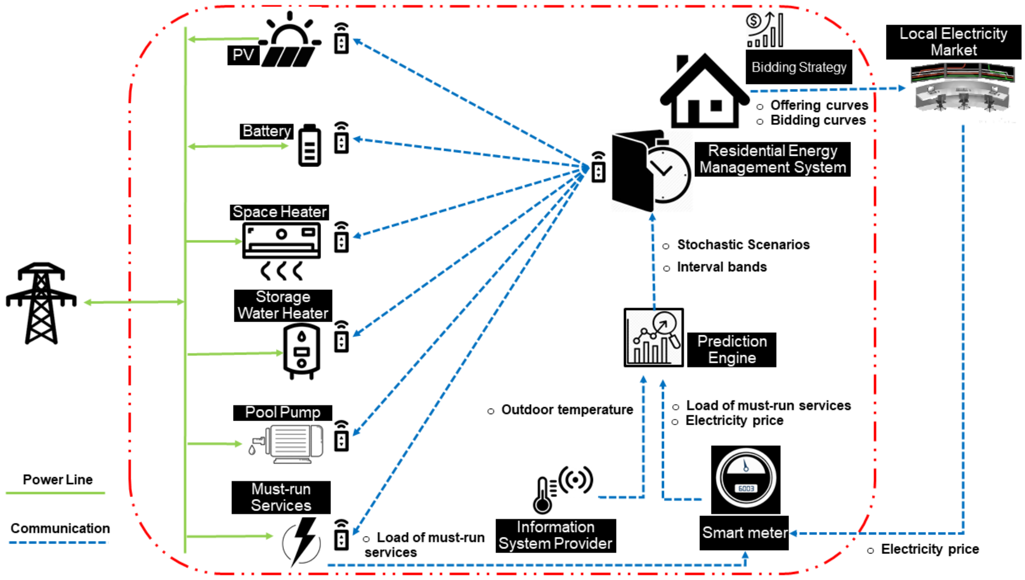

FIG. 4.2: A generic layout of our residential energy management system [Gazafroudi et al., 2019c].

distributed energy resource in the domestic energy system. The battery system acts as an energy storage system. Also, electrical loads consist of Space Heater (SH), storage water heater, pool pump, and must-run services.

$$\max EP = \sum_t[\lambda^{da}(t)(P^{da}_{sold}(t) - P^{da}_{net}(t))] \\ + \sum_\omega \pi_\omega[\sum_t(\lambda^{rt}_{sold}(t,\omega)\Delta P^{rt}_{sold}(t,\omega) - \lambda^{rt}_{net}(t,\omega)\Delta P^{rt}_{net}(t,\omega) \\ -V^S_{PV}S^{PV}(t,\omega) - \sum_j VOLL_j(t)ES^{rt}_j(t,\omega))]. \tag{4.2}$$

As seen in (4.2), the EP is represented as an objective function of the two-stage interval-stochastic residential energy management problem. The EP consists of two parts. The first part represents the profit of the day-ahead stage and the second part expresses the real-time expected profit. In the DA part, the revenue of selling the electrical energy to local market is stated as a first term, and the second term states the costs of buying the electrical energy from the market. In the RT part, they are presented in the following order: the revenue of extra energy sold in real-time, the cost of extra energy bought in real-time, PV's spillage cost, and the cost of loads' shedding. The constraints related to the DA and RT stages are represented in the following.

4.3.1.2 Day-ahead stage

As discussed further on, we account that the smart home can transact electrical energy in both day-ahead and real-time local electricity markets. Eqs. (4.3) and (4.4) represent the power flow limitation through the distribution line which ends at the home building. In this way, S_{max} expresses the maximum power capacity of the distribution line that links the smart home and the power grid (hereinafter, authors refer to the Smart HomE as "SHE" for short, note that the abbreviation does not intend to make any association with gender). Also, $v^{da}(t)$ is a binary variable which states the transacted energy status. In other words, SHE purchases energy from the local market when $v^{da}(t)$ is equal to 1, and SHE sells energy to the local market when $v^{da}(t)$ equals 0. Eqs. (4.3) and (4.4) guarantee that the SHE cannot act as a producer and a consumer, simultaneously. In this model, the smart home provides for its demand first and then SHE sells its extra energy to the local market.

$$0 \leq P_{net}^{da}(t) \leq S_{max} v^{da}(t), \forall t. \tag{4.3}$$

$$0 \leq P_{sold}^{da}(t) \leq S_{max}(1 - v^{da}(t)), \forall t. \tag{4.4}$$

Moreover, Eq. (4.5) expresses that the energy sold to the local market consists of two terms: the energy produced by the PV system, $P_{pv,out}^{da}(t)$, and the discharged energy, $P_{dis,out}^{da}(t)$, of the battery system; these are injected into the power grid in the day-ahead stage. Besides, the flexibility coefficient, γ, is multiplied by the discharged and charged energy of the battery in the day-ahead stage, obtaining a value between 0 and 1. If γ equals 0 it means that the battery is not considered in the day-ahead residential energy management problem. On the other hand, the battery is considered to have full capacity in the day-ahead stage of the problem when γ equals 1. Also, only the corresponding portion of the battery's capacity will be considered in the day-ahead stage when γ gets an amount between 0 and 1.

$$P_{sold}^{da}(t) = P_{pv,out}^{da}(t) + \gamma P_{dis,out}^{da}(t), \forall t. \tag{4.5}$$

Eq. (4.6) establishes the power balance equation due to the energy output of the PV system and the discharged energy of the battery injected into the home ($P_{pv,in}^{da}(t)$ and $P_{dis,in}^{da}(t)$, respectively), the electrical energy bought from the local market, $P_{net}^{da}(t)$, total energy consumption of the domestic loads, $EL^{da}(t)$, and charged energy of the battery system, $P_{ch}^{da}(t)$.

$$P_{net}^{da}(t) + P_{pv,in}^{da}(t) + \gamma P_{dis,in}^{da}(t) = EL^{da}(t) + \gamma P_{ch}^{da}(t), \forall t. \tag{4.6}$$

As discussed further in this section, the DA stage's uncertainty is modeled by interval bands in the two-stage interval-stochastic model. Eq. (4.7) presents the maximum and minimum bands of the price in the day-ahead local market. Hence, $\lambda^{pred}(t)$ and $\sigma_{price}^{up}(t)/\sigma_{price}^{dn}(t)$ are predicted price and upper/lower predicted price error, respectively. Also, price is the corresponding Optimistic Coefficient (OC) of the electricity price. The OC is a slack parameter for the decision-maker which can take amounts between 0 and 1. If α_{price} equals 0/1 the uncertainty of price is modeled as conservative/optimistic.

$$\lambda^{pred}(t) - \sigma_{price}^{dn}(t)(1 - \alpha_{price}) \leq \lambda^{da}(t) \leq \lambda^{pred}(t) + \sigma_{price}^{up}(t)\alpha_{price}, \forall t. \tag{4.7}$$

Moreover, the following constraints correspond to all devices in the smart home. The total potential energy generated by the PV system in each time period, $P_{pv,p}^{da}(t)$, is the sum of the produced PV's energy that is injected into the home, $P_{pv,in}^{da}(t)$, and the power grid, $P_{pv,out}^{da}(t)$ as represented in Eq. (4.8). Also, $k(t)$ is a binary variable which states the dispatched status of the PV system.

$$P_{pv,p}^{da}(t)k(t) = P_{pv,in}^{da}(t) + P_{pv,out}^{da}(t), \forall t. \tag{4.8}$$

Furthermore, our uncertainty modeling relies on confidence intervals for energy generation of the PV as well as price. Hence, Eq. (4.9) deals with the possibility of point forecasting error. This way, $P_{PV}^{pred}(t)$ and $+\sigma_{pv}^{up}(t)/\sigma_{pv}^{dn}(t)$ are predicted PV energy generation and upper/lower predicted energy error, respectively. Also, α_{pv} is the corresponded Optimistic Coefficient (OC) of the PV energy produced that can be between 0 and 1.

$$P_{PV}^{pred}(t) - \sigma_{pv}^{dn}(t)(1 - \alpha_{pv}) \leq P_{pv,p}^{da}(t) \leq P_{PV}^{pred}(t) + \sigma_{pv}^{up}(t)\alpha_{pv}, \forall t. \tag{4.9}$$

The battery is used based on the charging and discharging strategies in the residential energy management problem. Eq. (4.10) represents the state-of-charge (SOC) balance equation of the battery, where C_i is the initial state of charge in the battery.

$$C^{da}(t) = C^{da}(t-1) + P^{da}_{ch}(t)\eta_{H2B} - \frac{P^{da}_{dis}(t)}{\eta_{B2H}}, \forall t \geq 2. \tag{4.10}$$
$$C^{da}(t) = C_i + P^{da}_{ch}(t)\eta_{H2B} - \frac{P^{da}_{dis}(t)}{\eta_{B2H}}, \forall t = 1.$$

Eq. (4.11) presents the maximum and minimum limitations of the battery's SOC.

$$P_b^{min} \leq C^{da}(t) \leq P_b^{max}, \forall t. \tag{4.11}$$

The ramping upper and lower constraints related to the SOC are expressed in (4.12).

$$-w^{min} \leq C^{da}(t) - C^{da}(t-1) \leq w^{max}, \forall t \geq 2. \tag{4.12}$$
$$-w^{min} \leq C^{da}(t) - C_i \leq w^{max}, \forall t = 1.$$

Maximum and minimum limitations of the discharged and charged energy of the battery are stated in (4.13) and (4.14), respectively.

$$0 \leq P^{da}_{dis}(t) \leq w^{max} u^{da}(t), \forall t. \tag{4.13}$$
$$0 \leq P^{da}_{ch}(t) \leq w^{min}(1 - u^{da}(t)), \forall t. \tag{4.14}$$

Eq. (4.15) represents that the total discharged energy of the battery system, $P^{da}_{dis}(t)$, is the sum of discharged energies that are injected into the home, $P^{da}_{dis,in}(t)$, and the power grid, $P^{da}_{dis,out}(t)$, in the day-ahead stage.

$$P^{da}_{dis}(t) = P^{da}_{dis,in}(t) + P^{da}_{dis,out}(t), \forall t. \tag{4.15}$$

In our proposed model, it is considered that the day-ahead electrical loads are equal to the predicted load as seen in (4.16), and their corresponding equations are defined only in the real-time stage. Moreover, for the sake of simplicity, the uncertainty of the electrical loads is not considered in this section.

$$EL^{da}(t) = EL^{pred}(t), \forall t. \tag{4.16}$$

4.3.1.3 Real-time stage

In the DA stage the smart home can exchange energy with the LEM. However, in contrast to the DA stage, stochastic programming is used to model the uncertainty of the electricity price and PV energy generation in the RT stage, and the prices of sold and bought electricity can be different in the RT stage. The power balance equation in the RT is expressed in Eq. (4.17) to represent the mismatch between the DA transacted energy and RT expected exchanged energy. According to Eq. (4.17), the sum of energy bought in the DA and RT markets, $P^{da}_{net}(t)$ and $\Delta P^{rt}_{net}(t,\omega)$, produced energy of the PV system in the RT, $P^{rt}_{pv}(t,\omega)$, and discharged energy of the battery in the RT, $P^{rt}_{dis}(t,\omega)$, equal total electrical energy consumption in the RT, $EL^{rt}(t,)$, charged energy of the battery in the RT, $P^{rt}_{ch}(t,\omega)$, the energy sold to the local market in the DA and RT, $P^{da}_{sold}(t)$ and $\Delta P^{rt}_{sold}(t,\omega)$, minus total energy loss, $ES^{rt}(t,\omega)$.

$$\begin{aligned} P^{da}_{net}(t) + P^{rt}_{pv}(t,\omega) + P^{rt}_{dis}(t,\omega) + \Delta P^{rt}_{net}(t,\omega) = EL^{rt}(t,\omega) - ES^{rt}(t,\omega) \\ P^{rt}_{ch}(t,\omega) + P^{da}_{sold}(t) + \Delta P^{rt}_{sold}(t,\omega), \forall t, \omega. \end{aligned} \tag{4.17}$$

Eq. (4.18) presents the power flow limitation in a distribution line that ends at the smart home. It is noticeable that both, Eqs. (4.17) and (4.18), are coupling constraints that cause the DA and RT problems to be solved simultaneously.

$$S_{max} \leq P^{da}_{net}(t) + \Delta P^{rt}_{net}(t,\omega) - P^{da}_{sold}(t) - \Delta P^{rt}_{sold}(t,\omega) \leq S_{max}, \forall t, \omega. \tag{4.18}$$

In addition, Eqs. (4.19) and (4.20) ensure that the smart home cannot be a producer and a consumer in the same scenario in the real-time stage.

$$0 \leq \Delta P^{rt}_{net}(t,\omega) \leq S_{max} v^{rt}(t,\omega), \forall t, \omega. \tag{4.19}$$

$$0 \leq \Delta P^{rt}_{sold}(t,\omega) \leq S_{max}(1 - v^{rt}(t,\omega)), \forall t, \omega. \tag{4.20}$$

Eq. (4.21) represents the energy output equation of PV in the real-time stage. According to (4.21), $P_{pv}^{scen}(t,\omega)$ presents the stochastic potential PV energy generation, and $S^{pv}(t,\omega)$ is the spilled energy of the PV system.

$$P_{pv}^{rt}(t,\omega) = P_{pv}^{scen}(t,\omega) - S^{pv}(t,\omega), \forall t, \omega. \tag{4.21}$$

As well as Eq. (4.8), Eq. (4.22) presents the total energy generated by the PV system in the RT stage that is the sum of energy produced by the PV which is injected into the home, $P_{pv,in}^{rt}(t,\omega)$, and the energy grid, $P_{pv,out}^{rt}(t,\omega)$.

$$P_{pv}^{rt}(t,\omega) = P_{pv,in}^{rt}(t,\omega) + P_{pv,out}^{rt}(t,\omega), \forall t, \omega. \tag{4.22}$$

The maximum and minimum bands of spilled PV energy produced are represented in (4.23).

$$0 \leq S^{pv}(t,\omega) \leq P_{pv}^{scen}(t,\omega), \forall t, \omega. \tag{4.23}$$

In the following, the battery system's constraints in the RT stage are stated in (4.24)-(4.29).

$$C^{rt}(t,\omega) = C^{rt}(t-1,\omega) + P_{ch}^{rt}(t,\omega)\eta_{H2B} - \frac{P_{dis}^{rt}(t,\omega)}{\eta_{B2H}}, \forall t \geq 2, \omega. \tag{4.24}$$

$$C^{rt}(t=1,\omega) = C_i + P_{ch}^{rt}(t=1,\omega)\eta_{H2B} - \frac{P_{dis}^{rt}(t=1,\omega)}{\eta_{B2H}}, t = 1, \forall \omega.$$

$$P_b^{min} \leq C^{rt}(t,\omega) \leq P_b^{max}, \forall t, \omega. \tag{4.25}$$

$$-w^{min} \leq C^{rt}(t,\omega) - C^{rt}(t-1,\omega) \leq w^{max}, \forall t \geq 2, \omega. \tag{4.26}$$

$$-w^{min} \leq C^{rt}(t,\omega) - C_i \leq w^{max}, t = 1, \forall \omega.$$

$$0 \leq P_{dis}^{rt}(t,\omega) \leq w^{max} u^{rt}(t,\omega), \forall t, \omega. \tag{4.27}$$

$$0 \leq P_{ch}^{rt}(t,\omega) \leq w^{min}(1 - u^{rt}(t,\omega)), \forall t, \omega. \tag{4.28}$$

$$P_{dis}^{P} rt(t,\omega) = P_{dis,in}^{rt}(t,\omega) + P_{dis,out}^{rt}(t,\omega), \forall t, \omega. \tag{4.29}$$

In the context of this section, electrical loads consist of loads that can be controllable and/or shiftable, or not. In this section, Space Heater (SH) is a controllable load, Storage Water Heater (SWH) and Pool Pump (PP) are modeled as shiftable loads, and Must-Run Services (MRSs) are defined as a class of loads that are non-controllable and non-shiftable. Eqs. (4.30) and (4.31) represent the total electrical energy consumption and energy shedding in the RT stage.

$$\begin{aligned} E^{rt}(t,\omega) =_j EL_j^{rt}(t,\omega) = EL_{sh}^{rt}(t,\omega) + EL_{swh}^{rt}(t,\omega) \\ +EL_{pp}^{rt}(t,\omega) + EL_{mrs}^{rt}(t,\omega), \forall t,\omega. \end{aligned} \tag{4.30}$$

$$\begin{aligned} ES^{rt}(t,\omega) = \textstyle\sum_j ES_j^{rt}(t,\omega) = ES_{sh}^{rt}(t,\omega) + ES_{swh}^{rt}(t,\omega) \\ +ES_{pp}^{rt}(t,\omega) + ES_{mrs}^{rt}(t,\omega), \forall t,\omega. \end{aligned} \tag{4.31}$$

Space heater controls the indoor temperature at the desired temperature band. Eq. (4.32) states the linear equation between the indoor and outdoor temperature and the electrical consumption of the space heater. Here, θ_i^{in} is the initial indoor temperature which, in this model is assumed to equal the desired temperature, θ_{des}^{in}.

$$\begin{aligned} \theta^{in}(t+1,\omega) = e^{\frac{-1}{RC}}\theta^{in}(t,\omega) + R(1-e^{\frac{-1}{RC}})L_{sh}^{rt}(t,\omega) \\ +(1-e^{\frac{-1}{RC}})\theta^{out,pred}(t,\omega), \forall t \geq 2,\omega. \\ \theta in(t,\omega) = \theta_i^{in} = \theta_{des}^{in}, t = 1, \forall\omega. \end{aligned} \tag{4.32}$$

Eq. (4.33) represents that the indoor temperature is limited to 1 degree above and below the desired temperature.

$$-1 \leq \theta^{in}(t,\omega) - \theta_{des}^{in} \leq 1, \forall t,\omega. \tag{4.33}$$

Besides, the corresponding maximum and minimum bands of the space heater's load consumption in (4.34).

$$0 \leq L_{sh}^{rt}(t,\omega) \leq L_{sh}^{max}, \forall t,\omega. \tag{4.34}$$

Eq. (4.35) presents how energy consumption of the SH is determined based on its power consumption.

$$EL_{sh}^{rt}(t,\omega) = \frac{L_{sh}^{rt}(t,\omega) - L_{sh}^{rt}(t-1,\omega)}{2}, \forall t,\omega.$$
$$EL_{sh}^{rt}(t,\omega) = \frac{L_{sh}^{rt}(t,\omega) - L_{i}^{sh}}{2}, t = 1, \forall\omega. \tag{4.35}$$

Energy shedding constraint of the SH is expressed in (4.36).

$$0 \leq ES_{sh}^{rt}(t,\omega) \leq EL_{sh}^{rt}(t,\omega), \forall t,\omega. \tag{4.36}$$

The SWH is in charge of storing the heat in the water tank. The maximum and minimum constraints of the storage water heater's load consumption are stated in Eq. (4.37).

$$0 \leq L_{swh}^{rt}(t,\omega) \leq L_{swh}^{max}, \forall t,\omega. \tag{4.37}$$

Besides, Eq. (4.38) represents that the total energy consumption of the SWH should be equal to its maximum energy capacity, and it guarantees that the SWH is only a shiftable load, not a shavable load.

$$\textstyle\sum_{t=1}^{N_T} L_{swh}^{rt}(t,\omega) = U_{swh}^{max}, \forall\omega. \tag{4.38}$$

Also, Eq. (4.39) represents that relation between energy and load consumption of the SWH.

$$EL_{swh}^{rt}(t,\omega) = \frac{L_{swh}^{rt}(t,\omega) - L_{swh}^{rt}(t-1,\omega)}{2}, \forall t \geq 2,\omega.$$
$$EL_{swh}^{rt}(t,\omega) = \frac{L_{swh}^{rt}(t,\omega) - L_{i}^{swh}}{2}, t = 1, \forall\omega. \tag{4.39}$$

Eq. (4.40) states the energy shedding constraint related to the SWH.

$$0 \leq ES_{swh}^{rt}(t,\omega) \leq EL_{swh}^{rt}(t,\omega), \forall t,\omega. \tag{4.40}$$

The PP should not run more than TON hours in a day as represented in (4.41).

$$L_{pp}^{rt}(t,\omega) = L_{pp}^{max}, \forall t, \omega. \tag{4.41}$$

Besides, Eq. (4.42) represents when the PP is "ON" it consumes its maximum load capacity. In (4.41) and (4.42), $z(t,\omega)$ is a binary variable that represents the "ON"/ "OFF" status of the PP. This way, $z(t,\omega)$ is equal to 1 when the PP is "ON", and $z(t,\omega)$ equals 0 when the PP is "OFF".

$$sum_{t=1}^{N_T} z(t,\omega) \leq T_{ON}, \forall \omega. \tag{4.42}$$

The relation between the energy and power consumption of the PP is stated in (4.43).

$$EL_{pp}^{rt}(t,\omega) = \frac{L_{pp}^{rt}(t,\omega) - L_{pp}^{rt}(t-1,\omega)}{2}, \forall t \geq 2, \omega. \tag{4.43}$$
$$EL_{pp}^{rt}(t,\omega) = \frac{L_{pp}^{rt}(t,\omega) - L_{i}^{pp}}{2}, t = 1, \forall \omega.$$

Also, the limitations regarding the shedded energy of the PP is expressed in (4.44).

$$0 \leq ES_{pp}^{rt}(t,\omega) \leq EL_{pp}^{rt}(t,\omega), \forall t, \omega. \tag{4.44}$$

The MRSs include the loads that should be provided quickly - e.g. lighting, entertainment, etc. Hence, MRS are not dispatchable, and the quantity of them are determined based on the prediction as seen in (4.45).

$$0 \leq L_{mrs}^{rt}(t,\omega) \leq L_{mrs}^{pred}(t), \forall t, \omega. \tag{4.45}$$

The relation between the energy and power consumption and energy shedding of the MRSs are obtained the same as SH, SWH and PP as represented in (4.46) and (4.47), respectively.

$$EL_{mrs}^{rt}(t,\omega) = \frac{L_{mrs}^{rt}(t,\omega) - L_{mrs}^{rt}(t-1,\omega)}{2}, \forall t \geq 2, \omega. \tag{4.46}$$
$$EL_{mrs}^{rt}(t,\omega) = \frac{L_{mrs}^{rt}(t,\omega) - L_{i}^{mrs}}{2}, t = 1, \forall \omega.$$
$$0 \leq ES_{mrs}^{rt}(t,\omega) \leq EL_{mrs}^{rt}(t,\omega), \forall t, \omega. \tag{4.47}$$

All equations- which are represented above- described physical home system's objective and constraints, and our proposed model for optimal bidding strategy has not been represented up to now. In the following, we present an optimal bidding strategy for our proposed residential energy management system.

4.3.2 Optimal bidding strategy

The equations presented in this section derive optimal offering (when SHE is a producer) and biding (when SHE is a consumer) curves of the smart home for each decision-making time period in the DA and RT local electricity markets. In the context of this work, the offering curves should be ascending. However, the bidding curves should be descending. Eqs. (4.48) and (4.49) represent the offering model of the smart home in the RT stage.

$$\Delta P_{net}^{rt}(t,\omega) \geq \Delta P_{net}^{rt}(t,\omega^{'}), \forall \omega > \omega^{'} \& \lambda_{net}^{rt}(t,\omega) < \lambda_{net}^{rt}(t,\omega^{'}), \forall t. \tag{4.48}$$

$$\Delta P_{sold}^{rt}(t,\omega) \geq \Delta P_{sold}^{rt}(t,\omega^{'}), \forall \omega > \omega^{'} \& \lambda_{sold}^{rt}(t,\omega) > \lambda_{sold}^{rt}(t,\omega^{'}), \forall t. \tag{4.49}$$

As seen in the above constraints, Eq. (4.48) makes the descending bidding curves. On the other hand, Eq. (4.49) guarantees that the offering curves should be ascending. However, the above equations are not practical in an offering model of the smart home in the day-ahead stage because the uncertainty of PV energy generation and day-ahead electricity price is modeled through interval bands. In this situation, one solution is to use an iterative algorithm according to [Baringo and Conejo, 2011] to derive offering and bidding curves for the smart home in the day-ahead stage. However, the PV energy generation/electricity price will get its maximum/minimum amount in each iteration interval. Hence, using the iterative algorithm is not an appropriate solution for an offering model in the DA stage. This way, a new method for bidding strategy via interval-based scenarios is presented in this section as described in next subsection.

4.3.3 Two-stage Stochastic model

According to our proposed method, the scenarios for the day-ahead stage are come from the interval bands. This way, interval bands of the day-ahead PV energy generation and electricity price are divided into two scenarios that consist of: minimum and maximum bands (however, these scenarios can be extended). In this case, total day-ahead scenarios, N_{φ}, equals $N_{ib}^{N_p}$. In this way, N_{ib} and N_p represent number of number of scenarios in each interval band in each time period, and number of uncertain parameters.

Therefore, in this section, N_φ equals 4, Nib equals 2 as mentioned above, and Np is equal to 2 because only the uncertainty of the PV energy generation and electricity price is considered in this section. Also, the corresponding probability, , for all scenarios equal $\frac{1}{N_\varphi}$ which are equal to 0.25 $(=\frac{1}{4})$ in this section.

Therefore, new scenarios are added to the variables of the DA stage instead of interval bands of the PV energy generation and electricity price. The scenarios in the DA stage will be represented by . In this way, the expected profit based on the two-stage stochastic model of the HEMS is represented in (4.50).

$$\begin{gathered}\max EP = \sum_\varphi [\sum_t [\lambda^{da}(t,\varphi)(P^{da}_{sold}(t,\varphi) - P^{da}_{net}(t,))]] \\ + \sum_\omega \pi_\omega [\sum_t (\lambda^{rt}_{sold}(t,\omega)\Delta P^{rt}_{sold}(t,\omega) - \lambda^{rt}_{net}(t,\omega)\Delta P^{rt}_{net}(t,\omega) \\ -V^S_{PV} S^{PV}(t,\omega) - \sum_j VOLL_j(t) ES^{rt}_j(t,\omega))].\end{gathered} \tag{4.50}$$

As seen in (4.50), only variables and parameters of the day-ahead stage depend on φ in comparison to (4.2). In the following, Eqs. (4.3) -(4.18) will be redefined in (4.51) -(4.66), respectively. In this way, Eqs. (4.51) and (4.52) express the power flow limitation for the distribution line which ends at the building.

$$0 \leq P^{da}_{net}(t,\varphi) \leq S_{max} v^{da}(t,\varphi), \forall t,\varphi. \tag{4.51}$$

$$0 \leq P^{da}_{sold}(t,\varphi) \leq S_{max}(1 - v^{da}(t,\varphi)), \forall t,\varphi. \tag{4.52}$$

Eq. (4.53) represents that the energy sold to the local market consists of energy produced by the PV system discharged energy of the battery system.

$$P^{da}_{sold}(t,\varphi) = P^{da}_{pv,out}(t,\varphi) + \gamma P^{da}_{dis,out}(t,\varphi), \forall t,\varphi. \tag{4.53}$$

Eq. (4.54) states the power balance equation in the building.

$$P^{da}_{net}(t,\varphi) + P^{da}_{pv,in}(t,\varphi) + \gamma P^{da}_{dis,in}(t,\varphi) = EL^{da}(t,\varphi) + \gamma P^{da}_{ch}(t,\varphi), \forall t,\varphi. \tag{4.54}$$

Eq. (4.55) presents the scenarios for the day-ahead electricity price which are come from its interval bands.

$$\lambda^{da}(t,\varphi_1) = \lambda^{da}(t,\varphi_2) = \lambda^{pred}(t) - \sigma^{dn}_{price}(t)(1-\alpha_{price}), \forall t. \qquad (4.55)$$
$$\lambda^{da}(t,\varphi_3) = \lambda^{da}(t,\varphi_4) = \lambda^{pred}(t) + \sigma^{up}_{price}(t)\alpha_{price}, \forall t.$$

Eq. (4.56) represents the potential energy generated by the PV system.

$$P^{da}_{pv,p}(t,\varphi)k(t,\varphi) = P^{da}_{pv,in}(t,\varphi) + P^{da}_{pv,out}(t,\varphi), \forall t, \varphi. \qquad (4.56)$$

The scenarios for the day-ahead PV energy generation based on its interval bands are represented in (4.57).

$$P^{da}_{pv,p}(t,\varphi_1) = P^{da}_{pv,p}(t,\varphi_3) = P^{pred}_{PV}(t) - \sigma^{dn}_{pv}(t)(1-\alpha_{pv}), \forall t. \qquad (4.57)$$
$$P^{da}_{pv,p}(t,\varphi_2) = P^{da}_{pv,p}(t,\varphi_4) = P^{pred}_{PV}(t) + \sigma^{up}_{pv}(t)\alpha_{pv}, \forall t.$$

Eq. (4.58) expresses the state-of-charge (SOC) equation of the battery in the day-ahead stage.

$$C^{da}(t,\varphi) = C^{da}(t-1,\varphi) + P^{da}_{ch}(t,\varphi)\eta_{H2B} - \frac{P^{da}_{dis}(t,\varphi)}{\eta_{B2H}}, \forall t \geq 2, \varphi. \qquad (4.58)$$
$$C^{da}(t,\varphi) = C_i + P^{da}_{ch}(t,\varphi)\eta_{H2B} - \frac{P^{da}_{dis}(t,\varphi)}{\eta_{B2H}}, \forall t = 1, \varphi.$$

Eq. (4.59) represents the maximum and minimum bands of the battery's SOC.

$$P^{min}_{b} \leq C^{da}(t,\varphi) \leq P^{max}_{b}, \forall t, \varphi. \qquad (4.59)$$

The ramping upper and lower limitations related to the SOC are stated in (4.60).

$$-w^{min} \leq C^{da}(t,\varphi) - C^{da}(t-1,\varphi) \leq w^{max}, \forall t \geq 2, \varphi. \tag{4.60}$$
$$-w^{min} \leq C^{da}(t,\varphi) - C_i \leq w^{max}, \forall t = 1, \varphi.$$

Eqs. (4.61) and (4.62) represent maximum and minimum constraints of the discharged and charged energy of the battery, respectively.

$$0 \leq P^{da}_{dis}(t,\varphi) \leq w^{max} u^{da}(t,\varphi), \forall t, \varphi. \tag{4.61}$$

$$0 \leq P^{da}_{ch}(t,\varphi) \leq w^{min}(1 - u^{da}(t,\varphi)), \forall t, \varphi. \tag{4.62}$$

Eq. (4.63) presents that the total discharged energy of the battery system.

$$P^{da}_{dis}(t,\varphi) = P^{da}_{dis,in}(t,\varphi) + P^{da}_{dis,out}(t,\varphi), \forall t, \varphi. \tag{4.63}$$

As highlighted before, in this section, the uncertainty of the electrical loads is not seen in the day-ahead stage, and the day-ahead electrical loads are considered to be equal to their point forecasting as seen in (4.64).

$$EL^{da}(t,\varphi) = EL^{pred}(t), \forall t, \varphi. \tag{4.64}$$

Eq. (4.65) represents the power balance equation in the real-time stage.

$$P^{da}_{net}(t,\varphi) + P^{rt}_{pv}(t,\omega) + P^{rt}_{dis}(t,\omega) + \Delta P^{rt}_{net}(t,\omega) = EL^{rt}(t,\omega) - ES^{rt}(t,\omega) \tag{4.65}$$
$$+P^{rt}_{ch}(t,\omega) + P^{da}_{sold}(t,\varphi) + \Delta P^{rt}_{sold}(t,\omega), \forall t, \omega, \varphi.$$

Eq. (4.66) states the power flow constraints a distribution line which end at the building.

$$-S_{max} P^{da}_{net}(t,\varphi) + \Delta P^{rt}_{net}(t,\omega) - P^{da}_{sold}(t,\varphi) - \Delta P^{rt}_{sold}(t,\omega) S_{max}, \forall t, \omega, \varphi. \tag{4.66}$$

Hence, the offering model for deriving the offering and bidding curves of the smart home presented according to (4.67) and (4.68):

$$
\begin{aligned}
&P^{da}_{net}(t,\varphi) \geq P^{da}_{net}(t,\varphi^{'}), \forall \varphi > \varphi^{'} \& \lambda^{da}(t,\varphi) < \lambda^{da}(t,\varphi^{'}), \forall t. \qquad (4.67)\\
&P^{da}_{sold}(t,\varphi) \geq P^{da}_{sold}(t,\varphi^{'}), \forall \varphi > \varphi^{'} \& \lambda^{da}(t,\varphi) > \lambda^{da}(t,\varphi^{'}), \forall t.
\end{aligned}
$$

This way, according to the reformulated equations, the decision-making problem is represented below:

$$
\begin{aligned}
&\max(4.50)\\
&s.t.: (4.19) - (4.49), (4.51) - (4.68).
\end{aligned}
$$

The above model expressed our proposed optimal bidding strategy for the HEMS via two-stage stochastic programming.

4.4 Case studies

4.4.1 Cases

The residential system that has been used in [Gazafroudi et al., 2019c] is utilized as a test system in this section. The proposed Mixed Integer Linear Programming (MILP) is solved in GAMS 24.2.3 [Soroudi, 2017]. Also, Table 2 presents data of the proposed domestic system. In addition to data presented in Tables 4.1-4.4, S_{max} is considered to equal 10 kW, L^{mrs}_{i} equals 0 kW, and V^{S}_{PV} 1 \$/kWh.

Prediction, interval bands, and scenarios data are presented in Appendix Section.The loads prediction data is stated in Table 4.5. Table 4.6 presents the predicted day-ahead central forecasting and interval errors of price and PV energy generation. As it can be seen in Table 4.6, upper and lower forecasting errors are considered to be equal in this paper. Moreover, the real-time electricity price and PV energy generation scenarios are reduced to ten scenarios for each time period as presented in Tables 4.7 and 4.8, respectively. The corresponding probabilities of the real-time scenarios are stated in Table 4.9. It should be highlighted that the sold and bought electricity price in the real-time are considered to be equal in this case study. Hence, $\lambda^{rt}(t,\omega)$ is defined in Table 5 instead of $\lambda^{rt}_{net}(t,\omega)$ and $\lambda^{rt}_{sold}(t,\omega)$.

TAB. 4.1: Data of the battery [Gazafroudi et al., 2019c].

Battery		
η_{H2B}	Charging efficiency	0.90
η_{B2H}	Discharging efficiency	0.9
C_i	Initial state of the charge	0.48kWh
P_b^{max}	Maximum storage level	2.40 kWh
P_b^{min} Minimum storage level	0.48 kWh	
w^{max}	Maximum ramping rate	0.40 kWh
w^{min}	Minimum ramping rate	0.40 kWh

TAB. 4.2: Data of the space heater [Gazafroudi et al., 2019c].

Space heater		
L_i^{sh}	Initial load consumption	1.00 kW
θ_i^{in}	Initial indoor temperature	23°C
C	Thermal energy capacity	0.525 kWh/°C
R	Thermal resistance of the building	18 °C/kWh
L_{sh}^{max}	Maximum electrical consumption	5.525 kWh

TAB. 4.3: Data of the storage water heater [Gazafroudi et al., 2019c].

Storage water heater		
L_i^{swh}	Initial load consumption	0.00 kW
L_{swh}^{max}	Maximum electrical consumption	3.00 kW
U_{swh}^{max}	Daily energy consumption	10.46 kWh

TAB. 4.4: Data of the pool pump [Gazafroudi et al., 2019c].

Pool pump		
L_i^{pp}	Initial load consumption	0.00 kW
L_{pp}^{max}	Maximum electrical consumption	1.10 kW
T_{ON}	Maximum daily-hours	1.00 h

As mentioned before, the predicted day-ahead home's energy consumption and load of must-run services in the real-time do not depend on the scenarios in our proposed model, only their point forecasting is modeled in this section. Characteristics of the residential system are described in the following:

- Battery can store between 0.48 kWh and 2.4 kWh, and its maximum charging and discharging rates are 400 W. Charging and discharging rates represent maximum amount of power of the battery that can be charged or discharged in each

TAB. 4.5: Day-ahead predicted energy consumption of the home and predicted load of the must-run services in real-time [Gazafroudi et al., 2019c].

Time (h)	$\mathrm{EL}^{pred}(t)(kWh)$	$\mathrm{L}^{pred}_{mrs}(t)(kW)$
1	4.605	0.005
2	4.605	0.005
3	4.605	0.005
4	4.605	0.005
5	3.065	0.005
6	2.605	0.005
7	2.435	0.005
8	2.245	0.005
9	2.055	0.005
10	1.865	0.005
11	1.675	0.005
12	1.675	0.005
13	1.675	0.005
14	1.675	0.005
15	1.675	0.005
16	1.675	0.005
17	1.85	0.005
18	1.935	0.005
19	2.278	1.218
20	2.452	0.262
21	2.582	0.262
22	2.59	0.14
23	2.727	0.127
24	2.605	0.005

decision-making time step. Also, the charging and discharging efficiencies of the battery are 90%.

- Maximum load capacity of the space heater in each time period is equal to 5.525 kW.

- Daily energy capacity of the storage water heater is 10.46 kWh (180 lt). Also, it has a 3 kW heating element.

- The desired temperature of the building is assumed to equal 23°C. Furthermore, the thermal resistance of the building shell and C are equal to 18°C/kW and 0.525 kWh/°C, respectively.

TAB. 4.6: Central forecasting and interval forecasting error of the market price and the PV energy output in the day-ahead stage [Gazafroudi et al., 2019c].

Time (h)	$\lambda^{pred}(t)$	$\sigma^{dn}_{price}(t) = \sigma^{up}_{price}(t)$	$\mathrm{P}^{pred}_{pv}(t)$	$\sigma^{dn}_{pv}(t) = \sigma^{up}_{pv}(t)$
1	39.13	13.11	0	0
2	35.51	12.77	0	0
3	33.13	12.59	0	0
4	31.91	12.37	0	0
5	31.62	12.32	0	0
6	33.25	12.34	0	0
7	38.04	13.03	0.042	0.042
8	43.30	13.81	11.78	11.78
9	45.95	13.58	91.47	75.02
10	46.61	12.75	271.1	147.7
11	46.31	12.82	494.1	215.7
12	45.39	12.83	698.7	275.8
13	44.88	12.84	853.2	312.8
14	44.73	13.00	973.7	328.2
15	43.52	13.31	1066.1	312.7
16	42.42	13.74	1071.8	285.7
17	42.40	14.11	972.6	285.0
18	43.73	14.47	800.8	259.4
19	45.19	14.86	589.6	230.5
20	46.75	14.13	370.1	169.7
21	47.44	13.42	146.3	105.3
22	47.18	12.12	25.06	25.06
23	44.43	11.63	0.680	0.680
24	40.84	11.86	0	0

The assessment of the performance of the proposed residential energy management problem is done in two cases that are described as follows:

- Case 1: The residential energy management problem is solved by Mixed-Integer Linear Programming (MILP) through a two-stage stochastic optimal bidding strategy which. In this way, scenarios of the first stage come from interval bands, while stochastic scenarios are used in the second stage. In this case, influences of the optimistic and flexibility coefficients are assessed in the performance of the proposed residential energy management system based on the optimal bidding strategy.

TAB. 4.7: Scenarios of the market price in the real-time stage [Gazafroudi et al., 2019c].

Time (h)	$\lambda^{rt}(t,\omega_1)$	$\lambda^{rt}(t,\omega_2)$	$\lambda^{rt}(t,\omega_3)$	$\lambda^{rt}(t,\omega_4)$	$\lambda^{rt}(t,\omega_5)$	$\lambda^{rt}(t,\omega_6)$	$\lambda^{rt}(t,\omega_7)$	$\lambda^{rt}(t,\omega_8)$	$\lambda^{rt}(t,\omega_9)$	$\lambda^{rt}(t,\omega_{10})$
1	11.96	22.42	30.48	31.56	34.23	41.23	47.42	48.90	52.85	59.20
2	29.05	34.35	19.32	31.38	27.70	33.83	32.40	50.91	21.01	34.40
3	41.22	17.40	25.82	29.68	41.83	22.75	32.09	30.28	24.66	34.18
4	24.20	30.15	28.56	39.21	29.80	31.45	34.78	40.37	39.17	29.35
5	13.49	33.30	39.75	37.96	26.81	30.57	20.85	38.17	41.58	53.09
6	36.62	23.10	43.12	21.33	32.85	37.74	27.52	33.01	32.80	35.33
7	40.18	46.20	37.62	41.97	32.70	43.00	35.64	47.69	32.14	30.76
8	46.71	38.62	47.66	43.39	49.46	33.96	49.51	46.68	47.04	48.18
9	49.29	42.51	47.84	36.27	43.07	41.45	58.31	44.12	41.82	48.57
10	40.14	61.71	64.09	36.72	39.46	52.21	43.75	36.02	35.13	40.04
11	37.05	39.08	29.24	43.01	55.78	47.82	47.79	53.98	54.90	55.20
12	34.53	39.80	55.38	32.61	37.76	64.35	44.50	54.37	34.39	42.58
13	37.50	48.56	43.54	39.54	50.76	45.38	67.95	23.15	46.28	45.44
14	43.32	42.59	52.83	33.82	39.99	40.04	49.73	52.87	34.58	50.54
15	42.47	42.89	32.35	47.86	51.53	41.00	47.19	27.01	35.75	43.31
16	26.11	30.76	49.69	23.35	46.66	36.85	27.31	57.41	32.81	45.03
17	45.90	30.30	47.90	16.84	39.27	24.37	72.74	34.35	41.71	67.24
18	28.00	49.67	35.27	31.16	29.82	40.23	44.97	40.25	31.91	38.66
19	53.04	40.93	47.06	49.15	40.53	61.46	54.31	53.95	54.42	57.43
20	28.17	58.00	27.05	49.46	58.08	28.05	48.24	40.36	55.23	48.96
21	41.61	51.30	51.10	47.98	60.90	42.25	45.62	51.61	39.05	45.47
22	27.68	53.03	41.27	51.70	37.96	47.51	31.93	48.34	45.07	53.13
23	56.34	48.24	49.41	46.56	51.08	43.00	38.23	52.57	47.93	36.63
24	46.38	29.20	50.56	22.86	33.41	33.68	27.80	43.71	50.39	38.75

TAB. 4.8: Scenarios of the PV energy output in the real-time stage [Gazafroudi et al., 2019c].

Time (h)	$P_{pv}^{scen}(t,\omega_1)$	$P_{pv}^{scen}(t,\omega_2)$	$P_{pv}^{scen}(t,\omega_3)$	$P_{pv}^{scen}(t,\omega_4)$	$P_{pv}^{scen}(t,\omega_5)$	$P_{pv}^{scen}(t,\omega_6)$	$P_{pv}^{scen}(t,\omega_7)$	$P_{pv}^{scen}(t,\omega_8)$	$P_{pv}^{scen}(t,\omega_9)$	$P_{pv}^{scen}(t,\omega_{10})$
1	0	0	0	0	0	0	0	0	0	0
2	0	0	0	0	0	0	0	0	0	0
3 0	0	0	0	0	0	0	0	0	0	
4 0	0	0	0	0	0	0	0	0	0	
5 0	0	0	0	0	0	0	0	0	0	
6 0	0	0	0	0	0	0	0	0	0	
7 0	0	0	0	0	0	0	0	0	0	
8	7.22	26.69	0	0.37	20.80	22.48	17.71	6.50	9.91	13.30
9	80.52	140.6	125.7	99.96	34.55	69.55	107.6	84.43	97.65	63.73
10	203.5	206.9	287.6	195.2	307.8	278.8	320.7	210.3	275.2	160.0
11	531.6	607.5	526.4	452.9	585.5	530.4	476.0	507.5	554.5	513.9
12	895.5	666.1	654.8	864.2	747.0	832.3	586.4	676.5	725.1	610.2
13	745.8	792.3	405.0	994.4	1007.4	1015	805.3	791.6	788.1	1082
14	1165	637.2	899.8	994	1336.9	1138.9	825.7	810.4	1106.2	1049.4
15	916.0	1267.8	1024.5	1282.8	1003.9	1211.2	1074.9	1292.2	923.7	874.7
16	870.9	1306.8	1068.9	988.1	1077.7	1120	1246.6	861.8	903.7	1092.7
17	1152.4	938.9	1061.8	882.2	1072.9	1065.6	1083.8	1058.5	895	925.4
18	773.8	777.5	795.2	738.9	881.5	814.09	950.9	725	868.1	714.9
19	434.8	540.2	582.4	523.9	654.2	493.3	443.9	612.2	615.3	561.4
20	314.3	313.2	305.5	415.3	282.9	379.4	332.7	378.09	360.7	346
21	160.8	150.9	148.1	261.9	98.10	120.1	149.7	87.45	106.8	163
22	24	35.40	19.70	13.29	8.640	48.21	17.18	22.75	0	21.75
23	0.465	0	1.783	0.435	0.851	0	0.694	0.330	0.553	0.054
24	0	0	0	0	0	0	0	0	0	0

In this way, the stochastic optimal bidding strategy for the HEMS will be:

TAB. 4.9: Scenario Probabilities in the real-time stage [Gazafroudi et al., 2019c].

	ω_1	ω_2	ω_3	ω_4	ω_5	ω_6	ω_7	ω_8	ω_9	ω_{10}
ϕ_ω	0.07	0.10	0.10	0.09	0.08	0.11	0.12	0.08	0.11	0.13

$$\max(4.50)$$
$$s.t.: (4.19) - (4.49), (4.51) - (4.68).$$

- Case 2: The residential energy management problem is solved without considering the bidding strategy. In this case, the uncertainty of price and PV energy output in the day-ahead stage is modeled by both methods: Interval-based scenarios and interval bands. In this way, the performance of the system is evaluated according to the impacts of optimistic coefficients on both methods.

In the two-stage stochastic scenario-based method (hereinafter, this method is called InterStoch), the proposed residential energy management problem without the optimal bidding strategy will be:

$$\max(4.50)$$
$$s.t.: (4.19) - (4.47), (4.51) - (4.66).$$

However, for the two-stage interval-stochastic optimization method (hereinafter, this method is called Hybrid), the residential energy management problem without the optimal bidding strategy is represented in the following:

$$\max(4.2)$$
$$s.t.: (4.3) - (4.47).$$

Although InterStoch method optimizes the residential energy management problem by MILP, uncertainty modeling based on Hybrid method in our proposed energy management problem is solved by Mixed-Integer Non-Linear Programming (MINLP).

4.4.2 Results

4.4.2.1 Case 1: with optimal offering model

In this section, the performance of the proposed two-stage stochastic residential energy management problem is assessed taking into account optimal bidding strategy. In this way the performance of the proposed problem is evaluated based on the impacts of the optimistic coefficients of the PV energy output and electricity price, and flexibility coefficient on the expected profit of the system and transacted energy between the smart home and the local market.

a. Impact of α_{pv}, α_{price}, and γ

In this section, impacts of α_{pv} and price on total, day-ahead and real-time expected profits of the smart home are studied. Moreover, their influences on the exchanged energy through smart home and the local market is evaluated. In Fig. 4.3, impact of the α_{pv} on the expected profits of the system is studied considering α_{price} and γ equal 1. As seen in Fig. 4.4, increment of α_{pv} increases total expected profit, and the maximum amount of the total expected profit is where α_{pv} is equal to 1. However, the worst case is where α_{pv} equals 0, and the total expected profit of the system gets its minimum amount. Thus, modeling a residential energy management system considering α_{pv} equals 0 increases the robustness of the system. On the hand, the increment of price has a negative effect on the total expected profit of the system where α_{pv} and γ equal 0 and 1, respectively. This way, worst and robust case of the system is when α_{pv} equals 0 and α_{price} equals 1. Fig.4.5 demonstrates the impact of the flexibility coefficient on the expected costs in the worst case of the system when α_{pv} and α_{price} equal 0 and 1, respectively. As shown in Fig. 4.5, increment of the flexibility coefficient increases the total expected profit of the system. Hence, the maximum amount of the expected profit is where γ equals 1. In this case, the best case is more interested to model energy flexibility of the smart home since the best case to manage energy flexibility in the domestic energy management problem is where γ equals 1.

b. Optimal offering and bidding curves

In this section, optimal offering and bidding curves of the residential energy management problem through the two-stage stochastic model are represented. As in the day-ahead stage, the home energy management system only offers and bids one quantity for all price scenarios, since the optimal bought/sold energy curve of the smart home from/to

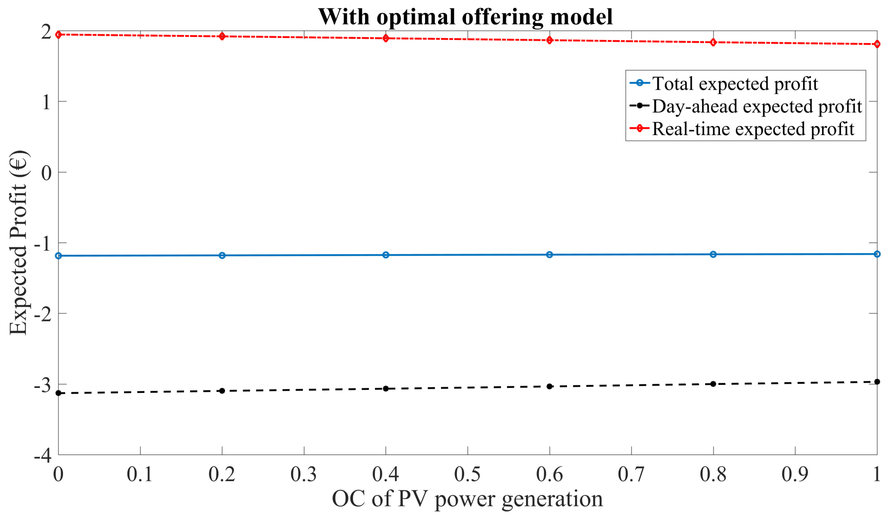

FIG. 4.3: Impact of α_{pv} on total, day-ahead and real-time expected profits of the residential energy management problem considering α_{price} and γ equal 1 [Gazafroudi et al., 2019c].

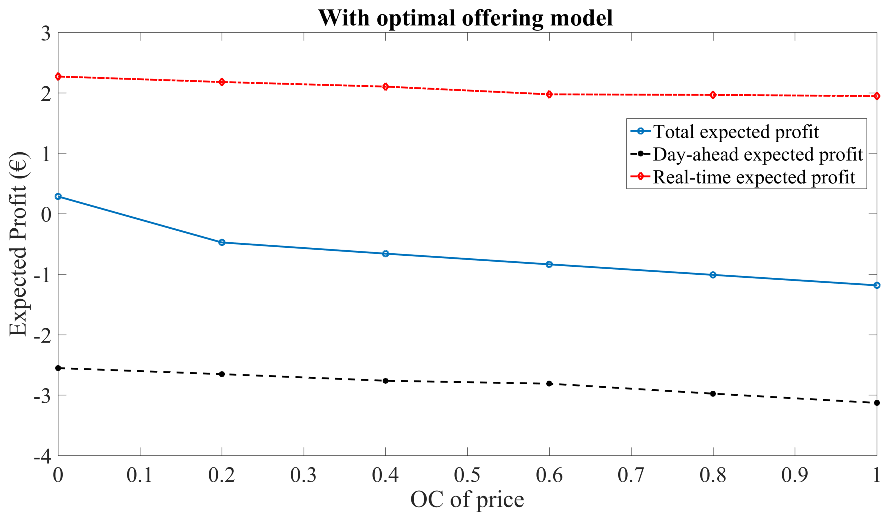

FIG. 4.4: Impact of α_{price} on total, day-ahead and real-time expected profits of the residential energy management problem considering α_{pv} equals 0 and γ equals 1 [Gazafroudi et al., 2019c].

the local market is shown in Fig. 4.6. As seen in Fig. 4.6, the offering set-points of the home in all scenarios and time steps in the day-ahead stage equal 0. It means that the proposed home is eager to participate only as a consumer in the day-ahead local market. However, Fig. 4.7 represents that the smart home acts as a prosumer, and SHE submits both its optimal and bidding curves to the real-time local market in all time steps. In Fig. 4.7, optimal offering and bidding curves are demonstrated at t=1, t=3, and t=6.

As it has been explained in Section 4.3, three types of electrical loads- controllable, shiftable and non-dispatchable- are defined in this section. In this way, the space heater is modeled as controllable load based on (4.32)-(4.34). Fig. 4.8 shows real-time expected

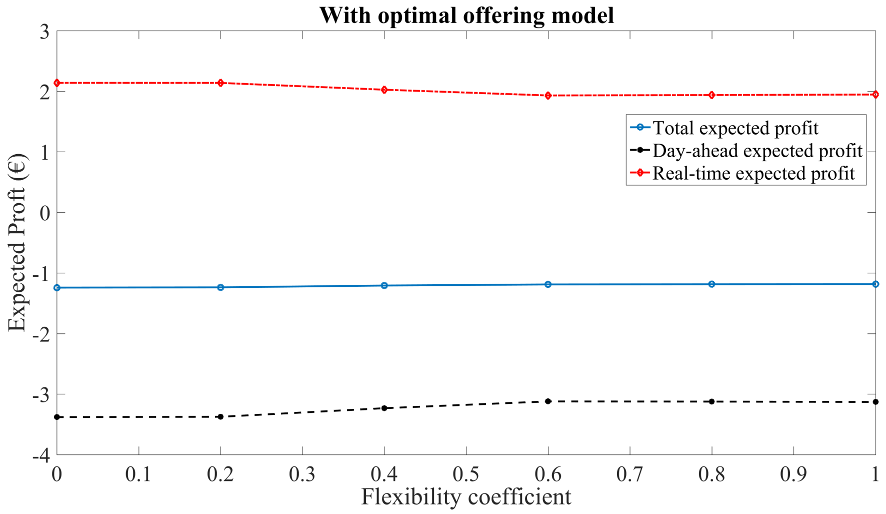

FIG. 4.5: Impact of γ on total, day-ahead and real-time expected profits of the residential energy management problem considering α_{pv} equals 0 and α_{price} equals 1 [Gazafroudi et al., 2019c].

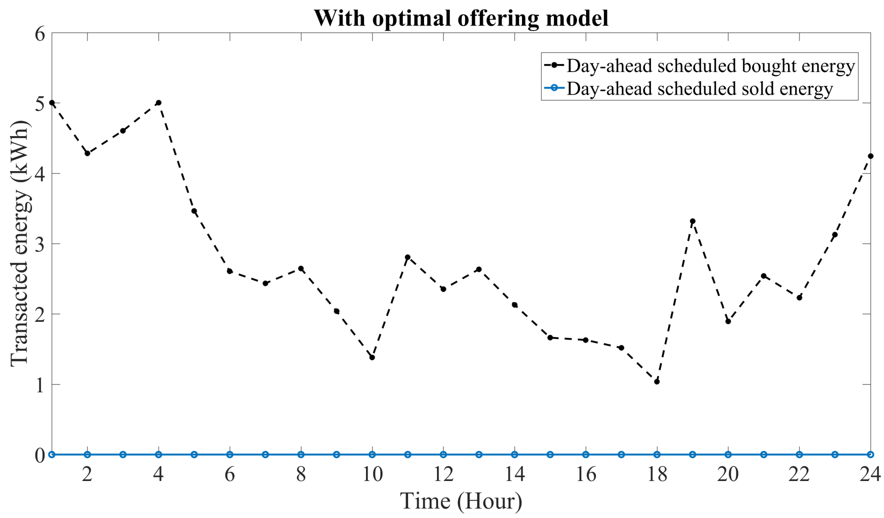

FIG. 4.6: The optimal scheduled transacted energy for the smart home in the day-ahead stage [Gazafroudi et al., 2019c].

electrical consumption of the space and indoor temperature. In the case study, it is considered that the desired indoor temperature of the home equals 23 . Hence, the real-time expected indoor temperature is constrained to 22 and 24 according to 4.33 as it is shown in Fig. 4.8. On the other hand, the Storage Water Heater (SWH) and Pool Pump (PP) are defined as shiftable loads in this system. Hence, shiftable loads are switched off in the time periods of higher electricity price. As shown in Table 4.7, electricity price is the highest amount in the time period from t=6 to t=15. Hence, both SWH and PP are not committed by the HEMS from t=6 to t=15 as shown in Fig. 4.9. Although the maximum daily operational time period of the PP has been assumed to be 1 hour ($T_{ON} = 1$), Fig. 4.9(b) shows the amount of real-time expected

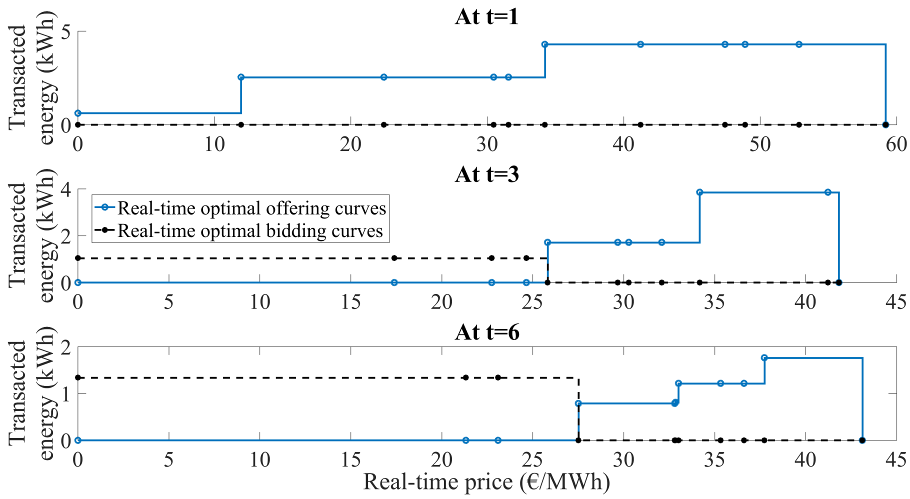

FIG. 4.7: The optimal bidding and offering curves for the smart home in t equals 1, 3, and 6 in the real-time stage [Gazafroudi et al., 2019c].

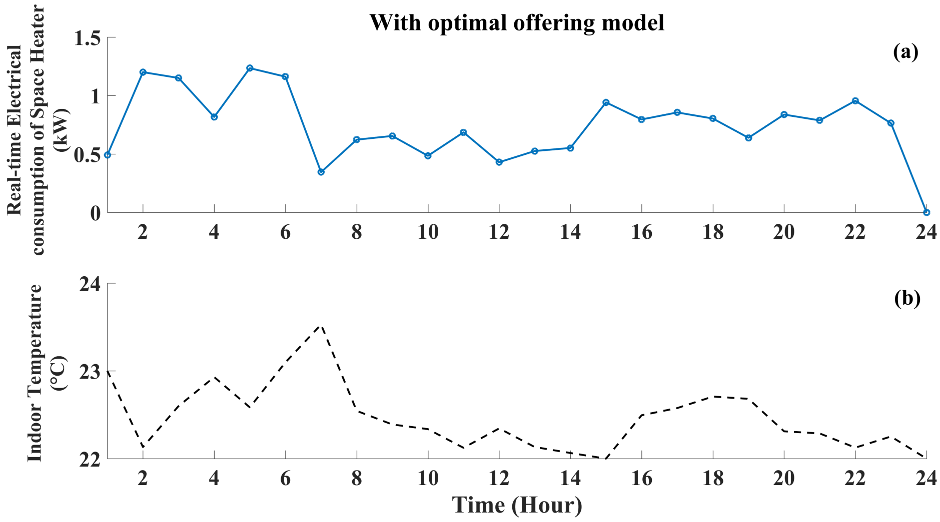

FIG. 4.8: Real-time expected electrical consumption of the space heater (a), real-time expected indoor temperature (b) in the optimal offering model of the HEMS [Gazafroudi et al., 2019c].

electrical consumption is nonzero in four time steps. For this reason, Fig. 4.9(b) presents expected electrical consumption of the PP in each time period of the residential energy management problem. In this way, real-time operation status on the PP ($z(t,\omega)$) is shown in Fig. 4.9(c). As it is seen in Fig. 4.9(c), $z(t,\omega)$ is only committed to one time period of each scenario. However, $z(t,\omega)$ is committed to six scenarios (ω_2, ω_3, ω_5, ω_6, ω_7, ω_{10}) in t=24, so real-time expected electrical consumption of the PP is the highest at t=24.

Fig. 4.10 shows the real-time expected state of charge of the battery. In this section, it is considered the battery' SOC is in the minimum storage level in the initial state (C_i=0.48 kWh). As it is shown in Fig. 4.10, the SOC of battery is at its minimum level of charge

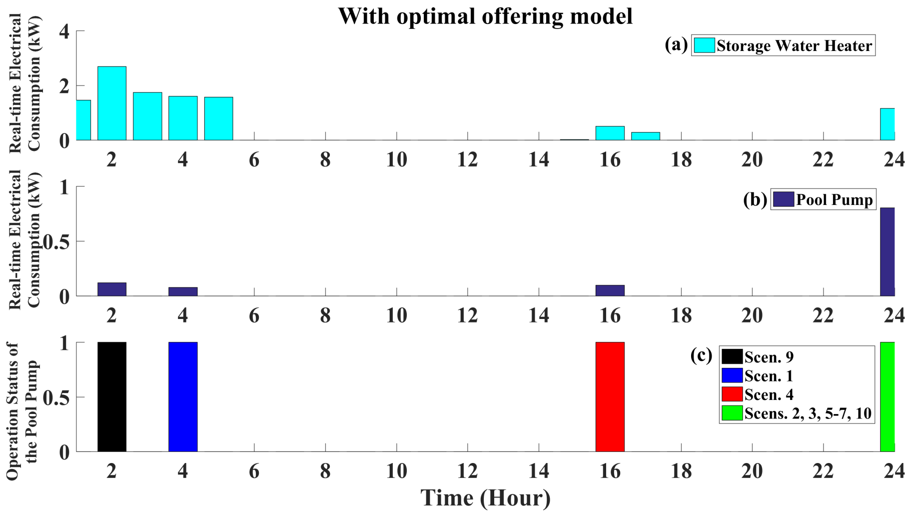

FIG. 4.9: Real-time expected electrical consumption of the storage water heater (a), real-time expected electrical consumption of the pool pump (b), real-time operation status of the pool pump (c) in optimal offering model of the HEMS [Gazafroudi et al., 2019c].

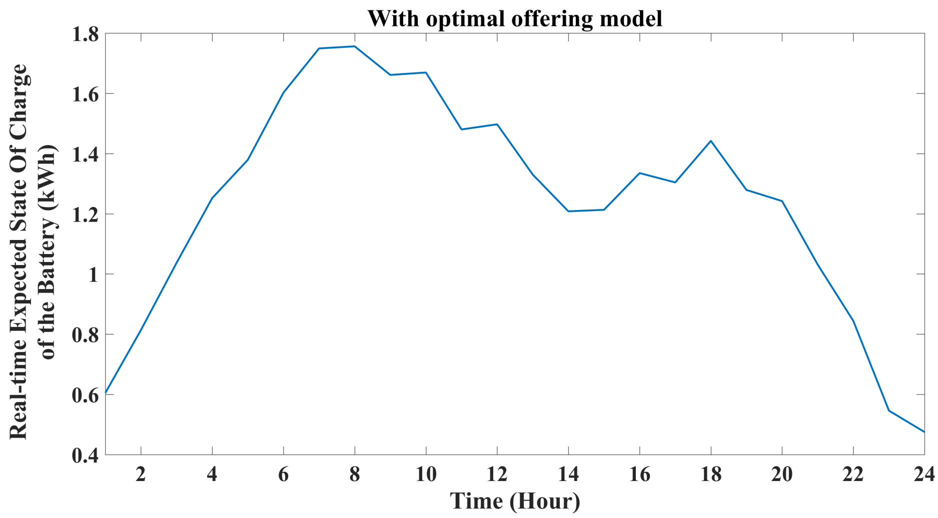

FIG. 4.10: Real-time expected state of charge of the battery in the optimal offering model of the HEMS [Gazafroudi et al., 2019c].

at t=24. Fig. 11 shows real-time SOC, charged energy, and energy discharged from the battery at t=1 (a), t=3 (b), and t=6 (c). By comparing Figs. 4.10 and 4.11, it can be deduced that there is not fixed incremental or decreasing relationship between the SOC of the battery and electricity price. Thus, the use of a battery as an energy storage system can provide energy flexibility to make optimal offering and bidding curves for the HEMS.

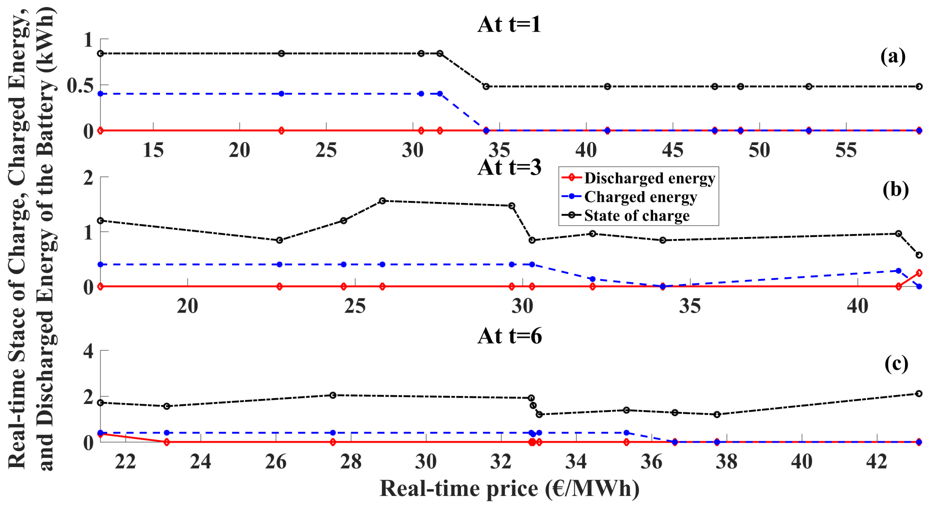

FIG. 4.11: Real-time state of charge, charged energy, and discharged energy of the battery at t=1 (a), t=3 (b), t=6 (c) [Gazafroudi et al., 2019c].

4.4.2.2 Case 2: without optimal offering model

In this section, performance of the proposed residential energy management problem is studied while constraints related to the optimal bidding strategy are not seen in the problem, and both proposed methods are used to model uncertainty of the PV energy generation and electricity price. In the following, the results of the system based on InterStoch and Hybrid methods are demonstrated and compared.

a. Results of the InterStoch method

In this section, the uncertainty of the system is modeled by the InterStoch method. Hence, effectiveness of the optimal bidding strategy that consists of constraints (4.48), (4.49), (4.67) and (4.68) is evaluated in this section.

As seen in Figs. 4.12 and 4.13, increment of the optimal coefficients of the PV energy generation and electricity price has positive and negative influence on the expected profit of the system. In other words, the worst case of the system is to consider that pv and price equal 0 and 1, respectively. In this way, in Fig. 4.14, the real-time offering and bidding curves of the domestic energy management system are assessed in the worst case without the optimal bidding strategy. Fig. 4.7 demonstrates the real-time bidding and offering curves in t=1, t=3, and t=6. As mentioned before, optimal offering and bidding curves must be ascending and descending, respectively. In Fig. 4.14, red circles indicate offering and bidding transacted energy steps that are descending and ascending, respectively, and they cause the offering and bidding curves to not be optimal. Hence, in non-optimal offering model, SHE is not able to submit its offering and bidding curves

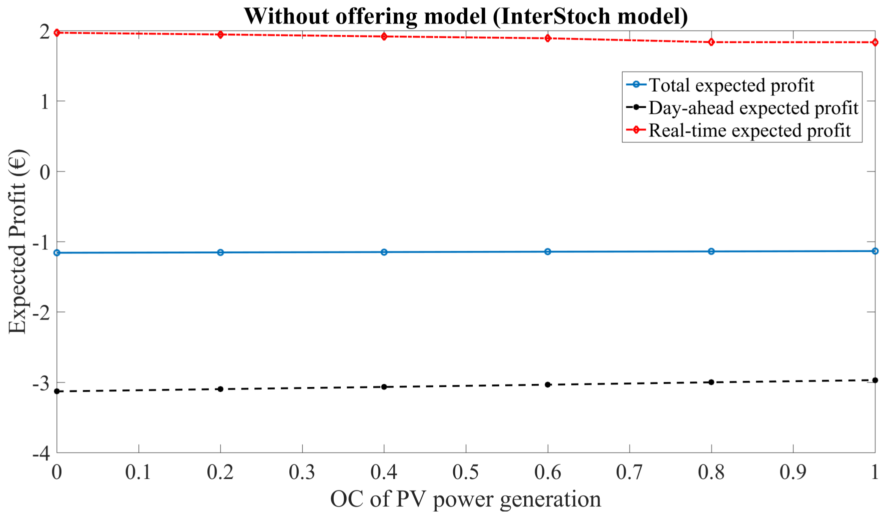

FIG. 4.12: Without offering model (InterStoch model): impact of α_{pv} on total, day-ahead and real-time expected profit of the residential energy management problem considering α_{price} and γ equal 1 [Gazafroudi et al., 2019c].

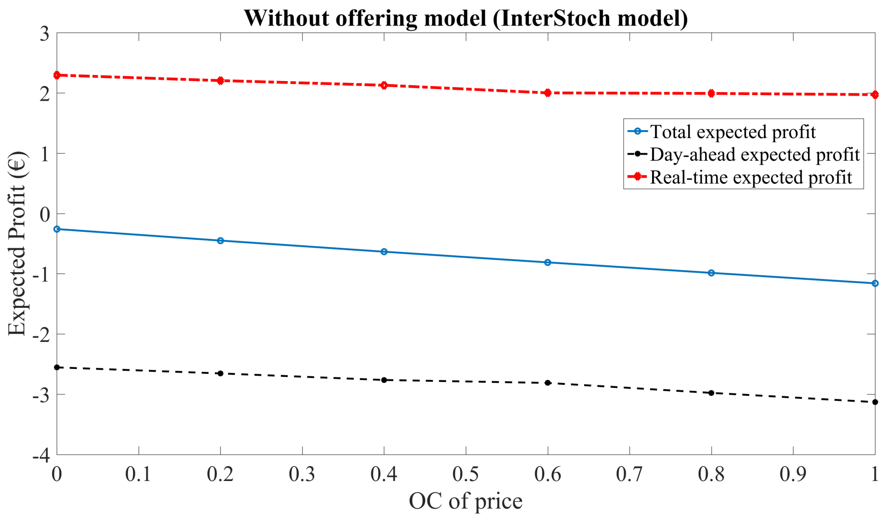

FIG. 4.13: Without offering model (InterStoch model): impact of α_{price} on total, day-ahead and real-time expected profit of the residential energy management problem considering α_{pv} equals 0 and γ equals 1 [Gazafroudi et al., 2019c].

to the local market so as to maximize its expected profit. This is because offering and bidding curves are not optimal in this Case. Hence, an appropriate strategy for SHE is to transact energy with other local market players- e.g. small consumers, producers, and prosumers- according to its optimum decisions in home energy management.

b. Results of the Hybrid method

In this section, the Hybrid method is used to model uncertainty of the PV's energy generation and electricity price in the residential energy management problem. In this

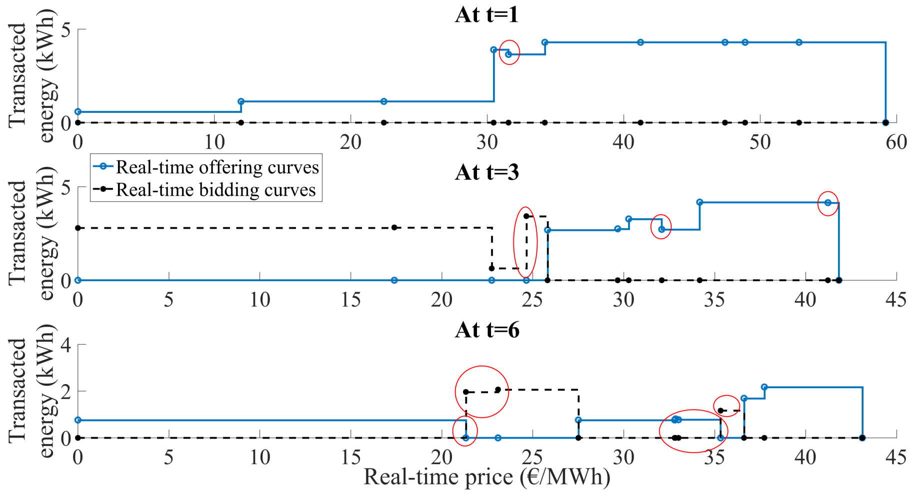

FIG. 4.14: Without offering model (InterStoch model): the bidding and offering curves for the smart home in t equals 1, 3, and 6 in the real-time stage [Gazafroudi et al., 2019c].

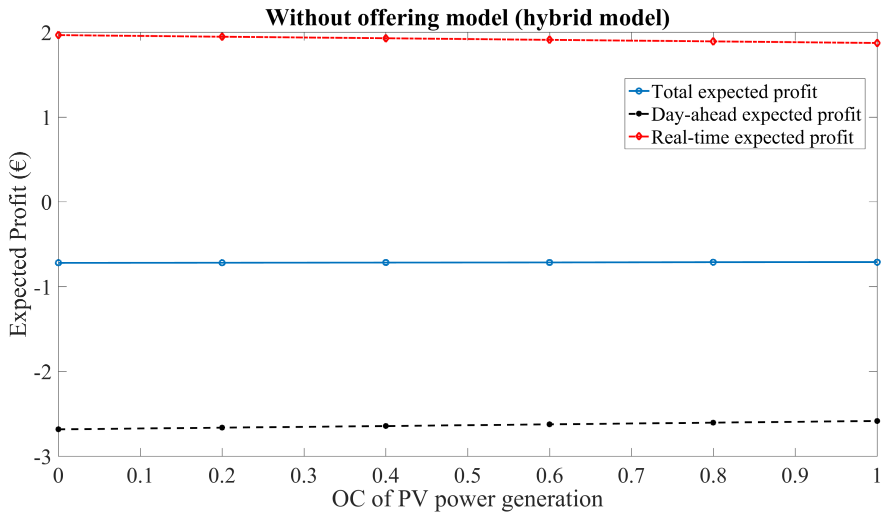

FIG. 4.15: Without offering model (Hybrid model): impact of α_{pv} on total, day-ahead and real-time expected profit of the residential energy management problem considering α_{price} and γ equal 1 [Gazafroudi et al., 2019c].

case, interval bands are defined to consider uncertainty in the day-ahead stage of our proposed energy management problem. Moreover, as it has been highlighted before, the optimization problem will be MINLP.

Fig. 4.15 demonstrates that increment of the optimistic coefficient of the PV energy generation increases the total expected profit of the system. However, increasing the price decreases the total expected profit as it is shown in Fig. 4.16. Hence, these facts state that impact patterns of the optimistic coefficients on the expected profit of the system are the same in both methods. Moreover, Fig. 4.17 proves that bidding and offering curves are not optimal in this case. By comparing between Tables 4 and 6, it

TAB. 4.10: Total expected profit of the residential energy management problem considering optimal and non-optimal strategies in the worst scenario (α_{pv} equals 0 and α_{price} equals 1) [Gazafroudi et al., 2019c].

	Non-optimal offering (hybrid method)	Non-optimal offering (InterStoch method)	Optimal offering
Day-ahead EP (€)	-2.684	-3.130	-3.130
Real-time EP (€)	1.965	1.971	1.945
Total EP (€)	-0.719	-1.159	-1.185

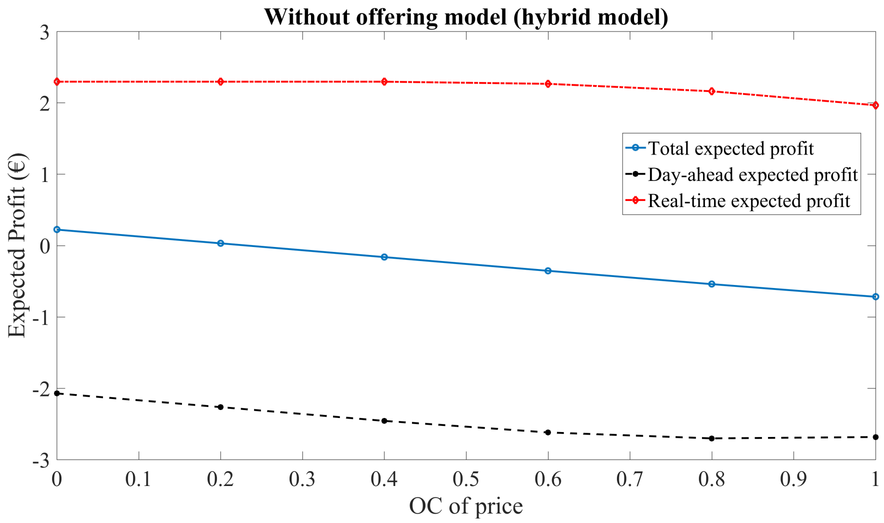

FIG. 4.16: Without offering model (Hybrid model): impact of α_{price} on total, day-ahead and real-time expected profit of the residential energy management problem considering α_{pv} equals 0 and γ equals 1 [Gazafroudi et al., 2019c].

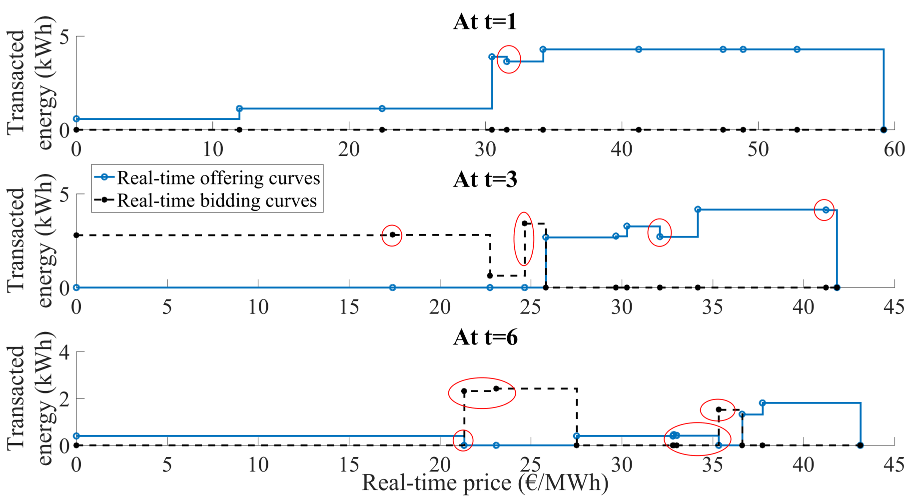

FIG. 4.17: Without offering model (Hybrid model): the bidding and offering curves for the smart home in t equals 1, 3, and 6 in the real-time stage [Gazafroudi et al., 2019c].

can be observed that the smart home is eager to act as a consumer in the model based on the hybrid method as opposed to the model based on the InterStoch method. The results of this eagerness can be seen in Table 5. In this way, although total and day-ahead expected profits of the system in the hybrid method is less than the InterStoch method, the real-time expected profit of the system in the InterStoch method is higher. For this reason, SHE prefers to play as a consumer in more scenarios in the hybrid method in comparison to the InterStoch one. Besides, Table 5 compares expected profits of the HEMS in non-optimal and optimal offering models in the worst scenario where PV equals 0 and price equals 1. As seen in Table 5, total EP of the HEMS is the highest when the non-optimal model is solved by hybrid method. Moreover, total EP of the system is lowest in optimal offering model of the HEMS. In other words, Table 5 shows that the InterStoch optimization method is more robust than the hybrid method because it provides a lower total expected profit of the system in this case study. Also, the optimal offering model is more robust than the non-optimal offering one.

4.5 Conclusions

In this chapter, a probabilistic scenario-based method was presented for the management of residential energy and energy trading with the local electricity market based on an optimal bidding strategy. Our residential energy management problem includes two stages: day-ahead and real-time. In the day-ahead stage, two methods have been proposed to model the uncertainty of electricity price and PV energy generation. Their uncertainty is modeled by interval bands and interval-based scenarios. In the real-time stage, stochastic scenarios have been used to consider the uncertainty affecting the system. In addition, energy flexibility is provided by a battery system. In our next chapter, we will model different energy management strategies in the power distribution systems based on a community of end-users (e.g. smart buildings) in order to look at how end-users can impact on local energy trading as price-maker agents.

Chapter 5

Local electricity trading structure (*estructura local del comercio de electricidad*)

VNiVERSiDAD D SALAMANCA

CAMPUS DE EXCELENCIA INTERNACIONAL

Local electricity trading structure (*estructura local del comercio de electricidad*)

5.1 Introduction

Power distribution systems are more active than their conventional structures due to demand response strategies and increment of distributed energy resources' power generation. Thus, centralized electricity markets cannot follow flexible behavior of end-users in the bottom layer of the distribution systems [Borlase, 2016]. Therefore, new market structures are required to provide energy flexibility based on decentralized manners. In this chapter, different strategies and structures are proposed to trade electricity in power distribution systems based on flexible behaviors of end-users.

The rest of this chapter is organized as follows. Section 5.2 describes a decentralized approach to manage energy flexibility by end-users in the distribution network. In Section 5.3, a monopolistic approach for the energy flexibility management problem is presented. Sections 5.4 and 5.5 propose iterative algorithm for trading electricity between the aggregators and the DSO, and between the end-users and the DSO, respectively. Finally, this chapter is concluded in Section 5.6.

5.2 Decentralized energy flexibility management

The appearance of end-users' flexible behavior based on DRPs has made the distribution layer of the power systems more active. In this way, energy transaction management through a decentralized manner could be an appropriate solution to improve the efficiency of energy trading in the power distribution networks. This section proposes a

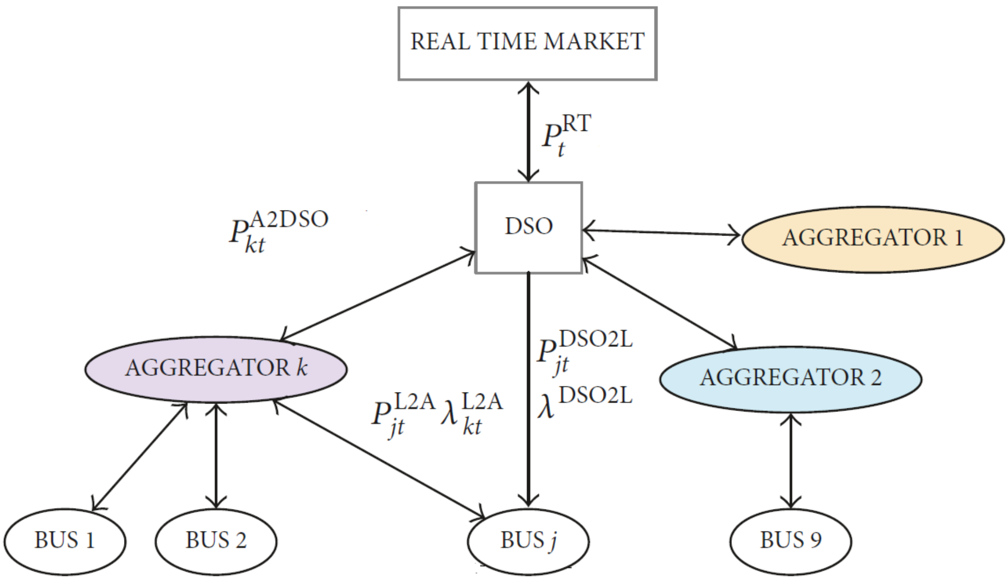

FIG. 5.1: Real-time energy transaction framework of the power distribution system [Zhang et al., 2018], [Prieto-Castrillo et al., 2018] and [Gazafroudi et al., 2018].

decentralized method to manage energy flexibility by end-users based on a bottom-up approach in distributed power systems. The results and discussions in this section are based on [Gazafroudi et al., 2018].

5.2.1 Energy flexibility management problem

In this section, real-time decentralized energy management problem is defined based on a bottom-up structure. Three types of players are introduced in the power distribution systems (e.g. end-users, aggregators, and the Distribution System Operator (DSO)). In this structure, the DSO is the only agent which is able to transact energy with the Real-Time Electricity Market (RTEM), $P_{t\omega}^{RT}$. Fig.5.1 describes the energy transaction problem schematically. According to the proposed approach, end-users trade energy flexibility with both aggregator (end-users can only transact energy flexibility with the aggregator from whom they bought their scheduled energy), $P_{jt\omega}^{L2A}$, and the DSO, $P_{jt\omega}^{DSO2L}$, at prices λ_{kt}^{L2A} and λ^{DSO2L}, respectively. In the next step, aggregators trade flexibility provided by end-users, $P_{kt\omega}^{A2DSO}$. Although the real-time flexibility transactions between end-users and aggregators, and aggregators and the DSO are two-way, end-users can only buy real-time energy from the DSO.

Hence, each end-user can either behave as upward or downward flexible load or not as represented in (5.1). A positive flexibility, $L_{jt\omega}^{F} > 0$, tends to reduce the scheduled load, whereas the end-user would increase its scheduled demand in a negative flexibility, $L_{jt\omega}^{F} <$

0. In other words, if $L^F_{jt\omega} > 0$, the corresponding customer decreases its day-ahead scheduled electrical demand in real-time. However, if $L^F_{jt\omega} < 0$, its real-time electrical demand is more than its day-ahead scheduled demand. Also, $L^{Shed}_{jt\omega}$ is the amount of load shedded by each end-user. Moreover, Eq. (5.2) represents that the real-time load of end-user j is not provided when all distribution lines (that are ended at end-user j) are not connected. Here, $ML_{ji\omega}$ is defined to express the status of lines between buses j and i. In this way, $ML_{ji\omega}$ equals 0 where the line between j and i is off. Thus, we find that:

$$L_{jt\omega} = L^C_{jt} - L^F_{jt\omega} - L^{Shed}_{jt\omega},\ \forall j,t,\omega. \tag{5.1}$$

$$L_{jt\omega} \leq (L^C_{jt} - L^F_{jt\omega}) \textstyle\sum_{j\neq i} ML_{ji\omega},\ \forall j,t,\omega. \tag{5.2}$$

Eq. (5.3) states load shedding constraints. Eq. (5.4) represents minimum and maximum limitations of energy flexibility. Flexibility splits itself into real-time traded energy with both the aggregator ($P^{L2A}_{jt\omega}$) and the DSO ($P^{DSO2L}_{jt\omega}$) as represented in (5.5).

$$0 \leq L^{Shed}_{jt\omega} \leq L^C_{jt}\ ,\forall j,t,\omega. \tag{5.3}$$

$$-\gamma_j L^C_{jt} \leq L^F_{jt\omega} \leq \gamma_j L^C_{jt}\ ,\forall j,t,\omega. \tag{5.4}$$

$$L^F_{jt\omega} = P^{L2A}_{jt\omega} - P^{DSO2L}_{jt\omega},\ \forall j,t,\omega. \tag{5.5}$$

As highlighted before, while the energy transacted through end-users and aggregators is bi-directional, end-users can only buy real-time energy from the DSO as seen in (5.6).

$$P^{DSO2L}_{jt\omega} \geq 0, \forall j,t,\omega. \tag{5.6}$$

In this section, it is considered that end-users can play as shiftable loads to provide flexibility as represented in (5.7). Also, end-users can be constrained over all end-users that are aggregated by the same aggregator, A_k, in each time step as seen in (5.8). In this way, Eq. (5.8) increases the sustainability of electrical loads in the each region of the distributed power system. Here, costumers that are limited to (5.7) are called economic followers. However, costumers who are limited to (5.8) are known as reliability followers in this section.

$$\textstyle\sum_t L^F_{jt\omega} = 0\ ,\forall j,\omega. \tag{5.7}$$

$$\textstyle\sum_{j\in A_k} L^F_{jt\omega} = 0\ ,\forall t,\omega. \tag{5.8}$$

Eqs. (5.9) and (5.10) represent power flow and balancing equations in each bus of the distribution network, respectively.

$$P_{jit\omega} = B_{ji}(\theta_{jt\omega} - \theta_{it\omega}), \forall j \neq i, t, \omega. \tag{5.9}$$

$$P^{L2A}_{jt\omega} - P^{DSO2L}_{jt\omega} = \textstyle\sum_{j \neq i} P^{Flow}_{jit\omega} ML_{ji\omega}, \forall j, t, \omega. \tag{5.10}$$

Moreover, not only the exchanged energy must be balanced in all bus nodes, but also the transacted energy should be balanced in each layer of the power distribution grid. Hence, the total flexibility traded between the end-users and the aggregators should be transacted through aggregators and the DSO as represented in (5.11). Thus, the balancing equation in the layer of the DSO for energy exchange between the DSO and the RTEM, aggregators, and end-users is presented in (5.12).

$$P^{A2DSO}_{kt\omega} = \textstyle\sum_{j \in A_k} P^{L2A}_{jt\omega}, \forall k, t, \omega. \tag{5.11}$$

$$P^{RT}_{t\omega} = \textstyle\sum_j P^{DSO2L}_{jt\omega} - \sum_k P^{A2DSO}_{kt\omega}, \forall t, \omega. \tag{5.12}$$

As highlighted before, end-users are classified as economic and reliability followers in this section. In this way, customers are able to express their desired reliability level to guarantee their desired electrical demand considering the uncertainty of the power distribution grid. The Demand Factor (DF)- which which has been introduced in [Gazafroudi et al., 2015], [Pinto et al., 2017], [Gazafroudi et al., 2017c] and [Gazafroudi et al., 2019b]- is modified in this work as represented in (5.13). Eqs. (5.13) and (5.14) represent DF_j as a positive variable that is limited to 1. On the one hand, when $DF_j = 1$, end-user j has the highest reliability level. On the other hand, end-user j has the lowest reliability level if $DF_j = 0$. Besides, a flexible function for Value of Lost Load (VOLL) is needed to consider the desired reliability level of each end-user. Therefore, end-users who have higher amounts of $VOLL$, have higher amounts of the DF as represented in (5.15).

$$DF_j = \textstyle\sum_{t,\omega} \pi_\omega \left(\frac{L^C_{jt} - L^{Shed}_{jt\omega}}{L^C_{jt}}\right), \forall j \tag{5.13}$$

$$DF^{Des}_j \leq DF_j \leq 1, \forall j \tag{5.14}$$

$$VOLL_{jt} = \left(\frac{DF^{Des}_j}{\sum_j DF^{Des}_j} + 1\right) VOLL^{Base}_t, \forall j, t \tag{5.15}$$

Here, the objective function of end-users is defined as their Expected Cost (EC) which should be minimized. The proposed objective function, Eq. (5.16), derives from trade-off between energy bought from the DSO at price λ^{DSO2L} and flexibility trade with the corresponding aggregator k at price λ_{kt}^{L2A} integrated over time.

$$OF_{j\in A_k} = \sum_{\omega} \pi_\omega (\lambda^{DSO2L} \sum_t P_{jt\omega}^{DSO2L} - \sum_t \lambda_{kt}^{L2A} P_{jt\omega}^{L2A} + \sum_t VOLL_{jt} L_{jt\omega}^{Shed}) \tag{5.16}$$

5.2.2 Simulation results

5.2.2.1 Case study

In this section, a 33-bus test system is used from [Zhang et al., 2018], [Prieto-Castrillo et al., 2018], [Mithulananthan et al., 2016] and [Gazafroudi et al., 2018] as seen in Fig. 5.2. Three regions have been introduced that are operated by their corresponding aggregators. In this way, the energy price is different in each region as shown in Table 5.1. The basic cost of $VOLL$ is presented in Table 5.2. Here, it is considered that $\lambda^{DSO2L} = 0.6$ [€/kWh] according to [Zhang et al., 2018], [Prieto-Castrillo et al., 2018] and [Gazafroudi et al., 2018]. The proposed energy management approach is evaluated based on impacts of distribution lines' uncertainty, and flexibility strategies. Also, the proposed Linear Programming (LP) model is solved in GAMS 24.0.2 [?].

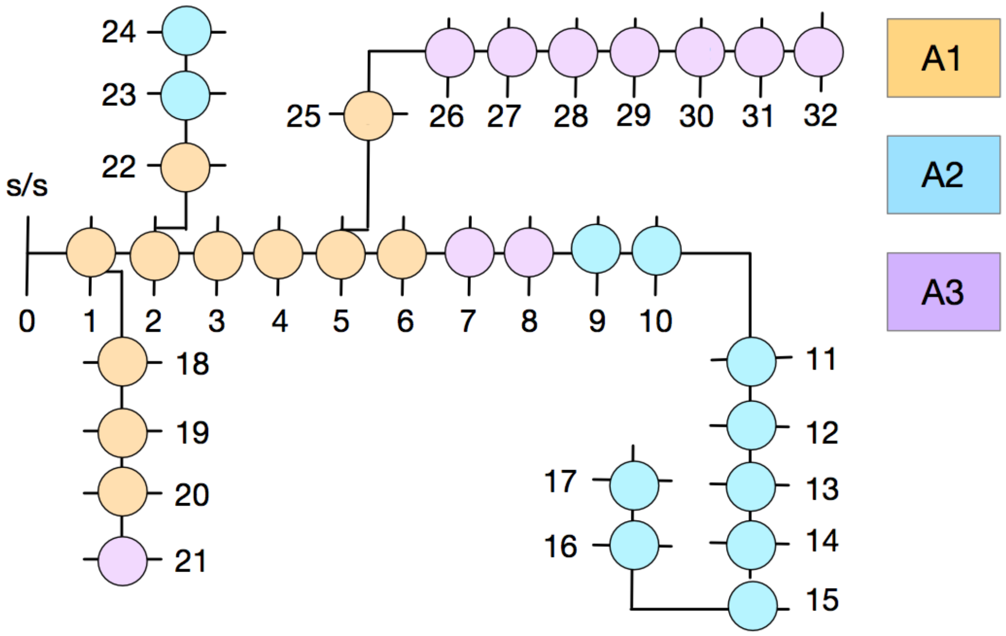

Fig. 5.2: The 33-bus test system and aggregators [Zhang et al., 2018], [Prieto-Castrillo et al., 2018], [Mithulananthan et al., 2016] and [Gazafroudi et al., 2018].

TAB. 5.1: Price of energy traded between end-users and aggregators [Zhang et al., 2018], [Prieto-Castrillo et al., 2018] and [Gazafroudi et al., 2018].

Time [h]	$\lambda_{k=1,t}^{L2A}$ [€/kWh]	$\lambda_{k=2,t}^{L2A}$ [€/kWh]	$\lambda_{k=3,t}^{L2A}$ [€/kWh]
1	0,05	0,08	0,06
2	0,05	0,08	0,07
3	0,05	0,09	0,07
4	0,04	0,07	0,05
5	0,11	0,18	0,15
6	0,12	0,20	0,16
7	0,13	0,22	0,17
8	0,15	0,24	0,19
9	0,16	0,25	0,20
10	0,24	0,41	0,33
11	0,26	0,42	0,36
12	0,28	0,43	0,37
13	0,25	0,40	0,32
14	0,18	0,26	0,21
15	0,15	0,24	0,20
16	0,14	0,22	0,18
17	0,15	0,25	0,19
18	0,20	0,36	0,30
19	0,21	0,36	0,29
20	0,22	0,41	0,30
21	0,24	0,42	0,33
22	0,12	0,22	0,16
23	0,11	0,19	0,15
24	0,06	0,09	0,07

5.2.2.2 Impact of lines uncertainty

In this section, the impact of distribution lines uncertainty on the total EC of all end-users is studied as seen in Eq. (5.17).

$$EC = \sum_{j} OF_j \tag{5.17}$$

Tab. 5.2: The basic $VOLL$ [Gazafroudi et al., 2018].

Time (h)	$VOLL_t^{Base}$ [€/kWh]
1	8
2	8
3	9
4	7
5	16
6	17
7	18
8	20
9	21
10	35
11	36
12	37
13	34
14	22
15	20
16	20
17	20
18	31
19	32
20	33
21	35
22	17
23	16
24	8

Hence, three scenarios are considered which consist of $C1$ (there is no uncertainty in the distribution lines), $C2$ (uncertainty of the distribution lines is considered without load-shedding cost), and $C3$ (line uncertainty and load-shedding cost are considered). It is noticeable that only Eq. (5.7) is considered as a flexible behavior of end-users in this section. In this way, end-users only act as shiftable loads, and their optimum decisions are made autonomously to manage flexibility.

As it is shown in Table 5.3, the EC is negative in both $C1$ and $C2$. In other words,

TAB. 5.3: The impact of line uncertainty [Gazafroudi et al., 2018].

	$C1$	$C2$	$C3$
EC [€]	-714.291	-171.02	1,851,328.747

TAB. 5.4: Impact of the end-users' flexible behavior [Gazafroudi et al., 2018].

	$F3$	$S3$	$FS3$
EC [€]	1,851,328.747	1,851,409.376	1,851,469.455

the proposed energy flexibility management approach brings a profit for all end-users in $C1$ and $C2$. However, the total expected costs of the end-users in $C2$ is less than $C1$ that it expresses the uncertainty of lines impacts negatively on the EC. In other words, the uncertainty of distribution lines causes load shedding in each end-user. Hence, this uncertainty increases the end-users' expected cost due to load shedding. Also, Table 5.3 represents the real effect of line uncertainty on the EC. However, the comparison between the ECs of $C2$ and $C3$ proves that the high amount of this cost is due to the load-shedding cost. This causes the importance of decreasing the line uncertainty where the distribution system operator are in charge of it.

5.2.2.3 The impact of flexible behavior

In this section, the impact of energy flexibility provided by end-users is assessed. To this end, another three scenarios are defined to evaluate shiftable and self-consumption flexible behaviors of the end-users. Moreover, this study is assessed considering assumptions in scenario $C3$ (the lines uncertainty and load-shedding cost are considered). Hence, the scenarios in this section include $F3$ (only shiftable constraint, Eq. (5.7), is considered), $S3$ (only self-consumption constraint, Eq. (5.8), is considered), and $FS3$ (both shiftable and self-consumption constraints, Eqs. (5.7) and (5.8), are considered).

In scenario $F3$, energy flexibility is managed independently by end-users in the bottom layer of the system. However, there is a need for coalition between end-users in $S3$ and $FS3$ to provide flexibility according to (5.8). Table 5.4 shows the flexible behavior of the end-users on relation to the EC. As it is shown in Table 5.4, Scenario $F3$ has the minimum amount of the total expected costs for the end-users. In other words, shiftable flexibility is more profitable than self-consumption flexibility for end-users. In addition, it would be concluded that the complete decentralized flexibility management system is more profitable for end-users than the scenario that flexibility provided by a coalition of end-users. However, scenarios $S3$ and $FS3$ improves the sustainability of the power distribution network.

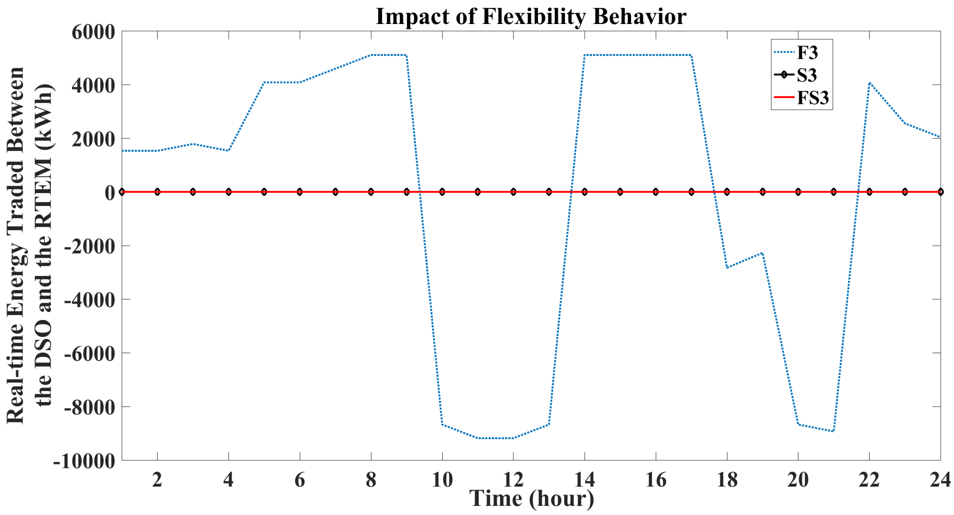

Fig. 5.3: Impact of flexibility behavior on the expected energy traded between the DSO and the RTEM [Gazafroudi et al., 2018].

As it is shown in Fig. 5.3, the expected traded energy through the DSO and the RTEM equals zero in scenarios $S3$ and $FS3$. However, in $F3$, the expected energy exchanged between the DSO and the RTEM is both positive and negative in different time periods in which it presents two-way energy transaction between the distribution network and the up-stream power grid. In other words, Fig. 5.3 shows that there is no energy transaction between the DSO and the RTEM considering self-consumption constraint, and it makes the power distribution system as a sustainable system which does not depend on the up-stream grid to provide its required energy.

In this section, the flexible behavior of end-users has been modelled to minimize the total expected cost for end-users considering uncertainty of distribution lines. However, the interaction between aggregators and the DSO and their expected costs have not been modelled in this section that will be discussed in Section ??.

5.3 Monopolistic approach to manage energy flexibility

In this section, a monopolistic approach based on a hierarchical structure is presented to manage energy flexibility in the distribution grid. According to our proposed monopolistic approach, all end-users and aggregators are able to manage their energy flexibility independently through a bottom-up approach considering the effects of interactions between players in the bottom layer of the power system.

5.3.1 Problem formulation

In this section, we remodel a real-time energy management problem to transact flexibility among three types of *agents* (e.g., end-users, aggregators, and the DSO). However, in Section **??**, it has been mentioned that there are three types of *players* in the system. *Agents* are one type of *players* which can make decisions independently with regard to energy flexibility management. Also, energy cost transaction is modelled in this section. Thus, aggregators transact energy flexibility, P_{kt}^{A2DSO}, with the DSO at price λ_{kt}^{A2DSO}. In the following, corresponding equations of each agent are described.

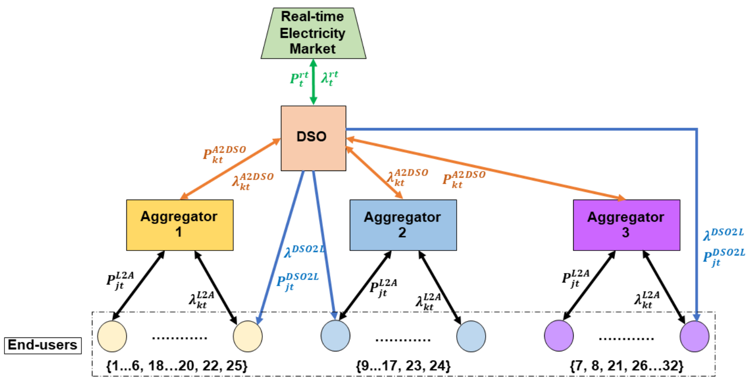

FIG. 5.4: Agents and real-time energy transaction framework of the distribution network [Zhang et al., 2018] and [Prieto-Castrillo et al., 2018].

For simplicity, uncertainty of distribution lines and load shedding cost are not considered in this section. Consequently, all equations are modified in this section. Each end-user can decrease or increase its scheduled load in real-time to provide either upward or downward flexible load, respectively, as represented in (5.18). Eq. (5.19) represents minimum and maximum limitations of energy flexibility. Here, γ_j is defined as a flexibility factor which can be set between 0 and 1. The flexible energy splits itself into the real-time exchanged energy with corresponding aggregator (P_{jt}^{L2A}) and the DSO (P_{jt}^{DSO2L}) as represented in (5.20). Moreover, Eq. (5.21) presents that the real-time energy transaction between the end-users and the DSO is one-way (from the DSO to end-users). In this section, four types of flexibility are defined that are provided by end-users or aggregators. Here, end-users are considered shiftable loads that provide energy flexibility as represented in (5.22). Besides, each end-user can be limited over all end-users that are aggregated by the same aggregator in each time step as seen in (5.23).

$$L_{jt} = L_{jt}^{C} - L_{jt}^{F},\ \forall j,t. \tag{5.18}$$

$$-\gamma_j L_{jt}^{C} \leq L_{jt}^{F} \leq \gamma_j L_{jt}^{C}\ ,\forall j,t. \tag{5.19}$$

$$L_{jt}^{F} = P_{jt}^{L2A} - P_{jt}^{DSO2L},\ \forall j,t. \tag{5.20}$$

$$P_{jt}^{DSO2L} \geq 0, \forall j,t. \tag{5.21}$$

$$\textstyle\sum_t L_{jt}^{F} = 0\ , \forall j. \tag{5.22}$$

$$\textstyle\sum_{j\in A_k} L_{jt}^{F} = 0\ , \forall t. \tag{5.23}$$

According to our hierarchical structure, the total flexibility transacted through end-users and aggregators should be exchanged through aggregators and the DSO as represented in (6.21). Moreover, Eqs. (5.25) and (5.26) are defined in the aggregators' layer to provide shiftable and self-sustainable traded real-time energy between aggregators and end-users as well as (5.22) and (5.23) which have been represented in the bottom layer of the system.

$$P_{kt}^{A2DSO} = \textstyle\sum_{j\in A_k} P_{jt}^{L2A}, \forall k,t. \tag{5.24}$$

$$\textstyle\sum_t P_{jt}^{L2A} = 0\ , \forall j. \tag{5.25}$$

$$\textstyle\sum_{j\in A_k} P_{jt}^{L2A} = 0\ , \forall t. \tag{5.26}$$

The maximum and minimum constraints of price of energy traded between aggregators and the DSO, λ_{kt}^{A2DSO}, are represented in (5.27). Besides, the balancing equation in the layer of the DSO to trade flexibility through the DSO and the RTEM, and rest of the agents is presented in (5.28).

$$\delta_{kt}\lambda_{kt}^{L2A} \leq \lambda_{kt}^{A2DSO} \leq \lambda_{t}^{RT}, \forall t,k. \tag{5.27}$$

$$P_{t}^{RT} = \textstyle\sum_j P_{jt}^{DSO2L} - \sum_k P_{kt}^{A2DSO}, \forall t. \tag{5.28}$$

In this way, the objective functions of end-users, aggregators, and the DSO are represented in (5.29), (5.30), and (5.31), respectively. In (5.29), the objective function of each end-user expresses its expected cost that should be minimized. Objective function of the end-user j consists of two terms. The first term represents the expected cost due to buy real-time energy from the DSO, and the second term states the expected profit due to sell energy flexibility to the aggregator. As represented in (5.30), the objective function consists of two terms which consists of the expected cost due to trading energy flexibility with the end-users, and the expected profit due to energy transaction with the DSO, (however, $\lambda_{kt}^{A2DSO}P_{kt}^{A2DSO}$ makes the problem non-linear). In (5.31), OF^{DSO} includes three terms consisting of the expected cost of energy transaction with aggregators, the expected cost of energy exchanged with the RTEM, and the expected profit due to selling energy to end-users.

$$OF_{j\in A_k}^{EU} = \lambda^{DSO2L}\sum_{t} P_{jt}^{DSO2L} - \sum_{t} \lambda_{kt}^{L2A}P_{jt}^{L2A}. \tag{5.29}$$

$$\begin{aligned} OF_{k}^{AG} &= \sum_{t}\sum_{j\in A_k} \lambda_{kt}^{L2A}P_{jt}^{L2A} \\ &- \sum_{t} \lambda_{kt}^{A2DSO}P_{kt}^{A2DSO}.\forall k \end{aligned} \tag{5.30}$$

$$\begin{aligned} OF^{DSO} &= \sum_{t} \lambda_{kt}^{A2DSO}P_{kt}^{A2DSO} + \sum_{t} \lambda_{t}^{RT}P_{t}^{RT} \\ &- \lambda^{DSO2L}\sum_{t}\sum_{j} P_{jt}^{DSO2L}. \end{aligned} \tag{5.31}$$

5.3.2 The MILP model

As mentioned in Section 5.3.1, $\lambda_{kt}^{A2DSO}P_{kt}^{A2DSO}$ makes non-linear the objective functions of the aggregators and of the DSO as represented in (5.30), and (5.31). In this section, we propose a model in which the DSO is in charge of determining the price of energy traded between aggregators and the DSO, λ_{kt}^{A2DSO}, to minimize its objective function, OF^{DSO}. Also, λ_{kt}^{A2DSO} is limited to maximum and minimum bands according to (5.27). In this way, if energy exchanged between aggregators and the DSO is positive, $P_{kt}^{A2DSO} \geq 0$, then the DSO sets the minimum band of price limitations. However, the DSO determines the maximum band of price limitation where the energy traded between the aggregators and the DSO is negative, $P_{kt}^{A2DSO} < 0$. Hence, we have:

IF $P_{kt}^{A2DSO} \geq 0 \rightarrow$

$$\lambda_{kt}^{A2DSO} = Min.\{\delta_{kt}\lambda_{kt}^{L2A}, \lambda_{t}^{RT}\} \rightarrow z_{kt} = 0.$$

ELSE $P_{kt}^{A2DSO} < 0 \rightarrow$

$$\lambda_{kt}^{A2DSO} = Max.\{\delta_{kt}\lambda_{kt}^{L2A}, \lambda_{t}^{RT}\} \rightarrow z_{kt} = 1.$$

Here, z_{kt} is defined as a binary variable which is determined by the DSO to represent states of electricity price. In the following, the nonlinear term is restated as seen in (5.32).

$$\begin{aligned}\lambda_{kt}^{A2DSO} P_{kt}^{A2DSO} = \{&\delta_{kt}\lambda_{kt}^{L2A}(1-z_{kt}) \\ &+ \lambda_t^{RT} z_{kt}\} P_{kt}^{A2DSO} = PP_{kt}, \forall t, k.\end{aligned} \tag{5.32}$$

$$PP_{kt} = PP_{kt}^{-} + PP_{kt}^{+}, \forall t, k. \tag{5.33}$$

$$PP_{kt}^{-} = \delta_{kt}\lambda_{kt}^{L2A}(1-z_{kt}) P_{kt}^{A2DSO}, \forall t, k. \tag{5.34}$$

$$PP_{kt}^{+} = \lambda_t^{RT} z_{kt} P_{kt}^{A2DSO}, \forall t, k. \tag{5.35}$$

As represented in (5.33), PP_{kt} is split into PP_{kt}^{-} and PP_{kt}^{+}. In this way, each of these nonlinear constraints, (5.34) and (5.35), can be redefined as mixed integer linear constraints according to Refs. [Garcés et al., 2009] and [Gazafroudi et al., 2017c]. Hence, Eq. (5.32) is redefined as presented in (5.36)-(5.40).

$$- z_{kt}M \leq PP_{kt}^{-} - \delta_{kt}\lambda_{kt}^{L2A} P_{kt}^{A2DSO} \leq z_{kt}M, \forall t, k. \tag{5.36}$$

$$\begin{aligned}- \gamma_j \delta_{kt}\lambda_{kt}^{L2A}(1-z_{kt}) \sum_{j\in A_k} L_{jt}^{C} &\leq PP_{kt}^{-} \\ &\leq \gamma_j \delta_{kt}\lambda_{kt}^{L2A}(1-z_{kt}) \sum_{j\in A_k} L_{jt}^{C}, \forall t, k.\end{aligned} \tag{5.37}$$

$$\begin{aligned}- (1-z_{kt})M &\leq PP_{kt}^{+} - \lambda_t^{RT} P_{kt}^{A2DSO} \\ &\leq (1-z_{kt})M, \forall t, k.\end{aligned} \tag{5.38}$$

$$\begin{aligned}- \gamma_j \lambda_t^{RT} z_{kt} \sum_{j\in A_k} L_{jt}^{C} &\leq PP_{kt}^{+} \\ &\leq \gamma_j \lambda_t^{RT} z_{kt} \sum_{j\in A_k} L_{jt}^{C}, \forall t, k.\end{aligned} \tag{5.39}$$

$$\begin{aligned}- \gamma_j z_{kt} \sum_{j\in A_k} L_{jt}^{C} &\leq PP_{kt}^{A2DSO} \\ &\leq \gamma_j (1-z_{kt}) \sum_{j\in A_k} L_{jt}^{C}, \forall t, k.\end{aligned} \tag{5.40}$$

Thus, Eqs. (5.36) and (5.37) represent Eq. (5.34). Also, Eqs. (5.38) and (5.39) express Eq. (5.35). Moreover, the relationship between the energy transacted through aggregators and the DSO, PP_{kt}^{A2DSO}, and its corresponding electricity price, λ_{kt}^{A2DSO}, is represented in (5.40). In 5.36 and 5.38, M represents a large positive parameter that gives enough freedom for variables between inequalities to be feasible. According to (5.40), z_{kt} equals 0 when PP_{kt}^{A2DSO} is positive. Besides, z_{kt} as a binary variable is equal to 1 when PP_{kt}^{A2DSO} is negative. Therefore, the objective functions of aggregators and the DSO should be redefined as they are represented in (5.41) and (5.42), respectively.

Hence, the respective energy management problems should be presented considering (5.33), and (5.36)-(5.40).

$$OF_k^{AG'} = \sum_t \sum_{j \in A_k} \lambda_{kt}^{L2A} P_{jt}^{L2A} - \sum_t PP_{kt}, \forall k. \tag{5.41}$$

$$\begin{aligned} OF^{DSO'} &= \sum_t PP_{kt} + \sum_t \lambda_t^{rt} P_t^{rt} \\ &- \lambda^{DSO2L} \sum_t \sum_j P_{jt}^{DSO2L}. \end{aligned} \tag{5.42}$$

5.3.2.1 Aggregators-based energy trading problem

Here, the decentralized energy management problem is modeled from the aggregators' perspective as seen in the following (Problem $M1$):

$$\begin{gathered} \min EC^{AG'} = \textstyle\sum_k OF_k^{AG'} \\ s.t.: (5.18) - (5.26), (5.28), (5.33), (5.36) - (5.40) \end{gathered}$$

Each aggregator transacts energy flexibility with the consumers that are in its region, and with the DSO. However, aggregators are not able to exchange energy with other aggregators and their corresponding end-users. Moreover, all four types of definitions of flexibility can be considered in this approach.

5.3.2.2 Consumers-based energy trading problem

In this section, the energy flexibility management problem is modeled decentralize which is solved by consumers. Thus, end-users manage their energy flexibility autonomously. Also, consumers can only provide shiftable loads and energy transaction with the aggregator, Eq. (5.22) and (5.25), respectively. Hence, Eqs. (5.23) and (5.26) are not provided in this approach as they require a coalition of the consumers in the aggregators' layer. Each end-user transacts energy flexibility with its corresponding aggregator. Besides, end-users are able to buy real-time energy from the DSO. Therefore, the consumers-based decentralized energy flexibility management problem is modeled in the following (Problem $M2$):

$$\min EC^{EU} = \sum_j OF_j^{EU}$$
$$s.t. : (5.18) - (5.22), (5.24) - (5.25), (5.28), (5.33), (5.36) - (5.40)$$

Hence, this problem is decomposed into j independent problems in which each end-user manages its own energy flexibility without being in a coalition with other end-users. However, in $M1$, the flexibility management problem is decomposed into k independent problems from the perspective of aggregators. In this way, end-users are able to provide only shiftable loads, because Eqs. (5.23) and (5.26) are not considered in this approach which requires cooperation between end-users to improve sustainability of the power distribution grid.

5.3.3 Evaluation of the Monopolistic Approach

In this section, a 33-bus test system- which has been demonstrated in Fig. 5.2- is used to assess the proposed monopolistic approach to manage energy flexibility. The energy price in the real-time electricity market and energy price which is traded in aggregators' regions are shown in Table 5.5. Also, we assume that $\gamma_j = 0.1$ and $\delta_{kt} = 1.1$ according to Ref. [Prieto-Castrillo et al., 2018].

In the monopolistic approach, the energy management problem is modeled from the perspective of one group of agents- e.g. end-users (consumers) or aggregators. In this way, for the consumer-based (Problem $M2$), three scenarios are defined to study the impact of flexibility constraints on the energy management problem. Additionally, for the aggregator-based (Problem $M1$), impact of energy flexibility is assessed in five scenarios. These scenarios are presented in Table 5.6.

Table 5.7 shows the impact of flexibility on total expected costs for end-users, aggregators, and the DSO in the monopolistic approach. As presented in Table 5.7, EC^{EU}, $EC^{AG'}$, and $EC^{DSO'}$ are negative in $C1$. In other words, energy flexibility transaction brings profit to all end-users, aggregators and the DSO. It is because of the bottom-up energy flexibility flow from end-users to aggregators, from aggregators to the DSO, and from the DSO to the RTEM. In $C2$ and $C3$, the total expected cost for aggregators is positive. In these scenarios, there are bidirectional energy transactions between end-users and aggregators, aggregators and the DSO, and the DSO and the RTEM as seen in Fig. 5.5. Also, end-users has no desire to buy real-time energy from the DSO.

TAB. 5.5: Prices of energy traded between consumers and aggregators and real-time energy price [Zhang et al., 2018] and [Prieto-Castrillo et al., 2018].

Time	$\lambda^{L2A}_{k=1,t}$ [€/kWh]	$\lambda^{L2A}_{k=2,t}$ [€/kWh]	$\lambda^{L2A}_{k=3,t}$ [€/kWh]	λ^{RT}_{t}h¿h [€/kWh]
1	0.05	0.08	0.06	0.13
2	0.05	0.08	0.07	0.12
3	0.05	0.09	0.07	0.15
4	0.04	0.07	0.05	0.11
5	0.11	0.18	0.15	0.30
6	0.12	0.20	0.16	0.32
7	0.13	0.22	0.17	0.35
8	0.15	0.24	0.19	0.40
9	0.16	0.25	0.20	0.42
10	0.24	0.41	0.33	0.66
11	0.26	0.42	0.36	0.71
12	0.28	0.43	0.37	0.74
13	0.25	0.40	0.32	0.69
14	0.18	0.26	0.21	0.50
15	0.15	0.24	0.20	0.41
16	0.14	0.22	0.18	0.40
17	0.15	0.25	0.19	0.42
18	0.20	0.36	0.30	0.60
19	0.21	0.36	0.29	0.65
20	0.22	0.41	0.30	0.67
21	0.24	0.42	0.33	0.70
22	0.12	0.22	0.16	0.35
23	0.11	0.19	0.15	0.28
24	0.06	0.09	0.07	0.15

TAB. 5.6: Flexibility scenarios.

Scenario	*Min.*	*s.t.*
$C1$	EC^{EU}	(5.18)-(5.21), (5.24), (5.28), (5.33) and (5.36)-(5.40).
$C2$	EC^{EU}	(5.18)-(5.22), (5.24), (5.28), (5.33) and (5.36)-(5.40).
$C3$	EC^{EU}	(5.18)-(5.21), (5.24)-(5.25), (5.28), (5.33) and (5.36)-(5.40).
$A1$	$EC^{AG'}$	(5.18)-(5.21), (5.24), (5.28), (5.33) and (5.36)-(5.40).
$A2$	$EC^{AG'}$	(5.18)-(5.21), (5.23)-(5.24), (5.28), (5.33) and (5.36)-(5.40).
$A3$	$EC^{AG'}$	(5.18)-(5.22), (5.24), (5.28), (5.33) and (5.36)-(5.40).
$A4$	$EC^{AG'}$	(5.18)-(5.21), (5.24), (5.26), (5.28), (5.33) and (5.36)-(5.40).
$A5$	$EC^{AG'}$	(5.18)-(5.21), (5.24)-(5.25), (5.28), (5.33) and (5.36)-(5.40).

Fig. 5.6 shows the energy traded between aggregator 2 and the DSO, their corresponding electricity price, and $z_{(k=2)t}$. As seen in Fig.5.6(c), $z_{(k=2)t}$ is equal to 1 when $P^{A2DSO}_{(k=2)t}$

Tab. 5.7: Total expected costs for end-users, aggregators, and the DSO in the monopolistic approach.

	$C1$	$C2$	$C3$	
EC^{EU} [€]	-2394.438	-714.291	-714.291	
$EC^{AG'}$ [€]	-239.444	733.548	749.681	
$EC^{DSO'}$ [€]	-2273.819	-1461.078	-1489.181	
	$A1$	$A2$ & $A3$	$A4$	$A5$
EC^{EU} [€]	870.642	3178.062	-30.991	1917.450
$EC^{AG'}$ [€]	-239.444	-239.444	-0.262	0
$EC^{DSO'}$ [€]	-2869.32	-2938.618	-23.309	-30.217

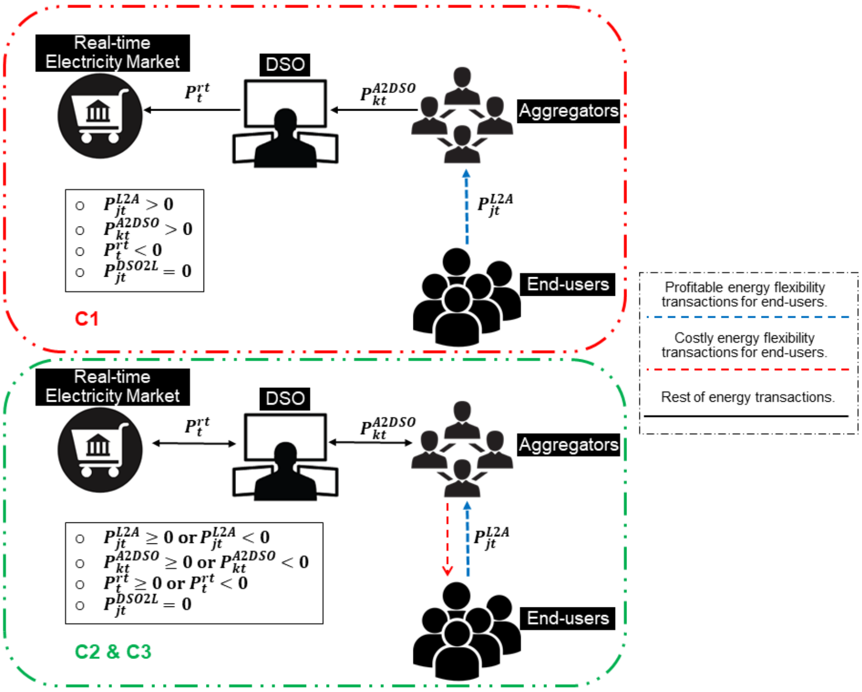

Fig. 5.5: Real-time energy flexibility transaction flows through end-users, aggregators, the DSO, and the RTEM in the monopolistic approach from perspective of end-users.

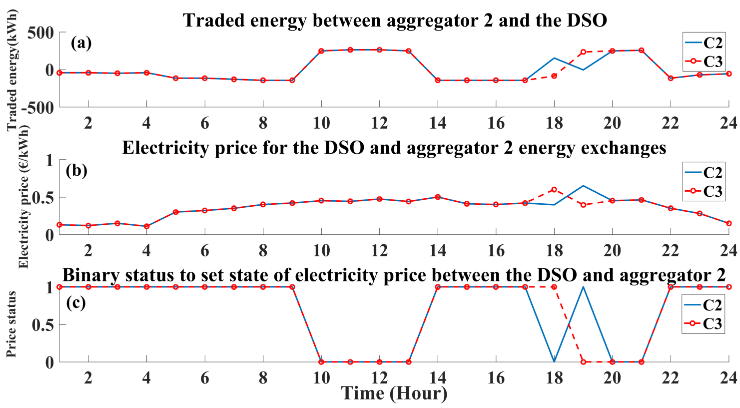

Fig. 5.6: Traded energy (a) electricity price (b), and z_{kt} (c) between aggregator 2 and the DSO in $C2$ and $C3$ in monopolistic approach.

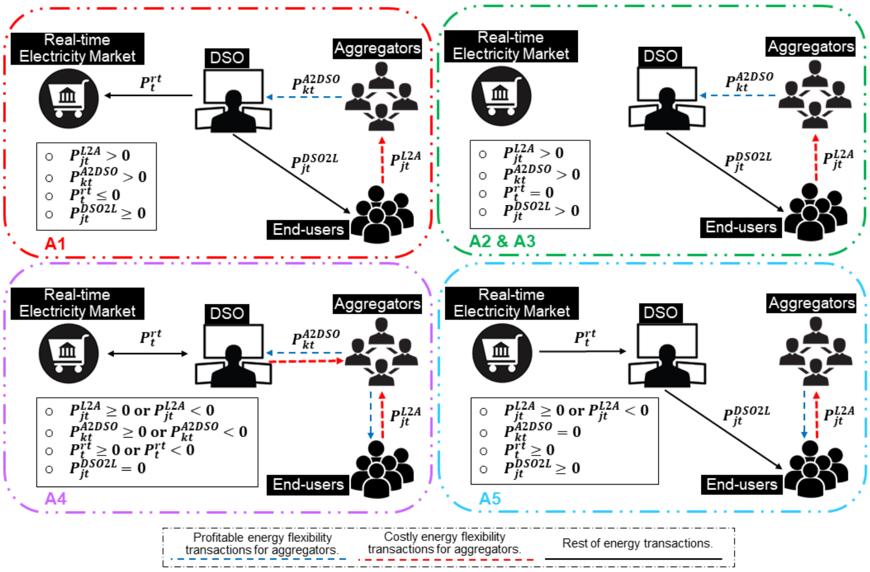

FIG. 5.7: Real-time energy flexibility transaction flows through end-users, aggregators, the DSO, and the RTEM in the monopolistic approach from perspective of aggregators.

is negative. Furthermore, $z_{(k=2)t}$ equals 0 when $P^{A2DSO}_{(k=2)t} \geq 0$. In this way, optimal scenarios (instead of $C1$) for aggregators and the DSO are $C2$ and $C3$, respectively. Thus, the DSO allows end-users for decentralized management of their own energy flexibility because this approach is profitable for them in all scenarios. However, if aggregators are players who are in charge of making policies for their corresponding end-users, $C2$ and $C3$ are not profitable for aggregators. In this way, aggregators do not allow end-users for decentralized management of energy flexibility.

Moreover, Table 5.7 presents that $EC^{AG'}$ equals zero, and there is no energy exchanged between aggregators and the DSO in $A5$. Therefore, $A5$ cannot encourage aggregators as decision-makers in Problem $M1$. On the one hand, in $A4$, total expected costs for all agents are negative. In other words, $A4$ is profitable for all agents. On the other hand, the power distribution network is more sustainable and does not depend to the upstream grid in $A2$ and $A3$ as shown in Fig. 5.7. However, the DSO bought real-time energy from the RTEM in $A5$. Thus, $A5$ is the worst scenario in the monopolistic approach from the perspective of aggregators.

Although interaction between the aggregators and the DSO has been modelled in this section, an interplay model has not been addressed for energy trade management between end-users, aggregators and the DSO.

5.4 Iterative algorithm for trading electricity between aggregators and the DSO

In this section, an iterative algorithm is presented to manage the trade of energy among aggregators and the DSO, considering energy flexibility which is provided by the end-users. Thus, energy is transacted on the basis of a hierarchical structure among the real-time electricity market and the distribution network's players.

5.4.1 The proposed iterative algorithm

Here, an iterative algorithm is proposed to transact energy between aggregators and the DSO based on an MILP model of the energy trading problem which has been introduced in Section 5.3.2. In our proposed iterative algorithm, aggregators are in charge of determining the quantity of energy flexibility traded between aggregators and the DSO, P_{kt}^{A2DSO}. However, the DSO determines the electricity price of energy transaction among them, λ_{kt}^{A2DSO}. Thus, the DSO sets z_{kt} to represent states of the electricity price in the MILP model of the energy management problem. Algorithm 1 represents our proposed algorithm to trade flexibility through aggregators and the DSO as seen in Fig. 5.8.

According to Algorithm 1, aggregator k and the DSO make decisions regarding their own autonomous energy management problem considering interaction signals among aggregators and the DSO. In the following, the energy management problems of aggregators and the DSO are presented:

- Aggregators' problem (Problem A):

$$\min EC^{AG'} = \sum_k OF_k^{AG'}$$
$$s.t.: (5.18)-(5.20),(5.22)-(5.26),(5.33),(5.36)-(5.40)$$

- DSO's problem (Problem D):

$$\min EC^{DSO'} = OF^{DSO'}$$
$$s.t.: (5.21),(5.28),(5.33),(5.36)-(5.40)$$

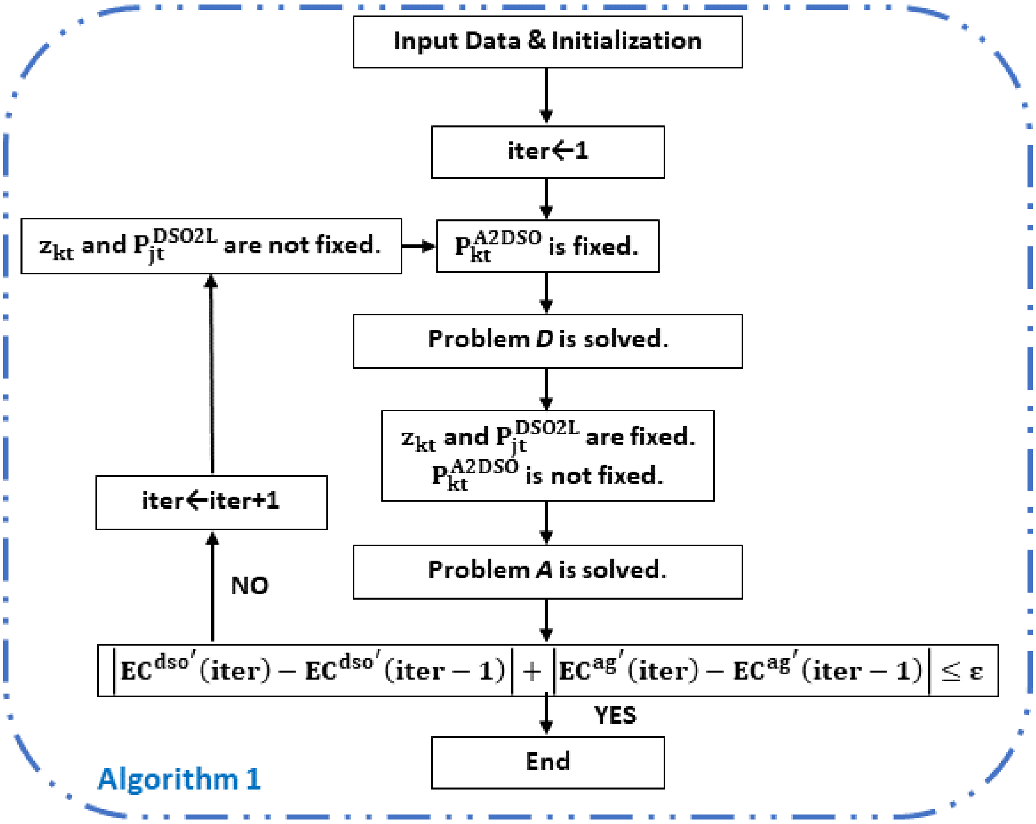

Fig. 5.8: Game-based interaction to transact energy between aggregators and the DSO.

In this structure, the energy flexibility provided by the bottom-layer of the power system is managed only by aggregators. The advantage of this model is that it directly manages the quantity of energy traded between aggregators and the DSO, P_{kt}^{A2DSO}. However, the drawlack of this approach is to not consider the expected profits and costs for end-users in decision-making where end-users are agents which are in charge of providing flexibility to the distribution network.

5.4.2 Assessment of the performance of the iterative algorithm

In this section, the impact of the proposed iterative algorithm on the expected cost for the aggregators and the DSO is studied. In this way, $A1$-$A3$ are considered to assess the performance of the energy management system. In $A1$, end-users are modelled as interruptible loads, shiftable loads- Eq. (5.22)- are modelled in $A2$, and self-consumption constraint- Eq. (5.23)- is considered to model the aggregation of end-users in $A3$. Table 5.8 shows total expected costs for aggregators and the DSO based on the proposed energy trading algorithm.

Tab. 5.8: Total expected costs for aggregators and the DSO based on the iterative algorithm.

	$EC^{AG'}$ [€]	$EC^{DSO'}$ [€]
$A1$	-239.444	-3339.466
$A2$	-143.924	-2413.909
$A3$	-72.618	-1753.407

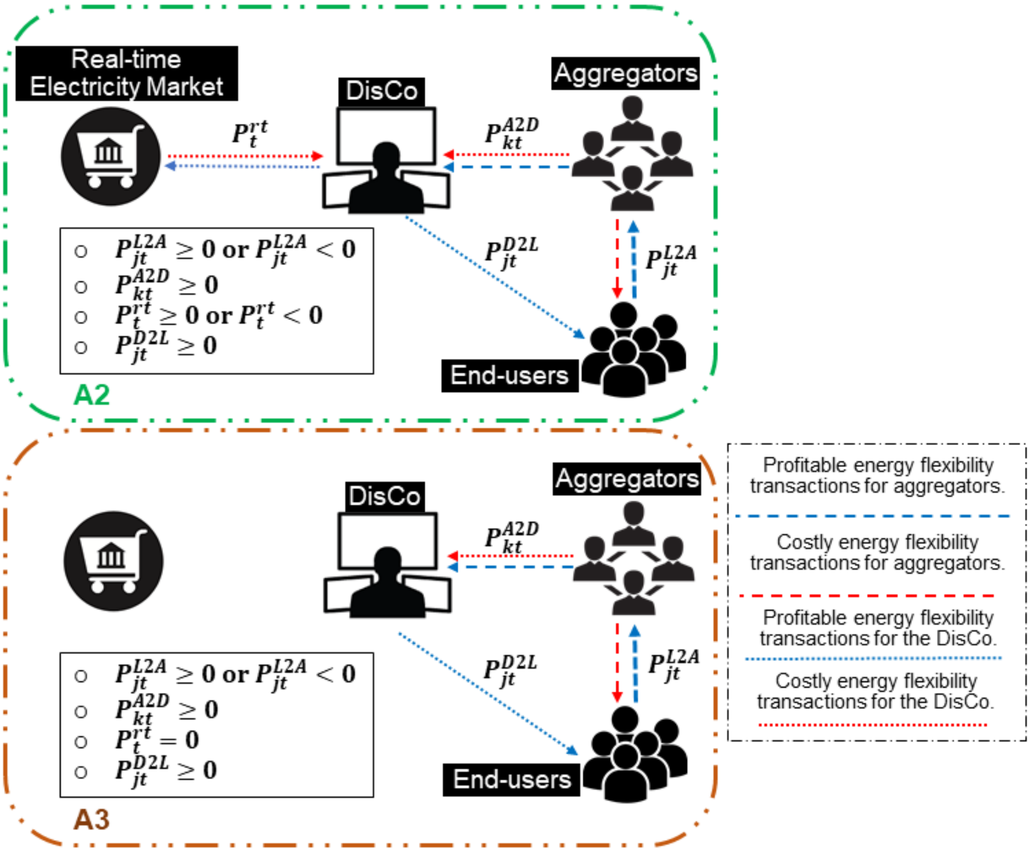

Fig. 5.9: Impact of flexibility scenarios on real-time energy transaction flows through end-users, aggregators, the DSO, and the RTEM based on the proposed iterative algorithm.

Instead of $A1$ which is an optimal scenario of the system in which all end-users play as interruptible loads, total expected costs of aggregators and the DSO are less in $A2$ in comparison with $A3$. In other words, $A2$ is a more profitable scenario for all players in the power distribution system in comparison with $A3$. However, the distribution network acts more sustainable in $A3$, because end-users, aggregators and the DSO make a closed-loop energy trading system as shown in Fig. 5.9. Thus, the power distribution network is more sustainable and does not depend on the upstream grid in $A3$, as shown in Figs. 5.9 and 5.10. Moreover, Fig. 5.11 shows flexible behavior of end-users $j3$, $j15$ and $j29$ as samples of end-users in regions of aggregators 1 to 3, respectively. As illustrated in Fig. 5.11, sample end-users present more dynamic and flexible behavior in $A2$ which increases the profit of end-users.

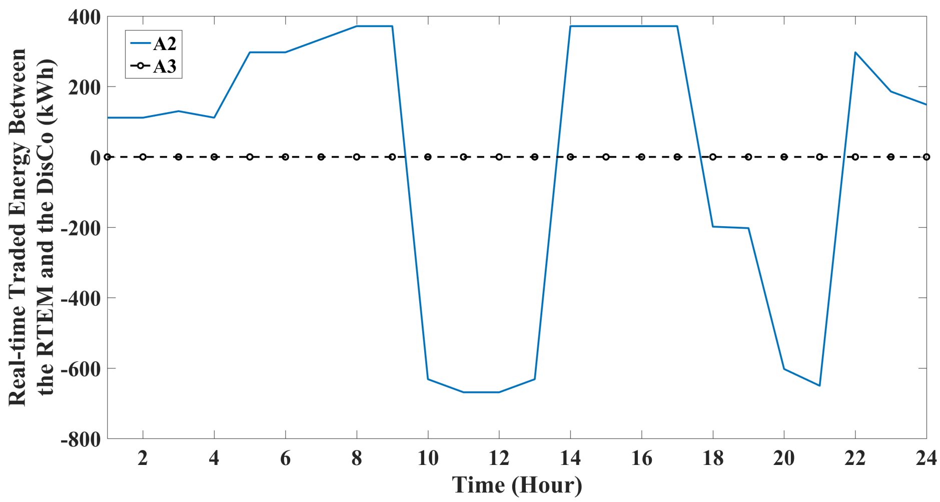

FIG. 5.10: Real-time energy exchanged between the DSO and the RTEM in *A*2 and *A*3.

	Scenario A2				Scenario A3		
	j3	j15	j29		j3	j15	j29
t1	-1.8	-1.8	-4.5	t1	0	0	0
t2	-1.8	-1.8	-4.5	t2	0	0	0
t3	-2.1	-2.1	-5.25	t3	0	0	0
t4	-1.8	-1.8	-4.5	t4	0	0	0
t5	-4.8	-4.8	-12	t5	0	0	0
t6	-4.8	-4.8	-12	t6	0	0	0
t7	-5.4	-5.4	-13.5	t7	0	0	0
t8	-6	-6	-15	t8	0	0	0
t9	-6	-6	-15	t9	0	0	0
t10	10.2	10.2	25.5	t10	10.2	-10.2	-25.5
t11	10.8	10.8	27	t11	10.8	-10.8	-27
t12	10.8	10.8	27	t12	10.8	-10.8	-27
t13	10.2	10.2	25.5	t13	10.2	-10.2	-25.5
t14	-6	-6	-15	t14	0	0	0
t15	-6	-6	-15	t15	0	0	0
t16	-6	-6	-15	t16	0	0	0
t17	-6	-6	-15	t17	0	0	0
t18	9	-3.6	-9	t18	9	-9	-22.5
t19	-3	9.6	24	t19	9.6	-9.6	-24
t20	10.2	10.2	25.5	t20	10.2	-10.2	-25.5
t21	10.5	10.5	26.25	t21	10.5	-10.5	-26.25
t22	-4.8	-4.8	-12	t22	0	0	0
t23	-3	-3	-7.5	t23	0	0	0
t24	-2.4	-2.4	-6	t24	0	0	0

FIG. 5.11: Energy flexibility (kWh) of end-users *j*3 (in region of aggregator 1), *j*15 (in region of aggregator 2), and *j*29 (in region of aggregator 3) in *A*2 and *A*3. Red and green colours represent negative and positive flexibilities, respectively.

5.5 Iterative algorithm for trading electricity between end-users and the DSO

Although the iterative algorithm proposed by us for transaction of energy between aggregators and the DSO directly manages the quantity of energy traded between aggregators and the DSO, the expected costs for end-users are not considered in the system's decision-making.

5.5.1 The proposed iterative algorithm

In the algorithm proposed by us, end-users and the DSO are agents who manage energy flexibility, and aggregators are considered as actors- who just follow decisions which are made by agents- in the power distribution network. Here, the energy management problem of the DSO is identical to the respective one in Section 5.4.1 (Problem D). Thus, the energy management problem of the end-users is:

- End-users' problem (Problem E):

$$\min EC^{EU'}$$
$$s.t. : (5.18) - (5.22), (5.24) - (5.26), (5.33), (5.36) - (5.40)$$

In Problem E, end-users manage their own energy flexibility independently and control the energy traded through the aggregators and the DSO. Furthermore, the DSO sets the electricity price of energy transaction between aggregators and the DSO based on Algorithm 2 which has been presented in Fig. 5.12.

5.5.2 Evaluation of iterative algorithms

In this section, the proposed energy flexibility management problem is evaluated based one a game between the end-users and the DSO, and a game between the aggregators and the DSO. Thus, the performance of the proposed iterative algorithms which we have defined to transact energy flexibility in the power distribution networks are assessed in this section.

In Algorithm 1, it has been defined that there is a game-based interaction between the aggregators and the DSO. Here, scenarios $A1$-$A5$ which have been presented in Table 5.6 are considered to assess the performance of the energy management system. As seen

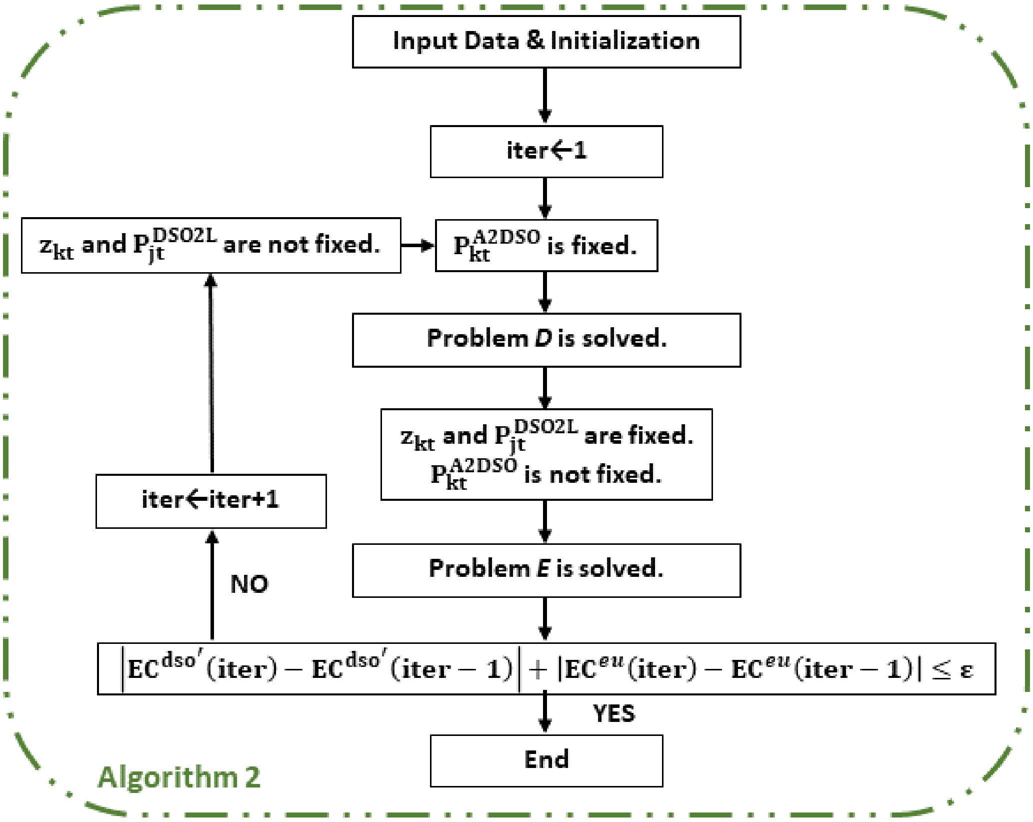

FIG. 5.12: Game-based interaction to transact energy between aggregators and the DSO.

TAB. 5.9: Total expected costs for end-users, aggregators, and the DSO in the game-based approach.

	EC^{eu} [€]	$EC^{ag'}$ [€]	$EC^{dso'}$ [€]
$A1$	157.767	-239.444	-3339.466
$A2$	1112.969	-143.909	-2413.909
$A3$	1826.025	-72.618	-1753.407
$A4$	2552.205	0	-1065.648
$A5$	2552.205	0	-1065.648
$C1$	159.767	-239.444	-8607.231
$C2$	1111.734	-100.082	-5612.034
$C3$	2552.205	0	-1065.648

in Table 5.9, EC^{EU} is positive in all scenarios which means that game-based interaction between the aggregators and the DSO is not profitable for end-users. Moreover, $EC^{AG'}$ equals zero in $A4$ and $A5$ because the aggregators do not transact any energy to the DSO as shown in Fig. 5.13. Thus, $A4$ and $A5$ cannot motivate aggregators to trade flexibility with the DSO. Instead of $A1$ which is an optimal scenario of the system that all end-users play as interruptible loads, total expected costs for all agents are less in $A2$ in comparison with $A3$. In other words, $A2$ is a more profitable scenario for all agents in the power distribution system in comparison with $A3$. However, the distribution

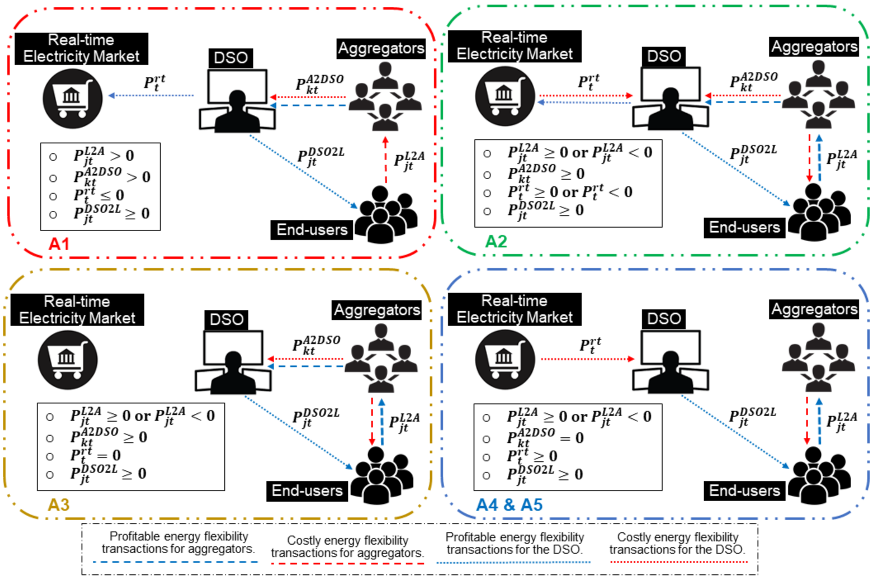

FIG. 5.13: Real-time energy flexibility transaction flows through end-users, aggregators, the DSO, and the RTEM in the game-based interaction between aggregators and aggregators and the DSO.

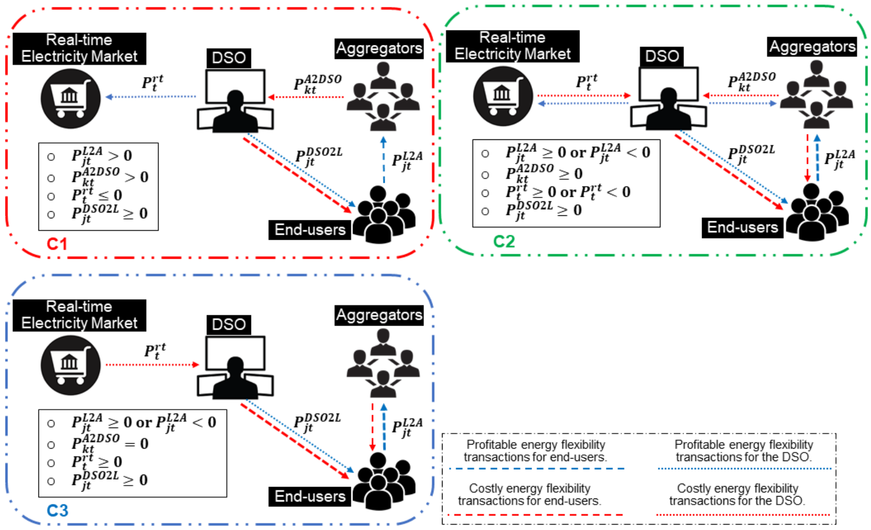

FIG. 5.14: Real-time energy flexibility transaction flows through end-users, aggregators, the DSO, and the RTEM in the game-based interaction between aggregators and end-users and the DSO.

network acts as a sustainable energy system in $A3$, because the DSO does not exchange energy with the real-time electricity market as seen in Fig. 5.15(a).

Algorithm 2 defines a game-based energy flexibility transaction between the end-users and the DSO. Hence, the aggregators are not decision-makers in the exchange of energy in Algorithm 2. The interaction between end-users and the DSO is studied in three scenarios, $C1$-$C3$, which have been presented in Table 5.6. As presented in Table 5.9,

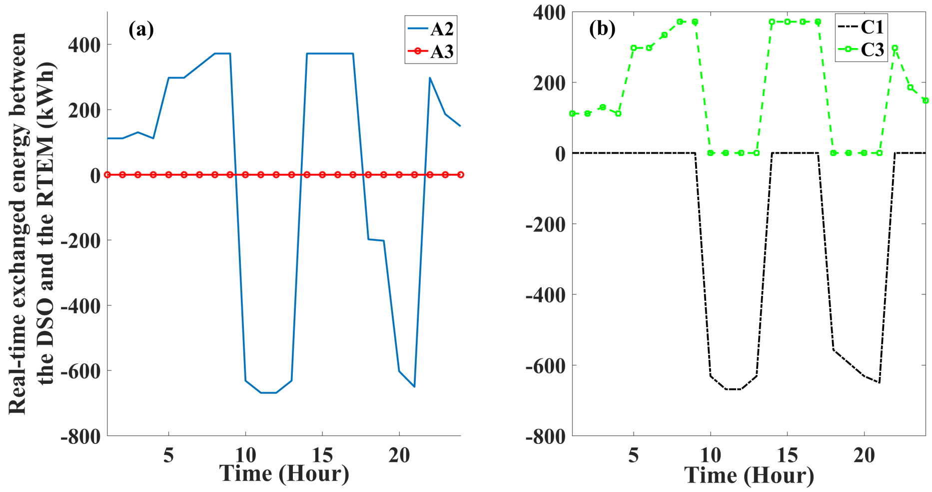

FIG. 5.15: Real-time energy exchanged between the DSO and the RTEM in $A2$ and $A3$ (a), in $C1$ and $C3$ (b) in game-based iterative algorithms.

$C1$ is an optimal scenario for all agents in this game. However, $C3$ is the worst scenario in which EC^{EU} is maximum, and the expected profit of the DSO is minimum. Also, $EC^{AG'}$ is equal to zero. In addition, in $C3$, the energy transaction between the DSO and the RTEM is one-way (from the RTEM to the DSO) which is not sufficient for the power distribution network as seen in Figs. 5.14 and 5.15(b).

5.6 Conclusions

In this chapter, we have presented decentralized, monopolistic and game-based approaches to manage energy flexibility among distribution network's agents. Also, the performance of the proposed approaches to manage energy flexibility has been assessed based on the impacts of flexible behaviors of the end-users and aggregators.

According to our decentralized approach, end-users manage their energy flexibility autonomously. Besides, two types of flexible behavior is defined- shiftable and self-consumption flexibility- for the end-users to provide the required energy flexibility in a cooperation with their corresponding aggregators. In this way, while end-users manage their own flexibility independently to provide the shiftable flexibility, the coalition of end-users is required to provide the self-consumption flexibility. Finally, it should be mentioned that this chapter has not modeled the impact of EVs on energy trading problem in the distribution network. In Chapter 6, we will discuss how energy management system can be modeled considering uncertainty of EV mobility in the distribution grid.

Chapter 6

Local electricity trading for EVs (*comercio local de electricidad para EVs*)

Chapter 6

Local electricity trading for EVs (*comercio local de electricidad para EVs*)

6.1 Introduction

The urbanization brings several challenges e.g. environmental, economical, energy, traffic for the future cities and in global overview for the planet earth [Shahidehpour et al., 2018]. In this way, smart cities have been introduced to build cites' infrastructure based on the cutting-edge technologies to support optimal multi-objective decisions [Arasteh et al., 2016]. In this way, smart cities make complex systems according to interconnected between subsystems which have been designed for different specific aims. For instance, smart transportation systems have been defined to manage transportation of public vehicles, monitor traffic based on mobility of vehicles consisting of EVs. On the other hand, the decision-making in energy management systems of distribution networks of smart cities plays an important role based on socioeconomic and energy reliability concerns in cities. Also, SGs have been defined as one of the most collective solutions in order to provide a solution for these concerns [Borlase, 2016]. Also, SGs provide two-way communication data transaction between system operators and customers in the bottom layers of the power systems. Moreover, SGs enable distribution grids to overcome uncertain impact of EVs' mobility. The DRP is one of the results of this restructuring to adjust the electrical demand in distribution networks based on price-based or incentive-based DRPs [Siano, 2014]. Thus, the end-users are able to behave more flexible in the restructured environment of the power system [Gazafroudi et al., 2017a], [Siano and Sarno, 2016] and [Graditi et al., 2018]. In other words, the end-users can behave as active customers in the SGs to play as a consumer or a virtual producer by decreasing their scheduled electrical demand in local energy management systems [Kok et al., 2009]. In this chapter, a stochastic energy management problem is defined to model expected energy flexibility provided by end-users based on uncertainty of EV's mobility in power distribution grids. Three strategies are presented to manage energy flexibility and operation of EVs through the end-users and the central coordinator in the power distribution system. In this way, the uncertainty of EVs' mobility is modeled by a stochastic energy management problem. Also, end-users are modeled as shiftable and interruptible loads to provide energy flexibility. According to the proposed strategies, energy flexibility and charging operation of EVs are managed by end-users decentralize, centralize, and partial centralize through a bottom-up approach.

The rest of this chapter is organized as follows. Section 6.2 introduces the proposed formulation for the energy management problem. The proposed strategies to manage energy flexibility and charging operation of EVs are described in Section 6.3. In Section 6.4, the results of simulation studies are illustrated. Finally, the findings are concluded in Section 6.5.

6.2 Problem formulation

In this section, a real-time energy flexibility management problem decentralized in the bottom layer of the distribution network is defined. Fig. 6.1 displays a schematic overview of this section. In this model, two types of players have been defined as further discussed in this chapter. The first type of players is called *agent* which can make the decision independently to manage energy flexibility. The Second type of player is called *actor* which follows the decisions of the agents. In this way, the agents consist of end-users and aggregators. However, only one of the end-users or aggregators can be agents that it depends on the chosen strategies for managing the flexibility in the system. On the other hand, EVs are defined as the actors who are considered in the flexibility management problem but are not decision-makers. In this way, the real-time energy flexibility is traded through a decentralized, bottom-up approach. The end-users can transact the energy flexibility only with their corresponding aggregators in a bilateral energy transaction. However, the aggregators can exchange energy with the RTEM. It should be noted that the aggregators are considered as the price-takers in the RTEM in this model. Fig. 6.2 shows the proposed bottom-up structure to manage energy flexibility in distribution grids. Moreover, in Fig. 6.2, corresponding structure for energy transaction between end-users, aggregators, and EVs are introduced. Each end-user (as an independent agent) can manage its real-time energy considering constraints related to its scheduled load. Thus, decrements/increments of the scheduled load can provide upward/downward flexible energy. Besides, charging and discharging of EVs increases

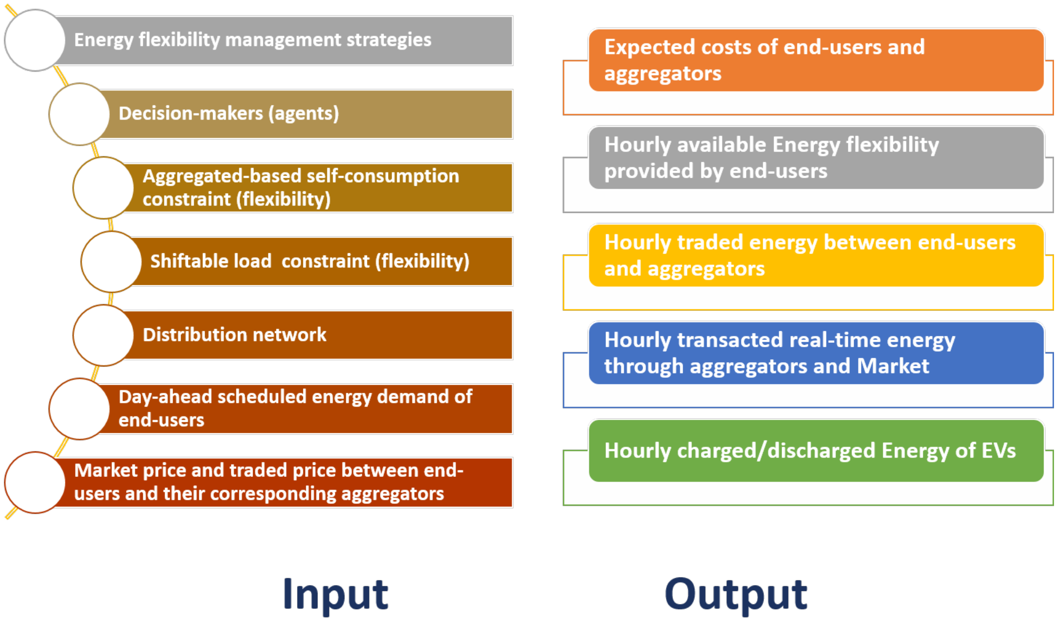

FIG. 6.1: Schematic overview of proposed energy flexibility management model [Gazafroudi et al., 2019a].

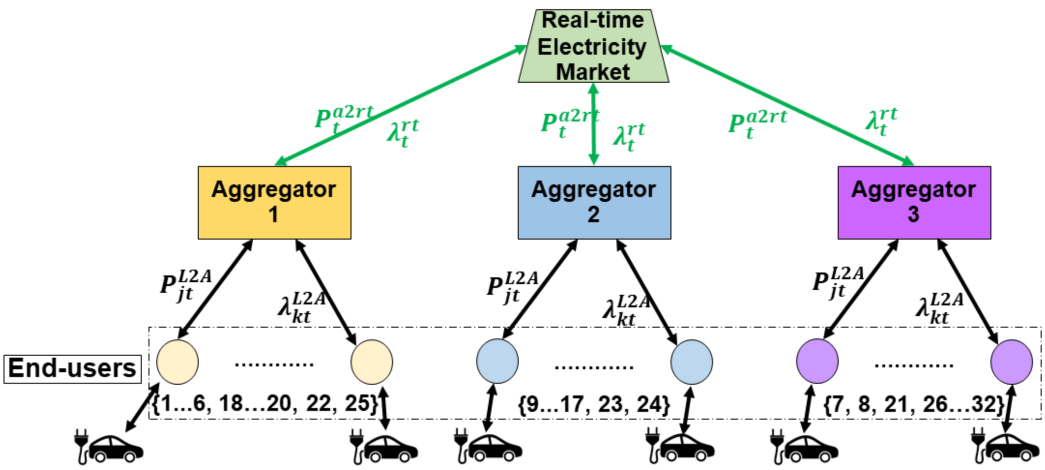

FIG. 6.2: General structure for real-time energy transaction considering EVs mobility in the distribution network [Gazafroudi et al., 2019a].

and decreases the real-time demand of end-users as represented in (6.1). Here, β_j is defined as a coefficient to consider the charging operation of EVs in energy flexibility management problem. The utilization of EV is not considered in the energy management problem if β_j equals zero. Eq. (6.2) represents the minimum and maximum limitations of the energy flexibility which is defined as a portion of the scheduled load. In this section, the end-users are considered only as shiftable loads to provide energy flexibility (6.3). Thus, the transacted energy between end-user j and its corresponding aggregator is expressed in (6.4).

$$L_{jt\omega} = L^C_{jt} - L^F_{jt\omega} + \beta_j P^{CH,C}_{jt\omega} - \beta_j P^{DIS,C}_{jt\omega}, \forall j, \omega, t. \tag{6.1}$$

$$-\sigma_{jt} L^C_{jt} \leq L^F_{jt\omega} \leq \sigma_{jt} L^C_{jt}, \forall j, \omega, t. \tag{6.2}$$

$$\sum_t L^F_{jt\omega} = 0 \ , \forall j, \omega. \tag{6.3}$$

$$L^F_{jt\omega} + \beta_j P^{DIS,C}_{jt\omega} - \beta_j P^{CH,C}_{jt\omega} = P^{L2A}_{jt\omega}, \forall j, \omega, t. \tag{6.4}$$

In this way, EVs can be utilized according to the energy management strategies by end-users or aggregators in the distribution network. The SOC balancing equation of EV i is represented in (6.5) and (6.6). Here, $EA_{it\omega}$ is a binary parameter, representing the availability of EV i at all buses of the network to be charged or discharged. If $EA_{it\omega}$ equals 0, the EV is in streets, then $Mob_{it\omega}$ presents amount of discharged power due to mobility of EV i. In other words, $Mob_{it\omega}$ equals 0 when $EA_{it\omega}$ is equal to 1. Also, C^0_i presents the initial SOC of EV i.

$$C_{it\omega} = C_{i,t-1,\omega} + EA_{it\omega} P^{CH}_{it\omega} \eta_{B2V} - EA_{it\omega} P^{DIS}_{it\omega} / \eta_{V2B} \\ - Mob_{it\omega}, \forall i, \omega, t \geq 2. \tag{6.5}$$

$$C_{i,t=1,\omega} = C^0_i + EA_{it\omega} P^{CH}_{it\omega} \eta_{B2V} - EA_{it\omega} P^{DIS}_{it\omega} / \eta_{V2B} \\ - Mob_{it\omega}, \forall i, \omega, t = 1. \tag{6.6}$$

Maximum and minimum limitations of EVs' SOC are presented in (6.7). Also, the ramp constraints of EVs' SOC are stated in (6.8) and (6.9).

$$C^{min}_i \leq C_{it\omega} \leq C^{max}_i, \forall i, \omega, t. \tag{6.7}$$

$$-r^{min} \leq C_{it\omega} - C_{i,t-1,\omega} \leq r^{max}, \forall i, \omega, t \geq 2. \tag{6.8}$$

$$-r^{min} \leq C_{it\omega} - C^0_i \leq r^{max}, \forall i, \omega, t = 1. \tag{6.9}$$

The discharging and charging limitations are represented in (6.10) and (6.11), respectively. Here, $u_{it\omega}$ is a binary variable which represents state of the EV to be in charged or discharged mode. The EV is discharged if $u_{it\omega}$ equals 1.

$$0 \leq P^{DIS}_{it\omega} \leq r^{max} u_{it\omega}, \forall i, \omega, t. \tag{6.10}$$

$$0 \leq P^{CH}_{it\omega} \leq r^{min}(1 - u_{it\omega}), \forall i, \omega, t. \tag{6.11}$$

In this section, it is considered that each EV is utilized by each end-user. This means that each end-user can utilize more than one EV, but each EV is only utilized by one specific end-user. In this way, (6.12)-(6.14) represent equations to map EV i to end-user j. Here, $MEV_{jit\omega}$ is defined to indicate that EV i is located at end-user j at time t, and scenario ω.

$$C^{m}_{jit\omega} = MEV_{jit\omega} C_{it\omega}, \forall j, i, \omega, t. \tag{6.12}$$

$$P^{dis,m}_{jit\omega} = MEV_{jit\omega} P^{dis}_{it\omega}, \forall j, i, \omega, t. \tag{6.13}$$

$$P^{ch,m}_{jit\omega} = MEV_{jit\omega} P^{ch}_{it\omega}, \forall j, i, \omega, t. \tag{6.14}$$

As mentioned in the previous paragraph, each end-user can utilize more than one EV. Eqs. (6.15)-(6.17) state total amount of the SOC, discharged power, and charged power, respectively, that are managed by end-user j.

$$C^{C}_{jt\omega} = \sum_{i} C^{M}_{jit\omega}, \forall j, \omega, t. \tag{6.15}$$

$$P^{DIS,C}_{jt\omega} = \sum_{i} P^{DIS,M}_{jit\omega}, \forall j, \omega, t. \tag{6.16}$$

$$P^{CH,C}_{jt\omega} = \sum_{i} P^{CH,M}_{jit\omega}, \forall j, \omega, t. \tag{6.17}$$

Moreover, the SOC of each EV, when it leaves the charging station of each end-user should be greater than or equal 110% of its SOC when it enters the charging station (6.18). Thus, $IEV_{jit\omega}$ represents the binary status that EV i enters to charging station of end-user j as defined in (6.19). In other words, EV i enters to charging station of end-user j, if $IEV_{jit\omega}$ equals 1. On the other hand, $OEV_{jit\omega}$ expresses the state of EV i when it leaves the charging station of end-user j as represented in (6.20).

$$1.1 C^{M,IN}_{jit\omega} \leq C^{M,OUT}_{jit\omega}, \forall j, i, \omega. \tag{6.18}$$

$$C^{M,IN}_{jit\omega} = \sum_{t} IEV_{jit\omega} C^{M}_{jit\omega}, \forall j, i, \omega. \tag{6.19}$$

$$C^{M,OUT}_{jit\omega} = \sum_{t} OEV_{jit\omega} C^{M}_{jit\omega}, \forall j, i, \omega. \tag{6.20}$$

According to the bottom-up structure, the total flexibility transacted through end-users and aggregators should be traded between aggregators and the RTEM as represented in (6.21).

$$P^{A2RT}_{kt\omega} = \sum_{j \in A_k} P^{L2A}_{jt\omega}, \forall k, t, \omega. \tag{6.21}$$

In the next section, the proposed strategies to manage energy flexibility and EVs utilization are introduced.

6.3 Strategies to manage energy flexibility

Here, three strategies are defined to manage energy flexibility in distribution networks. In strategy-I, the end-users manage energy flexibility and charging operation of EVs in a decentralized approach. In the strategy-II, the end-users manage the energy flexibility in a decentralized way. However, the charging operation of EVs is managed centrally by a virtual agent called EVs coordinator. In strategy-III, both energy flexibility of end-users and charging operation of EVs are managed centrally by a virtual agent which is called local coordinator. These strategies are described in the following:

6.3.1 Strategy-I

In strategy-I, S_1, the charging operation of EVs is managed only by EV-owners. Thus, the corresponding expected cost of the EV is only considered in the objective function of the end-user (EV owner). In this way, the impact of the EV on its owner's expected cost is observed when the EV is available at its owner's building, and β_j is considered to be equal to 1. Here, the objective functions of end-users and aggregators are represented in (6.22) and (6.23), respectively. Eq. (6.22) states the expected cost of end-user j based on real-time energy flexibility transaction with its corresponding aggregator that should be minimized. In (6.23), the expected cost of aggregator k is represented which consists of the expected cost due to trading energy flexibility with its end-users, and the expected profit due to energy exchanging with the RTEM.

$$OF^{EU''}_{j\in A_k} = -\sum_{t} \lambda^{L2A}_{kt} P^{L2A}_{jt\omega}, \forall j. \tag{6.22}$$

$$OF^{AG''}_{k} = \sum_{t} \sum_{j\in A_k} \lambda^{L2A}_{kt} P^{L2A}_{jt\omega} - \sum_{t} \lambda^{rt}_{t} P^{A2RT}_{kt\omega}, \forall k. \tag{6.23}$$

In this way, the energy management problem of S_1 to operate energy flexibility of end-users and charging of EVs is modeled decentralized as formulated in the following problem ($P1$):

$$\min EC^{eu} = \textstyle\sum_j OF^{eu}_j$$
$$s.t. : (6.1) - (6.21)$$

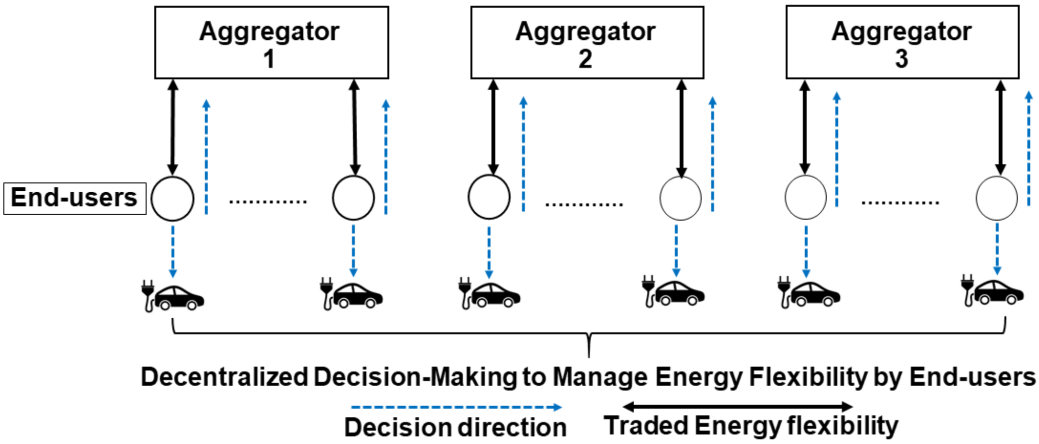

FIG. 6.3: Decentralized decision-making framework for energy flexibility management problem by end-users in Strategy-I [Gazafroudi et al., 2019a].

Fig. 6.3 shows real-time energy problem is managed decentralize by end-users to operate energy flexibility of charging of EVs in strategy one.

6.3.2 Strategy-II

In strategy-II, S_2, a sequential two-stage energy management problem is proposed. In stage-I, energy flexibility is managed autonomously by end-users without considering the EVs' constraints. However, in stage-II, charging mode of EVs is operated centralize by the EV Coordinator (EVC) while energy flexibility decisions were made by end-users in stage one. In energy management problem of stage one, β_j equals 0 to avoid the EVs utilization in decentralize decision-making of end-users. The proposed energy flexibility problem of stage one is presented in the following problem ($P2$):

$$\min EC^{EU''} = \textstyle\sum_j OF_j^{EU''}$$
$$s.t. : (6.1) - (6.4)$$

In the second stage, the EVC manages centralized charging of the EVs. Hence, the energy flexibility (which is the output of $P2$) is considered as an input in the energy management problem of stage two (Problem $P3$). Also, β_j equals 1 in the second stage. The objective function of the EVC, EC^{EVC}, is defined in (6.24). Here, ΔP_{jt}^{L2A} represents the change of traded energy between end-user j and aggregator k in stage-II compared to stage-I. The second term in (6.24) represents the expected cost of charging operation of EVs by end-users which are not their owners. Eqs. (6.25) and (6.26) state discharging and charging operation of EV i by end-users which are not the EV owner. Thus, $NEV_{jit\omega}$ is defined to map EV i to end-users who are not its owner. Also, OE_{ji} equals 1, if end-user j is the owner of EVi.

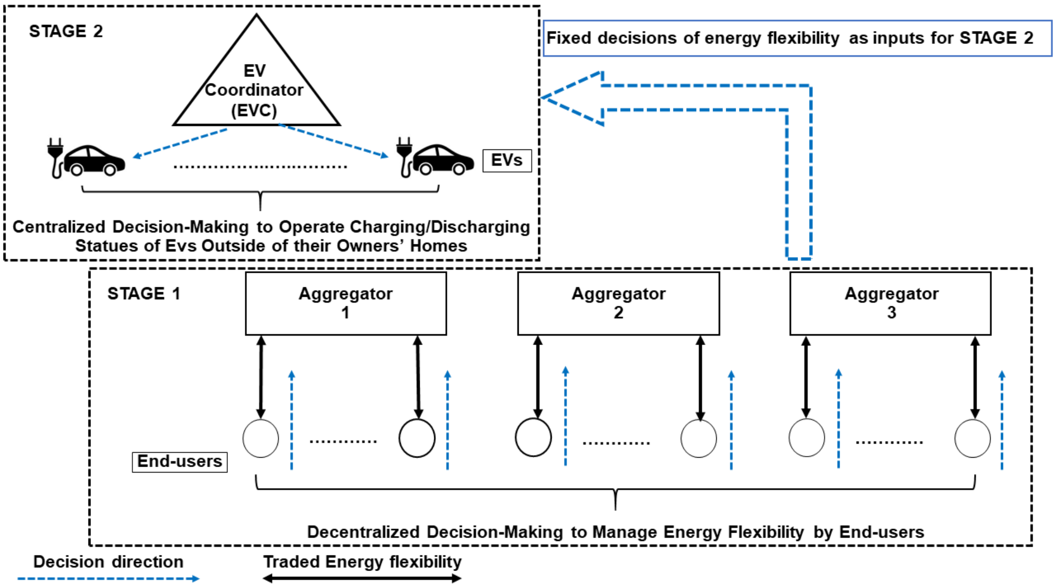

FIG. 6.4: Two-stage sequential decision-making framework to manage energy flexibility and charging state of EVs in Strategy-II [Gazafroudi et al., 2019a].

$$EC^{EVC} = \sum_{j} OF_{j}^{EU''} - \sum_{jt}(\lambda_{kt}^{L2A}\Delta P_{jt}^{L2A} + \sum_{i} OE_{ji}\sum_{k}\lambda_{kt}^{L2A}(P_{jit\omega}^{CH-} - P_{jit\omega}^{DIS-})). \quad (6.24)$$

$$P_{jit\omega}^{DIS-} = NEV_{jit\omega}P_{it\omega}^{DIS}, \forall j, i, \omega, t. \quad (6.25)$$

$$P_{jit\omega}^{CH-} = NEV_{jit\omega}P_{it\omega}^{CH}, \forall j, i, \omega, t. \quad (6.26)$$

Fig. 6.4 presents two-stage sequential energy management problem in strategy-II. In this way, $P3$ is:

$$\min EC^{EVC}$$
$$s.t.: (6.1) - (6.21), (6.25), (6.26)$$

6.3.3 Strategy-III

In strategy-III, S_3, charging operation of EVs and scheduling energy flexibility of end-users are managed in a centralized way by Local Coordinator (LC). The objective function of the LC, EC^{LC}, is represented in (6.27).

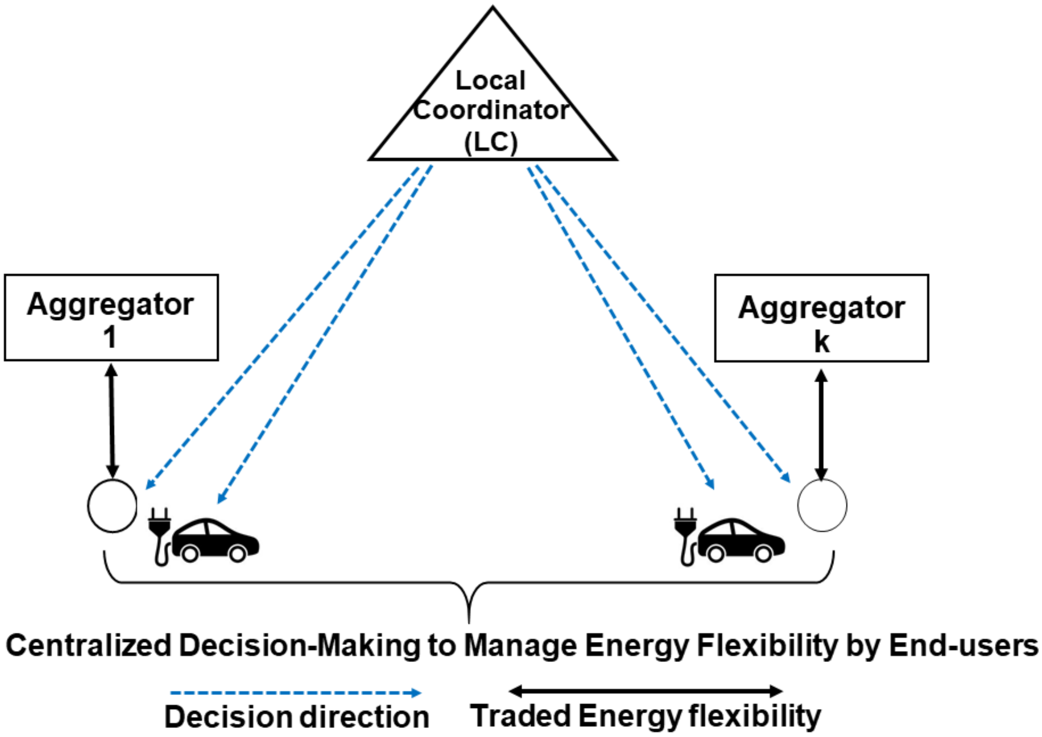

FIG. 6.5: Centralized decision-making framework to manage energy flexibility and charging state of EVs in Strategy-III [Gazafroudi et al., 2019a].

$$
\begin{aligned}
EC^{LC} = \sum_{jt} (OF_j^{EU''} \\
+ \sum_{i} OE_{ji} \sum_{k} \lambda_{kt}^{L2A} (P_{jit\omega}^{CH-} - P_{jit\omega}^{DIS-}))
\end{aligned}
\tag{6.27}
$$

As it is seen in (6.27), energy flexibility of end-users and charging operation of EVs are managed centralize by the LC. Fig.6.5 demonstrates centralized energy management problem in S_3. In the following, the energy management problem in strategy 3, $P4$, is represented:

$$
\begin{gathered}
\min EC^{LC} \\
s.t.: (6.1) - (6.21), (6.25), (6.26)
\end{gathered}
$$

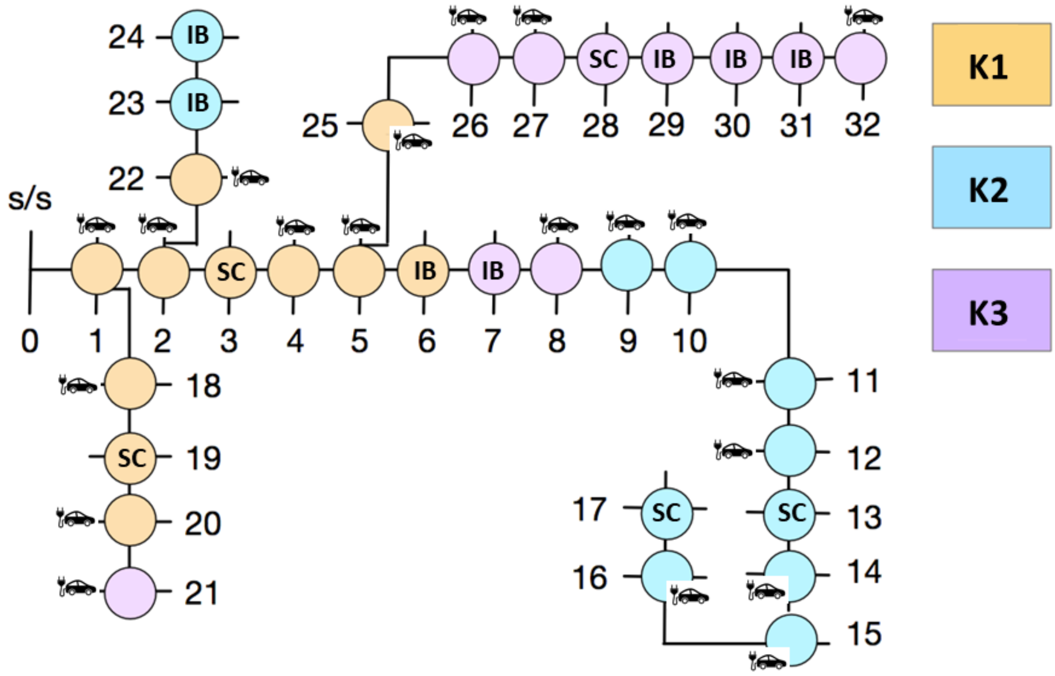

FIG. 6.6: A modified 33-bus test system with corresponding aggregators and PEVs owners [Gazafroudi et al., 2019a].

6.4 Simulation results

6.4.1 Case study

Here, a 33-bus test system which has been shown in Chapter 5 and has been modified in [Gazafroudi et al., 2019a] is used to evaluate the proposed strategies to manage energy flexibility and charging/discharging states of EVs as shown in Fig.6.6. Three regions are defined which aggregators have bilateral contracts with their corresponding end-users in the bottom layer of the system. Thus, the price of energy traded in each of these regions is different as shown in Table 6.1. Moreover, it is assumed there are three types of end-users consisting of residential buildings, industrial buildings (IB) and Shopping Centers (SC). In this way, for the sake of simplicity, EV owners are only allocated to residential buildings as seen in Fig. 6.6.

Table 6.2 presents EVs and their corresponding owners. In the stochastic problem, uncertain mobility of EVs is modeled by two probabilistic scenarios. In scenario one, it is assumed that EV i goes from its owner's residential building to an industrial building and comes back directly from that industrial building to the home. On the other hand, in scenario two, it is assumed that EV i stops at shopping in return path from industrial building to the home. In this way, corresponding probabilities of Scenarios one and two are considered 0.8 and 0.2, respectively. Mobility scenarios of EVs are presented

TAB. 6.1: Prices of traded energy between end-users and aggregators [Zhang et al., 2018], [Prieto-Castrillo et al., 2018] and [Gazafroudi et al., 2019a].

Time (h)	$\lambda^{L2A}_{k=1,t}$ [€/kWh]	$\lambda^{L2A}_{k=2,t}$ [€/kWh]	$\lambda^{L2A}_{k=3,t}$ [€/kWh]	λ^{RT}_{t} [€/kWh]
1	0.05	0.08	0.06	0.13
2	0.05	0.08	0.07	0.12
3	0.05	0.09	0.07	0.15
4	0.04	0.07	0.05	0.11
5	0.11	0.18	0.15	0.30
6	0.12	0.20	0.16	0.32
7	0.13	0.22	0.17	0.35
8	0.15	0.24	0.19	0.40
9	0.16	0.25	0.20	0.42
10	0.24	0.41	0.33	0.66
11	0.26	0.42	0.36	0.71
12	0.28	0.43	0.37	0.74
13	0.25	0.40	0.32	0.69
14	0.18	0.26	0.21	0.50
15	0.15	0.24	0.20	0.41
16	0.14	0.22	0.18	0.40
17	0.15	0.25	0.19	0.42
18	0.20	0.36	0.30	0.60
19	0.21	0.36	0.29	0.65
20	0.22	0.41	0.30	0.67
21	0.24	0.42	0.33	0.70
22	0.12	0.22	0.16	0.35
23	0.11	0.19	0.15	0.28
24	0.06	0.09	0.07	0.15

TAB. 6.2: PEVs and their corresponding owners [Gazafroudi et al., 2019a].

EV	EV owner	EV	EV owner
$i1$	$j1$	$i11$	$j15$
$i2$	$j2$	$i12$	$j16$
$i3$	$j4$	$i13$	$j18$
$i4$	$j5$	$i14$	$j20$
$i5$	$j8$	$i15$	$j21$
$i6$	$j9$	$i16$	$j22$
$i7$	$j10$	$i17$	$j25$
$i8$	$j11$	$i18$	$j26$
$i9$	$j12$	$i19$	$j27$
$i10$	$j14$	$i20$	$j32$

in Table 6.3. Also, Fig. 6.7 shows the corresponding location of EVs in different time steps after scenario reduction. Moreover, for the sake of simplicity, it is assumed that the characteristics of all EVs are the same. Minimum and maximum state of charge of EV i is between 1.77 and 5.9kWh, and its charging and discharging efficiencies are 90%.

	1	2	3	4	5	6	7	8	9	10	11	12	13	14	15	16	17	18	19	20	21	22	23	24
*j*1	1	1	1	1	1	1	1	1											1	1	1	1	1	1
*j*2	2	2	2	2	2	2	2	2	2											2	2	2	2	2
*j*3																			6	6				
																		16	16					
																			17	17				
*j*4	3	3	3	3	3	3	3	3	3	3												3	3	3
*j*5	4	4	4	4	4	4	4	4	4										4	4	4	4	4	4
*j*6									1	1	1	1	1	1	1	1	1	1						
								9	9	9	9	9	9	9	9	9	9							
								11	11	11	11	11	11	11	11	11	11							
								16	16	16	16	16	16	16	16	16	16							
*j*7									8	8	8	8	8	8	8	8	8	8						
									10	10	10	10	10	10	10	10	10	10						
									12	12	12	12	12	12	12	12	12	12						
									20	20	20	20	20	20	20	20	20	20						
*j*8	5	5	5	5	5	5	5	5													5	5	5	5
*j*9	6	6	6	6	6	6	6	6	6												6	6	6	6
*j*10	7	7	7	7	7	7	7	7													7	7	7	7
*j*11	8	8	8	8	8	8	8	8											8	8	8	8	8	8
*j*12	9	9	9	9	9	9	9											9	9	9	9	9	9	9
*j*13																								
*j*14	10	10	10	10	10	10	10	10											10	10	10	10	10	10
*j*15	11	11	11	11	11	11	11													11	11	11	11	11
*j*16	12	12	12	12	12	12	12	12											12	12	12	12	12	12
*j*17																		11	11					
*j*18	13	13	13	13	13	13	13	13	13										13	13	13	13	13	13
*j*19																		14	14	3	3			
*j*20	14	14	14	14	14	14	14	14												14	14	14	14	14
*j*21	15	15	15	15	15	15	15	15	15										15	15	15	15	15	15
*j*22	16	16	16	16	16	16	16													16	16	16	16	16
*j*23											3	3	3	3	3	3	3	3	3					
										13	13	13	13	13	13	13	13	13						
										15	15	15	15	15	15	15	15	15						
										17	17	17	17	17	17	17	17	17						
*j*24										4	4	4	4	4	4	4	4	4						
										6	6	6	6	6	6	6	6	6						
									14	14	14	14	14	14	14	14	14							
*j*25	17	17	17	17	17	17	17	17	17												17	17	17	17
*j*26	18	18	18	18	18	18	18											18	18	18	18	18	18	18
*j*27	19	19	19	19	19	19	19	19													19	19	19	19
*j*28																			5	5				
																			7	7				
																			19	19				
*j*29									5	5	5	5	5	5	5	5	5	5						
*j*30									7	7	7	7	7	7	7	7	7	7						
								18	18	18	18	18	18	18	18	18	18							
*j*31										2	2	2	2	2	2	2	2	2	2					
									19	19	19	19	19	19	19	19	19	19						
*j*32	20	20	20	20	20	20	20	20											20	20	20	20	20	20

EV 1	EV 2	EV 3	EV 4	EV 5	EV 6	EV 7	EV 8	EV 9	EV 10
1	2	3	4	5	6	7	8	9	10
EV 11	**EV 12**	**EV 13**	**EV 14**	**EV 15**	**EV 16**	**EV 17**	**EV 18**	**EV 19**	**EV 20**
11	12	13	14	15	16	17	18	19	20

FIG. 6.7: 24-hour location of PEVs in the 33-bus test system based on their expected mobility patterns after scenario reduction [Gazafroudi et al., 2019a].

It is noticeable that battery degradation cost of EVs are not considered in the proposed model because the problem is operated for 24 hours [Ahmadian et al., 2018]. Besides, EV's maximum charging and discharging rates are 3kW [Gazafroudi et al., 2017b].

TAB. 6.3: PEVs and their corresponding mobility path scenarios [Gazafroudi et al., 2019a].

EV	Mobility path in Scenario I	Mobility path in Scenario II
$i1$	$j1$-$j6$-$j1$	$j1$-$j6$-$j3$-$j1$
$i2$	$j2$-$j31$-$j2$	$j2$-$j29$-$j28$-$j2$
$i3$	$j4$-$j23$-$j4$	$j4$-$j23$-$j19$-$j4$
$i4$	$j5$-$j24$-$j5$	$j5$-$j24$-$j19$-$j5$
$i5$	$j8$-$j29$-$j8$	$j8$-$j29$-$j28$-$j8$
$i6$	$j9$-$j24$-$j9$	$j9$-$j24$-$j3$-$j9$
$i7$	$j10$-$j30$-$j10$	$j10$-$j30$-$j28$-$j10$
$i8$	$j11$-$j7$-$j11$	$j11$-$j7$-$j13$-$j11$
$i9$	$j12$-$j6$-$j12$	$j12$-$j6$-$j13$-$j12$
$i10$	$j14$-$j7$-$j14$	$j14$-$j7$-$j13$-$j14$
$i11$	$j15$-$j6$-$j15$	$j15$-$j6$-$j17$-$j15$
$i12$	$j16$-$j7$-$j16$	$j16$-$j7$-$j17$-$j16$
$i13$	$j18$-$j23$-$j18$	$j18$-$j23$-$j3$-$j18$
$i14$	$j20$-$j24$-$j20$	$j20$-$j24$-$j19$-$j20$
$i15$	$j21$-$j23$-$j21$	$j21$-$j23$-$j19$-$j21$
$i16$	$j22$-$j6$-$j22$	$j22$-$j6$-$j3$-$j22$
$i17$	$j25$-$j23$-$j25$	$j25$-$j23$-$j3$-$j25$
$i18$	$j26$-$j30$-$j26$	$j26$-$j30$-$j28$-$j26$
$i19$	$j27$-$j31$-$j27$	$j27$-$j31$-$j28$-$j27$
$i20$	$j32$-$j7$-$j32$	$j32$-$j7$-$j28$-$j32$

TAB. 6.4: Total expected costs of decision-makers in proposed strategies [Gazafroudi et al., 2019a].

EC^{eu} [€]	EC^{evc} [€]	EC^{lc} [€]
-745.514	-746.005	-746.005

TAB. 6.5: Total expected costs of aggregators in proposed strategies [Gazafroudi et al., 2019a].

	S_1	S_2	S_3
EC^{ag} [€]	-771.899	-774.388	-771.514

6.4.2 Economic evaluation of strategies

Here, the impacts of the proposed strategies to manage energy flexibility and operate charging mode of EVs are investigated. For this purpose, the total expected costs of end-users and aggregators are evaluated. Table 6.4 presents the expected costs of decision-makers in strategy-I (end-users), strategy-II (EV coordinator) and strategy-III (local coordinator). On the other hand, total expected cost of aggregator, $EC^{AG''} = \sum_k OF_k^{AG''}$, is shown in Table 6.5. Moreover, the expected costs of all end-users and aggregators are presented in Table 6.6. As it is seen in Tables 6.4, the total expected cost of end-users is more profitable in S_2 and S_3, because the profit due to charging operation

Tab. 6.6: Expected costs of aggregators and end-users in proposed strategies [Gazafroudi et al., 2019a].

OF_j^{eu}	S_1 [€]	S_2 [€]	S_3 [€]
$j0$	0.000	0.000	0.000
$j1$	-14.591	-14.594	-14.594
$j2$	-13.290	-13.287	-13.287
$j3$	-16.188	-16.203	-16.203
$j4$	-9.326	-9.347	-9.347
$j5$	-9.250	-9.262	-9.262
$j6$	-26.952	-27.047	-27.047
$j7$	-38.675	-38.688	-38.688
$j8$	-13.140	-13.141	-13.141
$j9$	-16.039	-16.037	-16.037
$j10$	-12.469	-12.464	-12.464
$j11$	-16.035	-16.041	-16.041
$j12$	-15.964	-15.917	-15.917
$j13$	-27.955	-27.965	-27.965
$j14$	-15.964	-15.984	-15.984
$j15$	-15.978	-15.960	-15.960
$j16$	-15.930	-15.945	-15.945
$j17$	-20.962	-20.973	-20.973
$j18$	-13.301	-20.973	-13.395
$j19$	-12.142	-12.154	-12.154
$j20$	-13.342	-19.001	-13.342
$j21$	-18.919	-13.273	-19.001
$j22$	-13.283	-98.060	-13.273
$j23$	-98.060	-97.885	-98.060
$j24$	-97.866	-9.248	-97.885
$j25$	-9.229	-9.248	-9.248
$j26$	-13.097	-13.104	-13.104
$j27$	-13.062	-13.068	-13.068
$j28$	-23.173	-23.212	-23.212
$j29$	-38.626	-38.630	-38.630
$j30$	-29.001	-29.032	-29.032
$j31$	-40.571	-40.605	-40.605
$j32$	-13.137	-13.141	-13.141
OF_k^{ag}	S_1 [€]	S_2 [€]	S_3 [€]
$k1$	-289.923	-289.908	-289.853
$k2$	-242.261	-244.755	-241.935
$k3$	-239.716	-239.726	-239.726

of EVs outside of their owner's home is considered in the objective function of their end-users. However, Table 6.5 shows that the total expected cost of aggregators in S_2 is higher than S_3. In this way, decentralized energy flexibility management by end-users is more profitable for end-users and aggregators in comparison with centralized energy flexibility management by the LC.

TAB. 6.7: Impact of energy flexibility on the total expected cost of aggregators [Gazafroudi et al., 2019a].

$EC^{AG''}$ [€]	S_1	S_2	S_3
C_1	-34.98	-34.90	-34.90
C_2	-771.899	-774.388	-771.514
C_3	-2548.243	-2548.163	-2548.163

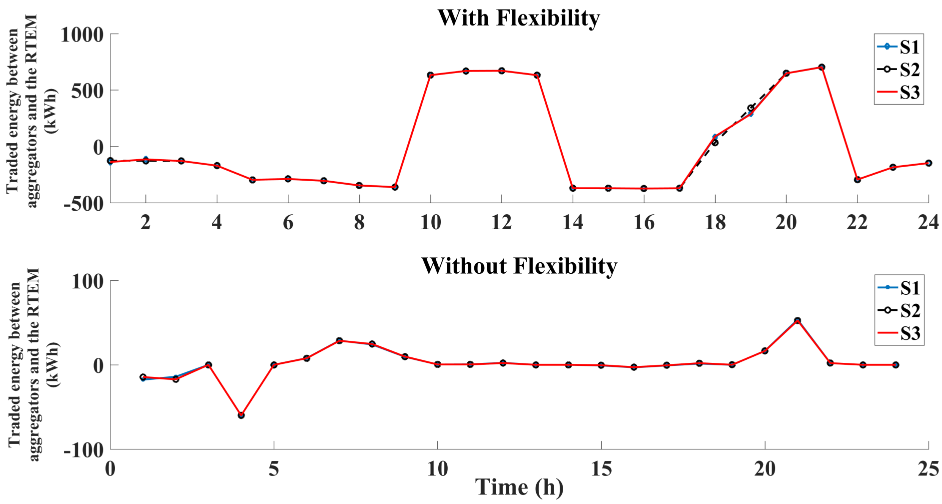

FIG. 6.8: Total Energy traded between real-time electricity market and aggregators with and without flexibility of end-users [Gazafroudi et al., 2019a].

Also, Table 6.6 represents that although S_2 is more profitable than S_3 for the majority of end-users and aggregators. For instance, the expected cost of aggregator $k3$ is the same in strategies two and three. On the other hand, although S_2 is more profitable strategy for the majority of end-users, but the expected profit of some end-users-e.g. $j21$, $j23$, $j24$- in S_3 is higher than S_2.

6.4.3 Energy flexibility evaluation

Here, the impact of energy flexibility on the expected cost of aggregators and total real-time energy transacted between the RTEM and aggregators is assessed. Table 6.7 shows the total expected cost of aggregators in the proposed energy management strategies in three cases. These cases includes considering: no energy flexibility ($L^F_{jt\omega} = 0$, C_1), shiftable flexibility (C_2), and interruptible load to provide energy flexibility (Eq. (6.3) is not considered, C_3). Also, Fig. 6.8 demonstrates the total energy traded through the RTEM and aggregators in C_1 and C_2.

As it is seen in Table 6.7, C_3 is the most profitable case to provide energy flexibility, since all end-users join as virtual energy producers to provide positive energy flexibility. Thus, the traded energy between end-users and their corresponding aggregators, and

TAB. 6.8: Impact of energy flexibility on expected costs of aggregators and end-users in Strategy-I based on aggregators' independent decisions [Gazafroudi et al., 2019a].

	Shiftable load constraint	SCA-based constraint
$OF^{ag}_{k_1}$[€]	-290.510	-29.545
$OF^{ag}_{k_2}$[€]	-244.921	-17.720
$OF^{ag}_{k_3}$[€]	-255.409	-9.502
EC^{eu}[€]	-731.352	-8.872

TAB. 6.9: Impact of agent-based decision-making on total expected costs of end-users and aggregators considering shiftable constraint in Strategy-I [Gazafroudi et al., 2019a].

	end-users-based	Aggregators-based
$EC^{EU''}$[€]	-745.514	-731.352
$EC^{AG''}$[€]	-771.899	-790.840

aggregators and the RTEM is based on a one-way bottom-up real-time energy transacted. Besides, the total expected cost of aggregators in C_1 is less than other cases which energy flexibility of end-users is not considered. In other words, the expected profit due to the operation of EVs is seen in C_1 which is maximum in S_1. As it is shown in Fig. 6.8, total energy traded with the RTEM is less in C_1 because only charging operating of EVs is seen in C_1. In other words, while C_2 is more profitable case for aggregators, the distribution network depends less to the RTEM in C_1. Hence, the power distribution grid is more sustainable in C_1.

6.4.4 Agent-based Decision-making Evaluation

In this section, the performance of the proposed energy management system is assessed based decisions which are made end-users or aggregators who are defined as agents in the system. Here, the impact of agent-based decision-making is studied in Strategy-I. In other words, the energy management problem is solved decentralized where end-users or aggregators are decision-makers based on Strategy-I. Moreover, another type of end-users' energy flexibility which is based on the coalition can be defined if aggregators are chosen as agents in the distribution grid. Eq. (6.28) represents Self-Consumption Aggregated (SCA)-based constraint.

$$\sum_{j \in A_k} L^F_{jt\omega} = 0 \ , \forall t, \omega. \tag{6.28}$$

According to (6.28), total energy flexibility which is traded between end-users and their corresponding aggregators in their region equals 0 in each time t and scenario ω. In other

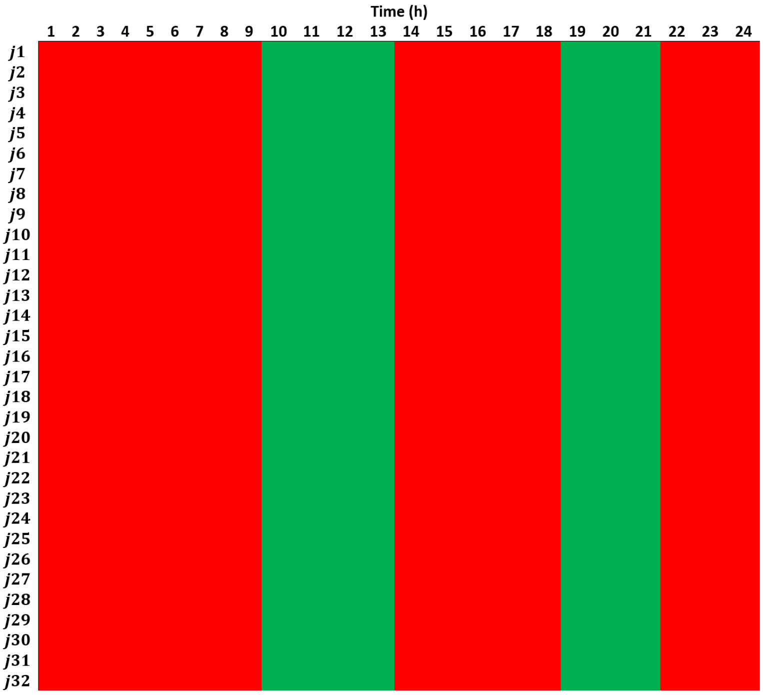

Fig. 6.9: Real-time energy flexibility provided by end-users in aggregators-based decision-making in Strategy-I considering shiftable load constraint [Gazafroudi et al., 2019a].

words, SCA loads increase the sustainability of the power distribution grids. Table 6.8 presents expected costs of aggregators and total expected cost of end-users considering SCA-based or shiftable load constraints when aggregators are agents in Strategy-I. As seen in Table 6.8, shiftable constraint is more profitable for aggregators and end-users. Besides, Table 6.9 shows the impact of agent-based decision-making on total expected costs of end-user and aggregators considering shiftable constraint in Strategy-I. it is concluded from Table 6.9 that aggregators-based decision-making is more profitable for aggregators. However, $EC^{EU''}$ is higher in end-users- based decision-making.

In addition, Figs. 6.9 and 6.10 demonstrate flexibility behavior of end-users where aggregators are agents in the system. As seen in Figs. 6.9 and 6.10, flexibility behavior of end-users is more dynamic under SCA-based constraint. In this way, it is seen that end-users represent different flexibility behavior in same time step. However, the flexibility behavior of end-users is the same under shiftable load constraint. All end-users provide positive energy flexibility as virtual energy producers in time steps 10, 11, 12, 13, 19, 20 and 21 when they are peak hours of the system according to Table 6.1. Moreover, Fig. 6.11 shows flexibility behavior of end-users under shiftable load constraint where end-users are decision-makers of the system. Although of the behavior of end-users constrained to shiftable loads are similar in end-user-based and aggregators-based decision-making, end-users have more dynamic behavior in end-user-based case, because they manage their corresponding flexibility autonomously

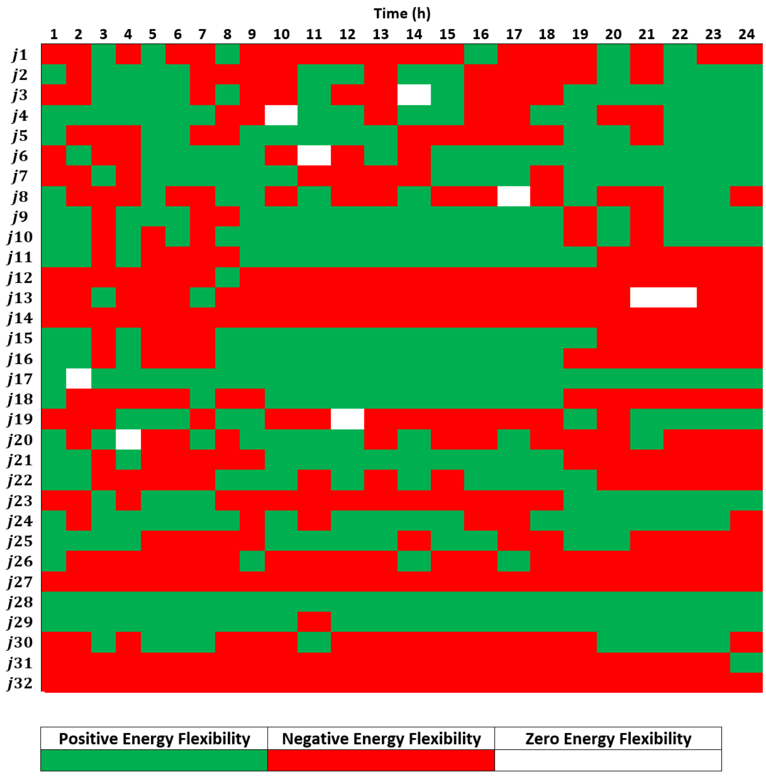

FIG. 6.10: Real-time energy flexibility provided by end-users in aggregators-based decision-making in Strategy-I considering CA-based constraint [Gazafroudi et al., 2019a].

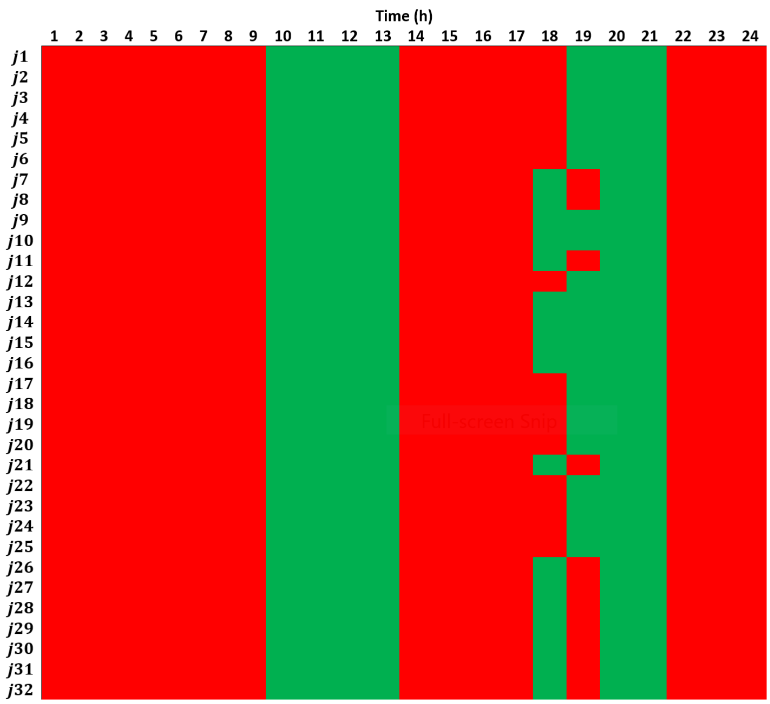

FIG. 6.11: Real-time energy flexibility provided by end-users in end-users-based decision-making in Strategy-I considering shiftable load constraint [Gazafroudi et al., 2019a].

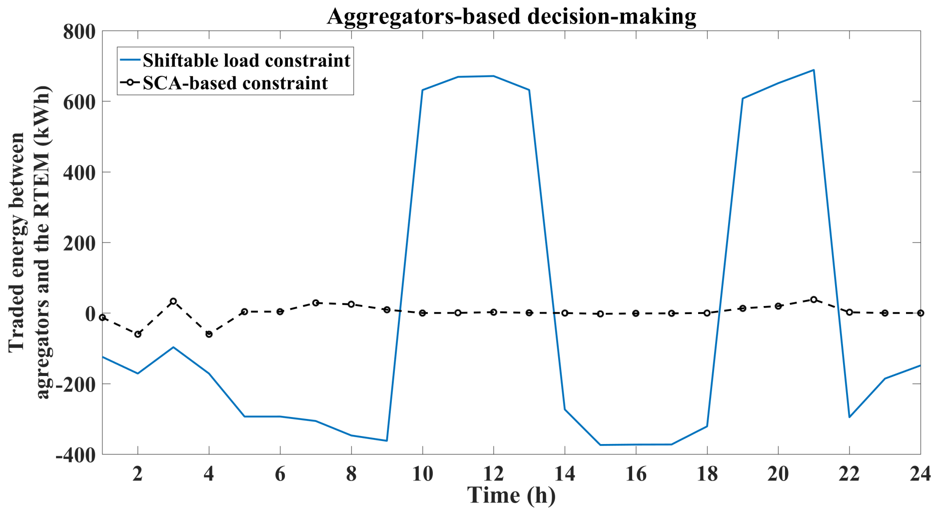

FIG. 6.12: Total Energy traded between real-time electricity market and aggregators in aggregators-based decision-making in Strategy-I considering shiftable load and SCA-based constraints [Gazafroudi et al., 2019a].

in this case; however, end-users follow decisions which are made by aggregators in the aggregators-based case.

In general, according to the simulation results, it is concluded that shiftable load constraint is more profitable for all agents in the system. On the other hand, flexibility behavior of end-users is more dynamic under SCA-based constraint. Fig. 6.12 demonstrates total transacted energy through the RTEM and aggregators under shiftable load and SCA-based constraints where aggregators play as agents in Strategy-I. According to Fig. 6.12, exchanged energy between aggregators and the RTEM is less under SCA-based constraint. In other words, SCA-based constraint increases the sustainability of the distribution network.

6.5 Conclusions

Smart cities have been defined to overcome urbanization's challenges, e.g., economic, energy and traffic. Smart cities consist of several subsystems to support optimal multi-objective decisions. Thus, interactions between these subsystems make smart cities as complex systems. In this chapter, the impact of future transportation systems on smart grids has been studied. This way, energy flexibility management of end-users and charging operation of EVs are modeled in the distribution grid. Three energy management strategies have been presented to deal with energy flexibility and operate EVs among players of the bottom-layer of the power system.

Also, EVs' mobility uncertainty has been modelled by stochastic programming. The proposed strategies are assessed based on the impact of flexibility behavior of end-users on expected costs of aggregators and traded energy between aggregators and electricity market. Moreover, the proposed strategies have been compared based on their impacts on the expected costs of distribution network's agents, energy flexibility provided by end-users and transacted energy between aggregators and real-time electricity market.

Chapter 7

Conclusions and future works (*conclusiones y trabajos futuros*)

VNiVERSiDAD
D SALAMANCA
CAMPUS DE EXCELENCIA INTERNACIONAL

Chapter 7

Conclusions and future works (*conclusiones y trabajos futuros*)

7.1 Introduction

This chapter summaries the main contributions of our Ph.D. work in Section 7.2. Also, the major results obtained from the case studies described in Chapters 3 to 6 and the findings in Section 7.7. Additionally, suggestions for future research works on the local electricity trading problems are described in Section 7.4.

7.2 Main contributions

This Ph.D. thesis has proposed a virtual organization architecture for energy trade between the agents (end-users, aggregators and the DSO) of the distribution network. Also, each of these agents and their interconnections have been described. In this work, a bottom-up approach has been proposed to trade energy from end-users, as *prosumer* agents which are able to provide two-way energy transaction, to aggregators and the DSO.

Thus, the organization-based multi-agent system of the smart home electricity system (as an example of the end-users) has been introduced. Then, the Home Energy Management System (HEMS) has been defined to model the flexible behavior of residential end-users and their uncertainty based on different types of optimization methods (e.g. interval, stochastic, and interval-stochastic). Furthermore, a probabilistic scenario-based method has been presented for the management of residential energy and energy trading with the local electricity market on the basis of an optimal bidding strategy. According to our optimal offering model, the HEMS is able to transact energy with other players in its neighborhood as a price-maker agent based on the peer-to-peer or the community-based energy trading approaches.

Then, we have proposed several approaches (e.g. decentralized, monopolistic and game-based) for the management of energy flexibility among the agents of the power distribution grid considering the flexible behavior of the end-users and the aggregators. Finally, the impact of future transportation systems on the smart grids has been studied. Thus, the management of the energy flexibility of end-users and the charging operations of EVs are modeled in the distribution grid. Three energy management strategies have been presented to deal with the energy flexibility and operation of EVs among players in the bottom-layer of the power system. Also, EV mobility uncertainty has been modelled by stochastic programming.

7.3 Research findings and conclusions

In this Ph.D. work, different case studies and problems have been presented. In this section, we classified our findings in four categories based on simulation results obtained in Chapters 3 to 6, respectively.

7.3.1 Home energy management system

The performance of the proposed home energy management problem has been evaluated by comparing it with the proposed interval-stochastic and the modified stochastic predicted bands optimization methods. Furthermore, we assessed the impact of the proposed energy flexibility model, of its prediction accuracy, and of the demand response program on the expected profit and transacted electrical energy of the system and on the reliability of the results. From the simulation, it is concluded that:

- Increasing the energy flexibility increases the total, day-ahead and real-time expected profits of the system.
- Increment of α increases the PV power produced in the day-ahead stage and day-ahead expected profit. However, α has a negative impact on the amounts of the real-time expected profit.
- Increment of the prediction accuracy has a smooth negative impact on the expected profit.
- The amount of the total expected profit in the worst case of the interval-stochastic method is less than its amount in the worst case of the modified stochastic

predicted bands method. Hence, the interval-stochastic method is more robust than the modified stochastic predicted bands method in modeling uncertainty in the proposed home energy management problem.

7.3.2 Optimal offering model for the HEMS

The proposed optimal offering model for the HEMS has been assessed in two different cases. Case 1 assessed the impacts of optimistic and flexibility coefficients on the HEMS considering the optimal bidding strategy. However, in case 2, the performance of the two different optimization methods- called InterStoch and Hybrid- in the HEMS has been evaluated without considering the optimal bidding strategy. According to the simulation results in our case study:

- The robustness of our proposed residential energy management system is increased where α_{pv} and α_{price}- the optimistic coefficients of PV power generation and electricity price- equal 0 and 1, respectively. In other words, increment in α_{pv} is in line with increment in the expected profit of the system. However, the increment in α_{price} has a negative impact on the HEMS' expected profit. In this way, the worst and robust case of the system is where α_{pv} equals 0 and α_{price} equals 1.
- Optimistic coefficients have the same pattern of impact on the system's expected profit in both InterStoch and Hybrid methods.
- The robustness of the InterStoch optimization method is higher than that of the Hybrid method because the total expected profit of the system is lower in the case study that is solved by the InterStoch optimization method. Besides, the Hybrid optimization method obtains suboptimal results because it is solved by MINLP, and it is not as efficient as the InterStoch optimization method.
- Our proposed optimal offering model for the residential energy management system is more robust than its non-optimal offering model because the optimal offering model brings lower expected profit to the system in the worst scenario where α_{pv} equals 0 and α_{price} equals 1.
- The increment in the flexibility coefficient is in line with the total expected profit of the system. Therefore, the best case of the system is where the flexibility coefficient equals 1.
- The proposed residential energy management system only offers and bids one quantity for all price scenarios in the day-ahead stage. In other words, modeling the domestic system with or without a bidding strategy demonstrates that it cannot

influence the smart home's behavior (as a consumer or producer) in the day-ahead local electricity market.

7.3.3 Local electricity trading structure

In this Ph.D. work, we have presented decentralized, monopolistic and game-based approaches for the management of energy flexibility among the agents of the distribution network.

The performance of the proposed decentralized approach has been evaluated in terms of its impact on the distribution line uncertainty and the flexible behavior of the end-users. On the basis of the simulations, it has been concluded that:

- The proposed energy flexibility management approach profitable for all consumers without considering the load-shedding cost.
- The distribution line uncertainty has a negative impact on the total expected costs for the end-users.
- End-users are able to manage their energy flexibility as independent agents considering only the shiftable flexibility constraint.
- The coalition of end-users is required to provide energy flexibility on the basis of the self-consumption flexibility constraint.
- End-users who only have shiftable flexibility behavior (economic followers) gain more profit than the ones who are limited to the self-consumption flexibility constraint (reliability followers).
- The self-consumption flexibility constraint increases the sustainability and reliability of the power distribution system. Thus, the distribution network does not depend on the up-stream grid to meet its energy needs.

According to the simulation results of the monopolistic and game-based approaches for energy flexibility management among the agents of the distribution network, it is found that:

- The monopolistic approach is profitable for all agents in the distribution network, if all end-users participate as interruptible loads.

- Aggregators have no desire to participate in DR programs to provide the energy flexibility exchanged between the end-users and the aggregators, because their expected costs is equal to zero.
- The power distribution system works as a sustainable energy system and does not depend on the upstream grid in scenarios considering the shiftable and the self-consumption flexibility constraints of the end-users.
- Game-based approach is costly for all end-users because the DSO is in charge of determining the price of energy transacted between the DSO and end-users in our proposed approach.
- In the game-based interaction between the aggregators and the DSO, the scenario considering the shiftable demand constraint is more profitable than the scenario considering the self-consumption demand constraint.
- The distribution network acts as a sustainable energy system considering the self-consumption demand constraint in the game-based interaction among the aggregators and the DSO.

7.3.4 Local electricity trading for EVs

We have modelled the energy flexibility management of end-users and the charging operation of the EVs in the distribution grid. Three energy management strategies have been presented to deal with the energy flexibility and operate EVs among players in the bottom-layer of the power system. In this way, main findings are concluded that:

- Decentralized energy flexibility management by end-users is the most profitable strategy for both end-users and aggregators.
- Two-stage stochastic sequential decision-making is the most profitable strategy for the majority of end-users since the profit from charging EVs outside of their owner's home is considered in their objective function.
- End-user's flexibility behavior is more profitable as an interruptible load than as a shiftable load.
- The expected profits due to the operation of EVs for aggregators are maximum in decentralized strategy.
- Shiftable load constraint is more profitable for all agents in the system.
- The sustainability of the distribution grid is increased considering the self-consumption aggregation-based constraint.

7.4 Recommendations for future works

Research regarding local electricity trading is a topic of broad and current interests whose development requires multi-disciplinary knowledge. Below, we present the possible objectives of future works:

- In this Ph.D. work, we presented different structures for local electricity trading (e.g. decentralized, centralized, game-based and partially-decentralized) among agents in the distribution network. However, the peer-to-peer (P2P) approach for the energy trade between end-users has not been discussed in this Ph.D. work because P2P energy trading is not practical in power systems based on the current infrastructure of the distribution networks.
- Pricing mechanisms is another direction in which this Ph.D. thesis can be improved in future works. The pricing mechanism is needed to provide a fair nodal electricity price for the end-users in the distribution network.
- The improvement the resiliency and security of digitalized energy systems is another research topic which is suggested for future works.
- The study of the applications of the Blockchain Technology (BT) is another future line of research. BT allows autonomous agents to negotiate and transact together with digitalized real assets e.g. energy and cryptocurrencies in power distribution system.
- Fog Computing is another suggested line of research in local electricity trading in power distribution grids. It makes it possible to operate on edge-to-edge devices e.g. smart meters. The edge fog collectors process the data generated by the sensors and network devices, and issue control commands to the actuators. They also filter the data to be consumed locally, and send the rest to the higher levels for visualization, real-time reporting and transaction analytics.

7.5 Introducción

Este capítulo resume las principales contribuciones de esta tesis en la Sección 7.6. Además, los principales resultados obtenidos de los estudios de caso descritos en los Capítulos 3 a 6 en la Sección ??. Además, en la Sección 7.8 se proponen posibles líneas de investigación futuras relacionadas con el comercio local de electricidad.

7.6 Contribuciones principales

Esta tesis doctoral ha propuesto una arquitectura de organización virtual para el comercio de energía entre los agentes (usuarios finales, agregadores y el gestor de la red de distribución) de la red de distribución. Asimismo, se ha descrito cada uno de estos agentes y las interconexiones entre ellos. En este trabajo, se ha propuesto un enfoque ascendente para el comercio de energía desde los usuarios finales, como agentes prosumidores capaces de proporcionar transacciones energéticas bidireccionales, hasta los agregadores y el gestor de la red de distribución.

Así, se ha introducido una organización basada en sistemas multiagente del sistema eléctrico de hogares inteligentes (como ejemplo de los usuarios finales). A continuación, se ha definido el sistema de gestión de la energía en el hogar (HEMS) para modelar el comportamiento flexible de los usuarios finales residenciales y su incertidumbre basándose en diferentes tipos de métodos de optimización (por ejemplo, intervalo, estocástico e intervalo-estocástico). Además, se ha presentado un método basado en escenarios probabilísticos para la gestión de la energía residencial y el comercio de energía con el mercado local de electricidad basado en una estrategia de licitación óptima. De acuerdo con nuestro modelo de oferta óptimo, el HEMS es capaz de realizar transacciones de energía con otros actores en su vecindario como un agente de fijación de precios de acuerdo con los enfoques de intercambio de energía entre pares o con la comunidad.

A continuación, hemos propuesto varios enfoques (por ejemplo, descentralizado, monopolístico y basado en juegos) para la gestión de la flexibilidad energética entre los agentes de la red de distribución de energía, teniendo en cuenta el comportamiento flexible de los usuarios finales y los agregadores. Por último, se ha estudiado el impacto de los futuros sistemas de transporte en las redes inteligentes. Así, la gestión de la flexibilidad energética de los usuarios finales y las operaciones de recarga de los vehículos eléctricos se modelan en la red de distribución. Se han presentado tres estrategias de gestión de la energía para gestionar la flexibilidad energética y el funcionamiento de los vehículos eléctricos entre los participantes de la capa inferior del sistema eléctrico.

Además, la incertidumbre provocada por la movilidad de los vehículos eléctricos se ha modelado mediante una programación estocástica.

7.7 Resultados y conclusiones de la investigación

En este trabajo doctoral, se han presentado casos de estudio y problemas diferentes. En esta sección, clasificamos nuestros resultados en cuatro categorías basadas en los resultados de la simulación obtenidos en los Capítulos 3 a 6

7.7.1 Sistema de gestión de energía en la hogar

El rendimiento del problema de gestión de la energía doméstica propuesto se ha evaluado comparándolo con los métodos de optimización de intervalos estocásticos propuestos y con los métodos de optimización de bandas estocásticas predichas modificadas. Se evaluó el impacto del modelo de flexibilidad energética y su exactitud de predicción. También, se evaluó el programa de respuesta de demanda en cuanto a las ganancias estimadas, la energía eléctrica tramitada y la confiabilidad de los resultados. A partir de la simulación, se concluye que:

- El aumento de la flexibilidad energética aumenta las ganancias totales esperadas del día siguiente y en tiempo real del sistema.
- El aumento de α incrementa la potencia fotovoltaica producida en la etapa del día siguiente y la ganancia esperada para esta etapa. Sin embargo, tiene un impacto negativo en la cuantía de la ganancia esperada en tiempo real.
- El aumento de la precisión de la predicción tiene un impacto negativo sobre las ganancias esperadas.
- La cuantía de la ganancia total esperada en el peor de los casos del intervalo estocástico es inferior a la cuantía de la ganancia en el peor de los casos del método de las bandas estocásticas predichas modificadas. Por lo tanto, el método estocástico por intervalos es más robusto que el método de bandas estocásticas predichas modificadas en la modelación de la incertidumbre en el problema de la gestión de la energía doméstica propuesto.

7.7.2 Modelo óptimo de oferta para el HEMS

El modelo de oferta óptimo propuesto para el HEMS se ha evaluado en dos casos diferentes. El Caso 1 evaluó el impacto de los coeficientes de optimismo y flexibilidad en el HEMS considerando la estrategia óptima de licitación. Sin embargo, en el caso 2, el rendimiento de los dos métodos de optimización diferentes -llamados InterStoch e Hybrid- en el HEMS se ha evaluado sin considerar la estrategia de licitación óptima. Según los resultados de la simulación de nuestro estudio de caso:

- Aumenta la robustez del sistema de gestión de la energía residencial propuesto, donde α_{pv} y α_{price} -los coeficientes de optimismo de la generación de energía fotovoltaica y el precio de la electricidad- son iguales a 0 y 1, respectivamente. En otras palabras, el incremento en α_{pv} está en línea con el incremento en la ganancia esperada del sistema. Sin embargo, el incremento del α_{price} tiene un impacto negativo en las ganancias esperadas del HEMS. De esta manera, el peor y más robusto caso del sistema es cuando α_{pv} es igual a 0 y el α_{price} es igual a 1.
- Los coeficientes de optimismo tienen el mismo patrón de impacto en las ganancias esperadas del sistema, tanto en el método InterStoch como en el método Hybrid.
- La robustez del método de optimización InterStoch es mayor que la del método Hybrid porque la ganancia total esperada del sistema es menor en el estudio de caso que se resuelve con el método de optimización InterStoch. Además, el método de optimización híbrido obtiene resultados subóptimos porque es resuelto por MINLP, y no es tan eficiente como el método de optimización InterStoch.
- El modelo de oferta óptimo que proponemos para el sistema de gestión de energía residencial es más robusto que el modelo de oferta no óptimo porque el modelo de oferta óptimo trae menores ganancias esperadas al sistema en el peor de los casos, donde α_{pv} es igual a 0 y el α_{price} es igual a 1.
- El incremento en el coeficiente de flexibilidad está en línea con la ganancia total esperada del sistema. Por lo tanto, el mejor caso del sistema es cuando el coeficiente de flexibilidad es igual a 1.
- El sistema de gestión de energía residencial propuesto sólo ofrece y licita una cantidad para todos los escenarios de precios en la etapa del día siguiente. En otras palabras, modelar el sistema doméstico con o sin una estrategia de licitación demuestra que no puede influir en el comportamiento de la vivienda inteligente (como consumidor o productor) en el mercado local de electricidad del día siguiente.

7.7.3 Estructura local del comercio de electricidad

En este trabajo de doctorado, hemos presentado enfoques descentralizados, monopolísticos y basados en juegos para la gestión de la flexibilidad energética entre los agentes de la distribución red.

El rendimiento del enfoque descentralizado propuesto se ha evaluado en términos de su impacto en la incertidumbre de la línea de distribución y el comportamiento flexible de los usuarios finales. Basándose en las simulaciones, se ha llegado a las siguientes conclusiones:

- El enfoque de gestión de la flexibilidad energética propuesto es viable para todos los consumidores sin tener en cuenta el coste de la reducción de la carga.
- La incertidumbre de la línea de distribución tiene un impacto negativo en los costes totales esperados para los usuarios finales.
- Los usuarios finales son capaces de gestionar su flexibilidad energética como agentes independientes teniendo en cuenta sólo la restricción de la flexibilidad cambiante.
- La coalición de usuarios finales debe proporcionar flexibilidad energética sobre la base de la restricción de la flexibilidad del autoconsumo.
- Los usuarios finales que sólo tienen un comportamiento de flexibilidad variable (seguidores económicos) obtienen más beneficios que los que se limitan a la restricción de flexibilidad de autoconsumo (seguidores de fiabilidad).
- La limitación de la flexibilidad del autoconsumo aumenta la sostenibilidad y la confiabilidad del sistema de distribución de energía. De este modo, la red de distribución no depende de la red de suministro para satisfacer sus necesidades energéticas.

De acuerdo con los resultados de la simulación de los enfoques monopolísticos y basados en juegos para gestión de la flexibilidad energética entre los agentes de la red de distribución, se descubre que:

- El enfoque monopolístico es viable para todos los agentes de la red de distribución, si todos los usuarios finales participan como cargas interrumpibles.
- Los agregadores no desean participar en programas de respuesta de demanda para proporcionar la flexibilidad energética intercambiable entre los usuarios finales y los agregadores, porque sus costos esperados son iguales a cero.

- El sistema de distribución de energía eléctrica funciona como un sistema energético sostenible y no depende de la red de suministro en los escenarios que consideran las limitaciones de flexibilidad de los usuarios finales, tanto en lo que se refiere a la capacidad de desplazamiento como al autoconsumo.
- El enfoque basado en juegos que proponemos, es costoso para todos los usuarios finales, ya que el gestor de la red de distribución se encarga de determinar el precio de la energía que se transfiere entre el gestor de la red de distribución y los usuarios finales.
- La red de distribución actúa como un sistema de energía sostenible teniendo en cuenta la restricción de la demanda de autoconsumo en la interacción basada en el juego entre los agregadores y el DSO.
- The distribution network acts as a sustainable energy system considering the self-consumption demand constraint in the game-based interaction among the aggregators and the DSO.

7.7.4 Comercio local de electricidad para EVs

Hemos modelado la gestión de la flexibilidad energética de los usuarios finales y la operación de carga de los vehículos eléctricos en la red de distribución. Se han presentado tres estrategias de gestión de la energía para abordar la flexibilidad energética y el funcionamiento de los EVs entre los actores de la capa inferior del sistema de energía. Se extraen las siguientes conclusiones de los hallazgos:

- La gestión descentralizada de la flexibilidad energética por parte de los usuarios finales es la estrategia más rentable tanto para los usuarios finales como para los agregadores.
- La toma de decisiones secuencial estocástica en dos etapas es la estrategia más rentable para la mayoría de los usuarios finales, ya que la ganancia que se obtiene al cobrar a los vehículos eléctricos fuera del hogar de sus propietarios se considera en su función objetiva.
- El comportamiento flexible del usuario final es más rentable como carga interrumpible que como carga desplazable.
- Las ganancias esperadas para los agregadores, producidas por la operación de los EV son máximas en la estrategia descentralizada.

- La restricción de carga desplazable es más rentable para todos los agentes del sistema.
- La sostenibilidad de la red de distribución se ve incrementada si se tiene en cuenta la restricción basada en la agregación de autoconsumo.

7.8 Recomendaciones para trabajos futuros

La investigación sobre el comercio local de electricidad es un tema de interés amplio y actual cuyo desarrollo requiere un conocimiento multidisciplinar. A continuación, presentamos los posibles objetivos de los trabajos futuros:

- En este trabajo de doctorado, presentamos diferentes estructuras para el comercio local de electricidad (por ejemplo, descentralizado, centralizado, basado en juegos y parcialmente descentralizado) entre los agentes de la red de distribución. Sin embargo, el enfoque P2P (peer-to-peer) para el comercio de energía entre usuarios finales no ha sido abordado en este trabajo de doctorado porque el comercio de energía P2P no es práctico en los sistemas de energía debido a la infraestructura actual de las redes de distribución.
- Los mecanismos de fijación de precios son también otro aspecto en el que se puede mejorar esta tesis doctoral en trabajos futuros. El mecanismo de fijación de precios debe proporcionar un precio nodal justo para los usuarios finales de la red de distribución.
- Mejorar la resistencia y la seguridad de los sistemas de energía digitalizados es otro tema de investigación que se planteará en trabajos futuros.
- El estudio de las aplicaciones de la Tecnología Blockchain (Blochchain Technology) es otra de las líneas de investigación futuras. BT permite a los agentes autónomos negociar y realizar transacciones junto con activos reales digitalizados, por ejemplo, energía y criptodivisas en el sistema de distribución de energía.
- El estudio de las aplicaciones de la Tecnología Blockchain (Blochchain Technology) es otra de las líneas de investigación futuras. BT permite a los agentes autónomos negociar y realizar transacciones junto con activos reales digitalizados, por ejemplo, energía y criptodivisas en el sistema de distribución de energía.

Appendix A

Publications and related works (*publicaciones y trabajos relacionados*)

VNiVERSiDAD
D SALAMANCA
CAMPUS DE EXCELENCIA INTERNACIONAL

Appendix A

Publications and related works (*publicaciones y trabajos relacionados*)

A.1 Introducción

In the following, a list of works is presented that have been published in international JCR journals and book chapters or have been presented at international conferences during this Ph.D. work. Also, international and national projects, that have been involved in this Ph.D. work, are presented in this section.

A.1.1 Published papers in international JCR journals

- **Gazafroudi AS**, Shafie-khah M, Heydarian-Forushani E, Hajizadeh A, Heidari A, Corchado JM, Catalão JP. Two-stage stochastic model for the price-based domestic energy management problem. International Journal of Electrical Power Energy Systems. 2019 Nov 1;112:404-16. **JCR 2017: 3.610, Q1**.

- **Gazafroudi AS**, Prieto J, Corchado JM. Virtual Organization Structure for Agent-Based Local Electricity Trading. Energies. 2019;12(8):1521. **JCR 2017: 2.676, Q2**.

- **Gazafroudi AS**, Soares J, Ghazvini MA, Pinto T, Vale Z, Corchado JM. Stochastic interval-based optimal offering model for residential energy management systems by household owners. International Journal of Electrical Power Energy Systems. 2019 Feb 1;105:201-19. **JCR 2017: 3.610, Q1**.

- **Gazafroudi AS**, Corchado JM, Keane A, Soroudi A. Decentralised flexibility management for EVs. IET Renewable Power Generation. 2019 Jan 4. **JCR 2017: 3.488, Q1**.
- Prieto-Castrillo F, **Gazafroudi AS**, Prieto J, Corchado JM. An ising spin-based model to explore efficient flexibility in distributed power systems. Complexity. 2018;2018. **JCR 2017: 1.829, Q2**.
- **Gazafroudi AS**, Shafie-Khah M, Abedi M, Hosseinian SH, Dehkordi GH, Goel L, Karimyan P, Prieto-Castrillo F, Corchado JM, Catalão JP. A novel stochastic reserve cost allocation approach of electricity market agents in the restructured power systems. Electric Power Systems Research. 2017 Nov 1;152:223-36. **JCR 2017: 2.856, Q2**.
- **Gazafroudi AS**, Prieto-Castrillo F, Pinto T, Prieto J, Corchado JM, Bajo J. Energy flexibility management based on predictive dispatch model of domestic energy management system. Energies. 2017;10(9):1397. **JCR 2017: 2.676, Q2**.

A.1.2 Published book chapters

- **Gazafroudi AS**, Shafie-khah M, Prieto-Castrillo F, Talari S, Corchado JM, Catalão JP. Evolving New Market Structures. In Pathways to a Smarter Power System, pp. 183-203. Academic Press, 2019.
- **Gazafroudi AS**, Shafie-khah M, Fitiwi DZ, Santos SF, Corchado JM, Catalão JP. Impact of Strategic Behaviors of the Electricity Consumers on Power System Reliability. In Sustainable Interdependent Networks II 2019 (pp. 193-215). Springer, Cham.
- Najafi S, Talari S, **Gazafroudi AS**, Shafie-khah M, Corchado JM, Catalão JP. Decentralized control of DR using a multi-agent method. In Sustainable interdependent networks 2018 (pp. 233-249). Springer, Cham.

A.1.3 Presented international conference papers

- **Gazafroudi AS**, Shafie-khah M, Corchado JM, Lotfi M, Catalão JPS. Iterative Algorithm for Electricity Trading in Distribution Networks. IEEE PES PowerTech Milano, June 2019.
- **Gazafroudi AS**, Prieto-Castrillo F, Pinto T, Corchado JM. Energy Flexibility Management in Power Distribution Systems: Decentralized Approach. In2018

International Conference on Smart Energy Systems and Technologies (SEST) 2018 Sep 10 (pp. 1-6). IEEE.

- Ebrahimi M, **Gazafroudi AS**, Corchado JM, Ebrahimi M. Energy Management of Smart Home Considering Residences' Satisfaction and PHEV. In2018 International Conference on Smart Energy Systems and Technologies (SEST) 2018 Sep 10 (pp. 1-6). IEEE.

- **Gazafroudi AS**, Pinto T, Prieto-Castrillo F, Corchado JM, Abrishambaf O, Jozi A, Vale Z. Energy flexibility assessment of a multi agent-based smart home energy system. In2017 IEEE 17th International Conference on Ubiquitous Wireless Broadband (ICUWB) 2017 Sep 12 (pp. 1-7). IEEE.

- **Gazafroudi AS**, Prieto-Castrillo F, Pinto T, Corchado JM. Organization-based multi-agent system of local electricity market: bottom-up approach. InInternational Conference on Practical Applications of Agents and Multi-Agent Systems 2017 Jun 21 (pp. 281-283). Springer, Cham.

- **Gazafroudi AS**, Prieto-Castrillo F, Pinto T, Jozi A, Vale Z. Economic evaluation of predictive dispatch model in MAS-based smart home. InInternational Conference on Practical Applications of Agents and Multi-Agent Systems 2017 Jun 21 (pp. 81-91). Springer, Cham.

- **Gazafroudi AS**, De Paz JF, Prieto-Castrillo F, Villarrubia G, Talari S, Shafie-khah M, Catalão JP. A review of multi-agent based energy management systems. InInternational Symposium on Ambient Intelligence 2017 Jun 21 (pp. 203-209). Springer, Cham.

- **Gazafroudi AS**, Pinto T, Prieto-Castrillo F, Prieto J, Corchado JM, Jozi A, Vale Z, Venayagamoorthy GK. Organization-based multi-agent structure of the smart home electricity system. In2017 IEEE Congress on Evolutionary Computation (CEC) 2017 Jun 5 (pp. 1327-1334). IEEE.

- **Gazafroudi AS**, Prieto-Castrillo F, Corchado JM. Residential energy management using a novel interval optimization method. In2017 4th International Conference on Control, Decision and Information Technologies (CoDIT) 2017 Apr 5 (pp. 0196-0201). IEEE.

A.1.4 Participation in projects

This Ph.D. work has been supported by the European Commission H2020 MSCA-RISE-2014: Marie Sklodowska-Curie project *DREAM-GO Enabling Demand*

Response for short and real-time Efficient And Market Based Smart Grid Operation. An intelligent and real-time simulation approach Ref. 641794. Also, This Ph.D. work has been supported by the Spanish Ministry, Ministerio de Economía y Competitividad and FEDER funds. Project. SURF: Intelligent System for integrated and sustainable management of urban fleets TIN2015-65515-C4-3-R. Moreover, Amin Shokri Gazafroudi acknowledge the support by the Ministry of Education of the Junta de Castilla y Leon and the European Social Fund through a grant from predoctoral recruitment of research personnel associated with the research project *Arquitectura multiagente para la gestión eficaz de redes de energía a través del uso de tecnicas de inteligencia artificial* of the University of Salamanca.

Bibliography (*bibliografía*)

Abrishambaf, O., Ghazvini, M. A. F., Gomes, L., Faria, P., Vale, Z., and Corchado, J. M. (2016a). Application of a home energy management system for incentive-based demand response program implementation. In *2016 27th International Workshop on Database and Expert Systems Applications (DEXA)*, pages 153–157. IEEE.

Abrishambaf, O., Gomes, L., Faria, P., Afonso, J. L., and Vale, Z. (2016b). Real-time simulation of renewable energy transactions in microgrid context using real hardware resources. In *2016 IEEE/PES Transmission and Distribution Conference and Exposition (T&D)*, pages 1–5. IEEE.

Ahmadian, A., Sedghi, M., Mohammadi-ivatloo, B., Elkamel, A., Golkar, M. A., and Fowler, M. (2018). Cost-benefit analysis of v2g implementation in distribution networks considering pevs battery degradation. *IEEE Transactions on Sustainable Energy*, 9(2):961–970.

Arasteh, H., Hosseinnezhad, V., Loia, V., Tommasetti, A., Troisi, O., Shafie-Khah, M., and Siano, P. (2016). Iot-based smart cities: a survey. In *Environment and Electrical Engineering (EEEIC), 2016 IEEE 16th International Conference on*, pages 1–6. IEEE.

Bahrami, S., Amini, M. H., Shafie-khah, M., and Catalao, J. P. (2018). A decentralized electricity market scheme enabling demand response deployment. *IEEE Transactions on Power Systems*, 33(4):4218–4227.

Bakirtzis, E. A., Ntomaris, A. V., Kardakos, E. G., Simoglou, C. K., Biskas, P. N., and Bakirtzis, A. G. (2014). A unified unit commitment—economic dispatch model for short-term power system scheduling under high wind energy penetration. In *11th International Conference on the European Energy Market (EEM14)*, pages 1–6. IEEE.

Baringo, L. and Conejo, A. J. (2011). Offering strategy via robust optimization. *IEEE Transactions on Power Systems*, 26(3):1418–1425.

Beaudin, M., Zareipour, H., and Schellenberg, A. (2012). Residential energy management using a moving window algorithm. In *2012 3rd IEEE PES Innovative Smart Grid Technologies Europe (ISGT Europe)*, pages 1–8. IEEE.

Borlase, S. (2016). *Smart grids: infrastructure, technology, and solutions.* CRC press.

Brazier, F., La Poutre, H., Abhyankar, A., Saxena, K., Singh, S., and Tomar, K. (2015). A review of multi agent based decentralised energy management issues. In *2015 International Conference on Energy Economics and Environment (ICEEE)*, pages 1–5. IEEE.

Bui, V.-H., Hussain, A., and Kim, H.-M. (2018). A multiagent-based hierarchical energy management strategy for multi-microgrids considering adjustable power and demand response. *IEEE Transactions on Smart Grid*, 9(2):1323–1333.

Caramanis, M., Ntakou, E., Hogan, W. W., Chakrabortty, A., and Schoene, J. (2016). Co-optimization of power and reserves in dynamic t&d power markets with nondispatchable renewable generation and distributed energy resources. *Proceedings of the IEEE*, 104(4):807–836.

Chai, B., Chen, J., Yang, Z., and Zhang, Y. (2014). Demand response management with multiple utility companies: A two-level game approach. *IEEE Transactions on Smart Grid*, 5(2):722–731.

Chen, Y., He, L., Guan, Y., Lu, H., and Li, J. (2017). Life cycle assessment of greenhouse gas emissions and water-energy optimization for shale gas supply chain planning based on multi-level approach: Case study in barnett, marcellus, fayetteville, and haynesville shales. *Energy conversion and management*, 134:382–398.

Chen, Y., He, L., Li, J., Cheng, X., and Lu, H. (2016a). An inexact bi-level simulation–optimization model for conjunctive regional renewable energy planning and air pollution control for electric power generation systems. *Applied energy*, 183:969–983.

Chen, Y., Lu, H., Li, J., Huang, G., and He, L. (2016b). Regional planning of new-energy systems within multi-period and multi-option contexts: a case study of fengtai, beijing, china. *Renewable and Sustainable Energy Reviews*, 65:356–372.

Cintuglu, M. H., Youssef, T., and Mohammed, O. A. (2018). Development and application of a real-time testbed for multiagent system interoperability: A case study on hierarchical microgrid control. *IEEE Transactions on Smart Grid*, 9(3):1759–1768.

Conejo, A. J., Carrión, M., Morales, J. M., et al. (2010). *Decision making under uncertainty in electricity markets*, volume 1. Springer.

Das, S. K., Cook, D. J., Battacharya, A., Heierman, E. O., and Lin, T.-Y. (2002). The role of prediction algorithms in the mavhome smart home architecture. *IEEE Wireless Communications*, 9(6):77–84.

Degefa, M. Z., Alahäivälä, A., Kilkki, O., Humayun, M., Seilonen, I., Vyatkin, V., and Lehtonen, M. (2016). Mas-based modeling of active distribution network: the simulation of emerging behaviors. *IEEE Transactions on Smart Grid*, 7(6):2615–2623.

Deng, R., Yang, Z., Hou, F., Chow, M.-Y., and Chen, J. (2015). Distributed real-time demand response in multiseller–multibuyer smart distribution grid. *IEEE Transactions on Power Systems*, 30(5):2364–2374.

Disfani, V. R., Fan, L., and Miao, Z. (2015). Distributed dc optimal power flow for radial networks through partial primal dual algorithm. In *2015 IEEE Power & Energy Society General Meeting*, pages 1–5. IEEE.

Faria, P. and Vale, Z. (2011). Demand response in electrical energy supply: An optimal real time pricing approach. *Energy*, 36(8):5374–5384.

Farmani, F., Parvizimosaed, M., Monsef, H., and Rahimi-Kian, A. (2018). A conceptual model of a smart energy management system for a residential building equipped with cchp system. *International Journal of Electrical Power & Energy Systems*, 95:523–536.

Fujimoto, Y., Kikusato, H., Yoshizawa, S., Kawano, S., Yoshida, A., Wakao, S., Murata, N., Amano, Y., Tanabe, S.-i., and Hayashi, Y. (2018). Distributed energy management for comprehensive utilization of residential photovoltaic outputs. *IEEE Transactions on Smart Grid*, 9(2):1216–1227.

Garcés, L. P., Conejo, A. J., García-Bertrand, R., and Romero, R. (2009). A bilevel approach to transmission expansion planning within a market environment. *IEEE Transactions on Power Systems*, 24(3):1513–1522.

Gazafroudi, A. S., Afshar, K., and Bigdeli, N. (2015). Assessing the operating reserves and costs with considering customer choice and wind power uncertainty in pool-based power market. *International Journal of Electrical Power & Energy Systems*, 67:202–215.

Gazafroudi, A. S., Corchado, J. M., Keane, A., and Soroudi, A. (2019a). Decentralised flexibility management for evs. *IET Renewable Power Generation.*

Gazafroudi, A. S., Pinto, T., Prieto-Castrillo, F., Prieto, J., Corchado, J. M., Jozi, A., Vale, Z., and Venayagamoorthy, G. K. (2017a). Organization-based multi-agent structure of the smart home electricity system. In *2017 IEEE Congress on Evolutionary Computation (CEC)*, pages 1327–1334. IEEE.

Gazafroudi, A. S., Prieto-Castrillo, F., Pinto, T., and Corchado, J. M. (2018). Energy flexibility management in power distribution systems: Decentralized approach. In

2018 International Conference on Smart Energy Systems and Technologies (SEST), pages 1–6. IEEE.

Gazafroudi, A. S., Prieto-Castrillo, F., Pinto, T., Prieto, J., Corchado, J. M., and Bajo, J. (2017b). Energy flexibility management based on predictive dispatch model of domestic energy management system. *Energies*, 10(9):1397.

Gazafroudi, A. S., Shafie-Khah, M., Abedi, M., Hosseinian, S. H., Dehkordi, G. H. R., Goel, L., Karimyan, P., Prieto-Castrillo, F., Corchado, J. M., and Catalão, J. P. (2017c). A novel stochastic reserve cost allocation approach of electricity market agents in the restructured power systems. *Electric Power Systems Research*, 152:223–236.

Gazafroudi, A. S., Shafie-khah, M., Fitiwi, D. Z., Santos, S. F., Corchado, J. M., and Catalão, J. P. (2019b). Impact of strategic behaviors of the electricity consumers on power system reliability. In *Sustainable Interdependent Networks II*, pages 193–215. Springer.

Gazafroudi, A. S., Soares, J., Ghazvini, M. A. F., Pinto, T., Vale, Z., and Corchado, J. M. (2019c). Stochastic interval-based optimal offering model for residential energy management systems by household owners. *International Journal of Electrical Power & Energy Systems*, 105:201–219.

Ghalelou, A. N., Fakhri, A. P., Nojavan, S., Majidi, M., and Hatami, H. (2016). A stochastic self-scheduling program for compressed air energy storage (caes) of renewable energy sources (ress) based on a demand response mechanism. *Energy conversion and management*, 120:388–396.

Ghazvini, M. A. F., Faria, P., Ramos, S., Morais, H., and Vale, Z. (2015). Incentive-based demand response programs designed by asset-light retail electricity providers for the day-ahead market. *Energy*, 82:786–799.

Graditi, G., Di Somma, M., and Siano, P. (2018). Optimal bidding strategy for a der aggregator in the day-ahead market in the presence of demand flexibility. *IEEE Transactions on Industrial Electronics*.

Growe-Kuska, N., Heitsch, H., and Romisch, W. (2003). Scenario reduction and scenario tree construction for power management problems. In *2003 IEEE Bologna Power Tech Conference Proceedings,*, volume 3, pages 7–pp. IEEE.

Hurtado, L., Nguyen, P., and Kling, W. (2015). Smart grid and smart building inter-operation using agent-based particle swarm optimization. *Sustainable Energy, Grids and Networks*, 2:32–40.

Jokic, A., Van Den Bosch, P., and Hermans, R. (2009). Distributed, price-based control approach to market-based operation of future power systems. In *Energy Market, 2009. EEM 2009. 6th International Conference on the European*, pages 1–6. IEEE.

Kahrobaee, S., Rajabzadeh, R. A., Soh, L.-K., and Asgarpoor, S. (2013). A multiagent modeling and investigation of smart homes with power generation, storage, and trading features. *IEEE Transactions on Smart Grid*, 4(2):659–668.

Kok, K., Karnouskos, S., Nestle, D., Dimeas, A., Weidlich, A., Warmer, C., Strauss, P., Buchholz, B., Drenkard, S., Hatziargyriou, N., et al. (2009). Smart houses for a smart grid. In *CIRED 2009-20th International Conference and Exhibition on Electricity Distribution-Part 1*, pages 1–4. IET.

Li, W., Logenthiran, T., and Woo, W. (2015). Intelligent multi-agent system for smart home energy management. In *2015 IEEE Innovative Smart Grid Technologies-Asia (ISGT ASIA)*, pages 1–6. IEEE.

Loia, V. and Vaccaro, A. (2014). Decentralized economic dispatch in smart grids by self-organizing dynamic agents. *IEEE Transactions on Systems, Man, and Cybernetics: Systems*, 44(4):397–408.

Lund, H. (2014). *Renewable energy systems: a smart energy systems approach to the choice and modeling of 100% renewable solutions*. Academic Press.

Ma, K., Yao, T., Yang, J., and Guan, X. (2016). Residential power scheduling for demand response in smart grid. *International Journal of Electrical Power & Energy Systems*, 78:320–325.

Manic, M., Wijayasekara, D., Amarasinghe, K., and Rodriguez-Andina, J. J. (2016). Building energy management systems: The age of intelligent and adaptive buildings. *IEEE Industrial Electronics Magazine*, 10(1):25–39.

Miao, Z. and Fan, L. (2018). A novel multi-agent decision making architecture based on dual's dual problem formulation. *IEEE Transactions on Smart Grid*, 9(2):1150–1160.

Mithulananthan, N., Hung, D. Q., and Lee, K. Y. (2016). *Intelligent network integration of distributed renewable generation*. Springer.

Momber, I., Siddiqui, A., San Román, T. G., and Söder, L. (2015). Risk averse scheduling by a pev aggregator under uncertainty. *IEEE Transactions on Power Systems*, 30(2):882–891.

Mustafa, M. A., Cleemput, S., and Abidin, A. (2016). A local electricity trading market: Security analysis. In *PES Innovative Smart Grid Technologies Conference Europe (ISGT-Europe), 2016 IEEE*, pages 1–6. IEEE.

Nasri, A., Kazempour, S. J., Conejo, A. J., and Ghandhari, M. (2016). Network-constrained ac unit commitment under uncertainty: a benders' decomposition approach. *IEEE transactions on power systems*, 31(1):412–422.

Nunna, H. K. and Srinivasan, D. (2017). Multiagent-based transactive energy framework for distribution systems with smart microgrids. *IEEE Transactions on Industrial Informatics*, 13(5):2241–2250.

Oliveira, P., Pinto, T., Morais, H., and Vale, Z. (2012). Masgrip—a multi-agent smart grid simulation platform. In *2012 IEEE Power and Energy Society General Meeting*, pages 1–8. IEEE.

Park, S., Lee, J., Bae, S., Hwang, G., and Choi, J. K. (2016). Contribution-based energy-trading mechanism in microgrids for future smart grid: A game theoretic approach. *IEEE Transactions on Industrial Electronics*, 63(7):4255–4265.

Pedrasa, M. A. A., Spooner, T. D., and MacGill, I. F. (2009). Scheduling of demand side resources using binary particle swarm optimization. *IEEE Transactions on Power Systems*, 24(3):1173–1181.

Pereira, R., Figueiredo, J., Melicio, R., Mendes, V. M. F., Martins, J., and Quadrado, J. (2015). Consumer energy management system with integration of smart meters. *Energy Reports*, 1:22–29.

Pinto, T., Gazafroudi, A. S., Prieto-Castrillo, F., Santos, G., Silva, F., Corchado, J. M., and Vale, Z. (2017). Reserve costs allocation model for energy and reserve market simulation. In *Intelligent System Application to Power Systems (ISAP), 2017 19th International Conference on*, pages 1–6. IEEE.

Pratt, A., Krishnamurthy, D., Ruth, M., Wu, H., Lunacek, M., and Vaynshenk, P. (2016). Transactive home energy management systems: The impact of their proliferation on the electric grid. *IEEE Electrification Magazine*, 4(4):8–14.

Prieto-Castrillo, F., Shokri Gazafroudi, A., Prieto, J., and Corchado, J. M. (2018). An ising spin-based model to explore efficient flexibility in distributed power systems. *Complexity*, 2018.

Roche, R., Blunier, B., Miraoui, A., Hilaire, V., and Koukam, A. (2010). Multi-agent systems for grid energy management: A short review. In *IECON 2010-36th Annual Conference on IEEE Industrial Electronics Society*, pages 3341–3346. IEEE.

Sajjadi, S. M., Mandal, P., Tseng, T.-L. B., and Velez-Reyes, M. (2016). Transactive energy market in distribution systems: A case study of energy trading between transactive nodes. In *2016 North American Power Symposium (NAPS)*, pages 1–6. IEEE.

Santos, G., Pinto, T., Morais, H., Sousa, T. M., Pereira, I. F., Fernandes, R., Praça, I., and Vale, Z. (2015). Multi-agent simulation of competitive electricity markets: Autonomous systems cooperation for european market modeling. *Energy Conversion and Management*, 99:387–399.

Santos, G., Pinto, T., Praça, I., and Vale, Z. (2016). Mascem: Optimizing the performance of a multi-agent system. *Energy*, 111:513–524.

Shafie-khah, M. and Catalão, J. P. (2015). A stochastic multi-layer agent-based model to study electricity market participants behavior. *IEEE Transactions on Power Systems*, 30(2):867–881.

Shahidehpour, M., Li, Z., and Ganji, M. (2018). Smart cities for a sustainable urbanization: Illuminating the need for establishing smart urban infrastructures. *IEEE Electrification Magazine*, 6(2):16–33.

Shokri Gazafroudi, A., Prieto, J., and Corchado, J. M. (2019). Virtual organization structure for agent-based local electricity trading. *Energies*, 12(8):1521.

Shokri Gazafroudi, A., Prieto-Castrillo, F., and Corchado, J. (2017). Residential energy management using a novel interval optimization method. In *Proceedings of the 4th International Conference on Control, Decision and Information Technology.*

Siano, P. (2014). Demand response and smart grids—a survey. *Renewable and Sustainable Energy Reviews*, 30:461 – 478.

Siano, P. and Sarno, D. (2016). Assessing the benefits of residential demand response in a real time distribution energy market. *Applied Energy*, 161:533 – 551.

Soares, J., Borges, N., Ghazvini, M. A. F., Vale, Z., and de Moura Oliveira, P. B. (2016). Scenario generation for electric vehicles' uncertain behavior in a smart city environment. *Energy*, 111:664–675.

Soares, J., Canizes, B., Ghazvini, M. A. F., Vale, Z., and Venayagamoorthy, G. K. (2017). Two-stage stochastic model using benders' decomposition for large-scale energy resource management in smart grids. *IEEE Transactions on Industry Applications*, 53(6):5905–5914.

Soroudi, A. (2017). *Power System Optimization Modeling in GAMS.* Springer International Publishing.

Soroudi, A. and Amraee, T. (2013). Decision making under uncertainty in energy systems: State of the art. *Renewable and Sustainable Energy Reviews*, 28:376–384.

Vale, Z., Morais, H., Faria, P., and Ramos, C. (2013). Distribution system operation supported by contextual energy resource management based on intelligent scada. *Renewable Energy*, 52:143–153.

Venayagamoorthy, G. K., Sharma, R. K., Gautam, P. K., and Ahmadi, A. (2016). Dynamic energy management system for a smart microgrid. *IEEE transactions on neural networks and learning systems*, 27(8):1643–1656.

Vrba, P., Mařík, V., Siano, P., Leitão, P., Zhabelova, G., Vyatkin, V., and Strasser, T. (2014). A review of agent and service-oriented concepts applied to intelligent energy systems. *IEEE transactions on industrial informatics*, 10(3):1890–1903.

Wang, Z. and Paranjape, R. (2017). Optimal residential demand response for multiple heterogeneous homes with real-time price prediction in a multiagent framework. *IEEE transactions on smart grid*, 8(3):1173–1184.

Warrington, J., Mariéthoz, S., Jones, C. N., and Morari, M. (2010). Predictive power dispatch through negotiated locational pricing. In *2010 IEEE PES Innovative Smart Grid Technologies Conference Europe (ISGT Europe)*, pages 1–8. IEEE.

Wi, Y.-M., Lee, J.-U., and Joo, S.-K. (2013). Electric vehicle charging method for smart homes/buildings with a photovoltaic system. *IEEE Transactions on Consumer Electronics*, 59(2):323–328.

Wu, H., Shahidehpour, M., Alabdulwahab, A., and Abusorrah, A. (2015). Thermal generation flexibility with ramping costs and hourly demand response in stochastic security-constrained scheduling of variable energy sources. *IEEE Transactions on Power Systems*, 30(6):2955–2964.

Wu, H., Shahidehpour, M., Alabdulwahab, A., and Abusorrah, A. (2016). A game theoretic approach to risk-based optimal bidding strategies for electric vehicle aggregators in electricity markets with variable wind energy resources. *IEEE Transactions on Sustainable Energy*, 7(1):374–385.

Zhang, C., Wang, Q., Wang, J., Pinson, P., Morales, J. M., and Østergaard, J. (2018). Real-time procurement strategies of a proactive distribution company with aggregator-based demand response. *IEEE Transactions on Smart Grid*, 9(2):766–776.

Zhang, D., Li, S., Sun, M., and O'Neill, Z. (2016). An optimal and learning-based demand response and home energy management system. *IEEE Transactions on Smart Grid*, 7(4):1790–1801.

Zhao, C., Dong, S., Li, F., and Song, Y. (2015). Optimal home energy management system with mixed types of loads. *CSEE Journal of Power and Energy Systems*, 1(4):29–37.